



**UNIVERSIDAD DE INVESTIGACIÓN DE  
TECNOLOGÍA EXPERIMENTAL YACHAY**

**Escuela de Ciencias Biológicas e Ingeniería**

**TÍTULO: Chontacuro (*Rhynchophorus palmarum*  
*larvae*) fatty acids and their potential medical  
applications against viral infections using  
bioinformatics tools**

Trabajo de integración curricular presentado como requisito  
para la obtención del título de Ingeniero Biomédico

**Autor:**

William Daniel Lituma González

**Tutor:**

PhD. Ruiz-Hinojosa María Gabriela

Urcuquí, marzo 2023

## AUTORÍA

Yo, **LITUMA GONZÁLEZ WILLIAM DANIEL**, con cédula de identidad 0704754365, declaro que las ideas, juicios, valoraciones, interpretaciones, consultas bibliográficas, definiciones y conceptualizaciones expuestas en el presente trabajo; así como, los procedimientos y herramientas utilizadas en la investigación, son de absoluta responsabilidad de el/la autora (a) del trabajo de integración curricular. Así mismo, me acojo a los reglamentos internos de la Universidad de Investigación de Tecnología Experimental Yachay.

Urcuquí, marzo 2023.



---

William Daniel Lituma González

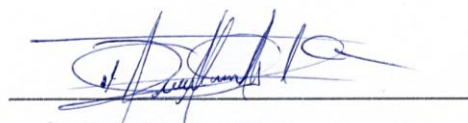
CI: 0704754365

## AUTORIZACIÓN DE PUBLICACIÓN

Yo, **LITUMA GONZÁLEZ WILLIAM DANIEL**, con cédula de identidad 0704754365, cedo a la Universidad de Investigación de Tecnología Experimental Yachay, los derechos de publicación de la presente obra, sin que deba haber un reconocimiento económico por este concepto. Declaro además que el texto del presente trabajo de titulación no podrá ser cedido a ninguna empresa editorial para su publicación u otros fines, sin contar previamente con la autorización escrita de la Universidad.

Asimismo, autorizo a la Universidad que realice la digitalización y publicación de este trabajo de integración curricular en el repositorio virtual, de conformidad a lo dispuesto en el Art. 144 de la Ley Orgánica de Educación Superior

Urcuquí, marzo 2023.



William Daniel Lituma González

CI:0704754365

## **DEDICATORIA**

*A aquella persona, la cual me ha acompañado tanto en mis logros y fracasos, mi madre. Además, a mi hermano que me enseñó, que no importa cuán difícil puedan ser las adversidades que una persona pase, con orden y paciencia, todo se logra.*

William Daniel Lituma González

## **AGRADECIMIENTOS**

Quiero agradecer a mi familia, mi mamá Rita y mi hermano Zalo. Son aquellas personas que no solo me apoyaron para lograr mis objetivos, sino también a plantearme nuevas metas.

Además, a mi tutora de tesis la doctora Ruiz-Hinojosa María Gabriela que formó parte del desarrollo de este trabajo curricular, tanto su guía y buenos consejos me impulsaron a continuar y no decaer.

William Daniel Lituma González

## Abstract

Known in the Kichwa language originally as, Chontacuro; it is the larvae of the South American palm weevil, *Rhynchophorus palmarum* (Linnaeus, 1758). The oil extracted from these larvae of the black palm weevil, *Rhynchophorus palmarum*, is used by indigenous kichwa groups in the Ecuadorian Amazon to treat and cure respiratory diseases and skin diseases wounds, calling this ancestral practice as zotherapy.

Based on the ethnopharmacological knowledge obtained, the hypothesis is raised that the use of *Rhynchophorus palmarum* oil can control different types of diseases of viral origin. Therefore, an investigation of the life cycle of the larva of *R. palmarum* was carried out. As well as the chemical composition of the South American palm weevil. In addition, the pharmacological applications of the fatty acids identified in *R. palmarum* within the human body are described. Also, the role of the ACE2 enzyme is described, in the viral infection caused by the SARS-CoV-2 virus, this enzyme will be the protein used in the molecular coupling against each fatty acid described in the chontacuro. Finally, a molecular docking is proposed, to represent the potential antiviral properties of *Rhynchophorus palmarum*.

**Keywords:** *Rhynchophorus palmarum*, fatty acids, bioinformatic, molecular docking, ACE2 protein, SARS-CoV-2 infection.

## Resumen

Conocido en la lengua kichwa originalmente como, Chontacuro; es la larva que proviene del picudo sudamericano de las palmeras, *Rhynchophorus palmarum* (Linnaeus, 1758). El aceite extraído de estas larvas del picudo negro, *Rhynchophorus palmarum*, es utilizado por los grupos indígenas kichwas de la Amazonía ecuatoriana para tratar y curar enfermedades respiratorias y heridas de enfermedades de la piel, denominando a esta práctica ancestral como zooterapia.

Con base en los conocimientos etnofarmacológicos obtenidos, se plantea la hipótesis de que el uso del aceite de *Rhynchophorus palmarum* puede controlar diferentes tipos de enfermedades de origen viral. Por ello, se llevó a cabo una investigación del ciclo vital de la larva de *R. palmarum*. Así como la composición química del picudo de la palmera sudamericana. Además, se describen las aplicaciones farmacológicas de los ácidos grasos identificados en *R. palmarum* dentro del organismo humano. También, se describe el papel de la enzima ACE2, en la infección viral causada por el virus SARS-CoV-2, esta enzima será la proteína utilizada en el acoplamiento molecular contra cada ácido graso descrito en el chontacuro. Finalmente, se propone un acoplamiento molecular, para representar las potenciales propiedades antivirales del *Rhynchophorus palmarum*.

*Palabras claves:* *Rhynchophorus palmarum*, ácidos grasos, bioinformática, acoplamiento molecular, proteína ACE2, infección del SARS-CoV-2.

## INDEX

<b>CHAPTER 1: Introduction and literature review</b>	<b>1</b>
<b>1.1. Introduction</b>	<b>1</b>
<b>1.2. Statement of the problem</b>	<b>3</b>
<b>1.3. Formulation of the problem</b>	<b>5</b>
1.3.1. Questions for guidance	5
<b>1.4. General and Specific Objectives</b>	<b>5</b>
1.4.1. General Objective	5
1.4.2. Specific Objectives	6
<b>CHAPTER 2: Rhynchophorus Palmarum: Biology</b>	<b>7</b>
<b>2.1. Life Cycle</b>	<b>10</b>
<b>2.2. Morphology</b>	<b>11</b>
<b>2.3. Rhynchophorus Palmarum as a plague.</b>	<b>14</b>
<b>2.4. Rhynchophorus Palmarum as a food.</b>	<b>15</b>
<b>CHAPTER 3: Rhynchophorus Palmarum: Fatty acid composition and potential medical properties.</b>	<b>17</b>
3.1.1. Fatty Acids	17
3.1.2. Ionization	19
3.1.3. Saturation	20
3.1.4. Fatty Acid Metabolism (Pelley, 2012)	22
<b>3.2. Variables used for food analysis of the proximate composition of Rhynchophorus palmarum.</b>	<b>29</b>
3.2.1. Moisture	29
3.2.2. Ashes	31
3.2.3. Fat Analysis	32
3.2.4. Protein Analysis (Chang, 2010)	34
3.2.5. Carbohydrate Analysis (BeMiller, 2010)	35
<b>3.3. Food analysis of R. palmarum larvae</b>	<b>37</b>
3.3.1. Fatty acid composition of R. palmarum larval oil	38
3.3.2. Proximal composition of Rhynchophorus palmarum larvae	39
3.3.3. Fatty acid composition of R. palmarum larvae sorted by palm type	39
<b>3.4. Medical properties of fatty acids identified in R. palmarum larvae.</b>	<b>41</b>
3.4.1. Caprylic acid (Octanoic acid)	41
3.4.2. Capric Acid (Decanoic acid)	42



3.4.3.	Lauric Acid (Dodecanoic acid)	43
3.4.4.	Myristic Acid (Tetradecanoic acid)	43
3.4.5.	Palmitic Acid (Hexadecanoic acid)	45
3.4.6.	Palmitoleic Acid ([Z]-Hexadec-9-enoic-acid)	46
3.4.7.	Margaric Acid (Heptadecanoic acid)	47
3.4.8.	Stearic Acid (Octadecanoic acid)	48
3.4.9.	Oleic Acid (cis-9-Octadecenoic acid)	48
3.4.10.	Linoleic Acid ([9Z-12Z]-octadeca-9,12-dienoic acid)	49
3.4.11.	Alpha-Linolenic Acid	51
3.4.12.	Arachidonic acid	52
3.4.13.	Heneicosanoic acid	53
3.4.14.	Behenic acid (Docosanoic acid)	54
3.4.15.	Tricosanoic acid	55
<b>CHAPTER 4: ACE2 Receptor for SARS-CoV-2</b>		<b>56</b>
<b>CHAPTER 5: Methodology</b>		<b>60</b>
<b>5.1</b>	<b>Structural retrieval</b>	<b>60</b>
<b>5.2.</b>	<b>Molecular Docking Studies.</b>	<b>61</b>
5.2.1.	Structure of natural compounds.	61
5.2.2.	Crystal structure of the SARS-CoV-2 protein spike (S) trimer and angiotensin-converting enzyme receptor 2 (ACE2)	62
5.2.3.	ACE2 protein optimization	65
5.2.4.	Revalidation of the crystal structure.	67
5.2.5.	Evaluate binding sites and pharmacological potential	68
5.2.6.	Docking with Autodock Vina and USCF Chimera	72
<b>CHAPTER 6: Results and Analysis</b>		<b>78</b>
<b>CHAPTER 7: Conclusions</b>		<b>85</b>
<b>Bibliography</b>		<b>87</b>

## **TABLE INDEX**

<b>Table 1.</b>	<i>Rhynchophorus palmarum</i> Taxonomy _____	<b>7</b>
<b>Table 2.</b>	<i>Rhynchophorus palmarum</i> distribution in America continent _____	<b>7</b>
<b>Table 3.</b>	Classification of fatty acids according to chain length _____	<b>18</b>
<b>Table 4.</b>	Important fatty acids in mammalian tissues _____	<b>19</b>
<b>Table 5.</b>	Degree of saturation of skin and digestive fat content oils from <i>Rhynchophorus palmarum</i> larvae expressed, expressed in percentages of g/100 g of total fat. _____	<b>38</b>
<b>Table 6.</b>	Proximal chemical composition (100g) of <i>R. palmarum</i> larvae. _____	<b>39</b>
<b>Table 7.</b>	Fatty acid composition of skin oil and digestive fat content of <i>Rhynchophorus palmarum</i> larvae according to the type of palm of origin (g/100 g of the total fatty acids). _____	<b>40</b>
<b>Table 8.</b>	Chemical structures of the fatty acids identified in the larvae of <i>R. palmarum</i> _____	<b>60</b>
<b>Table 9.</b>	Molecular docking results of each fatty acid identified in <i>R. palmarum</i> larvae with the ACE2 protein _____	<b>81</b>

## FIGURES INDEX

<b>Figure 1.</b>	<i>Geographical Distribution of R. palmarum.</i>	<b>8</b>
<b>Figure 2.</b>	<i>Palm infected by Bursaphelenchus cocophilus</i>	<b>8</b>
<b>Figure 3.</b>	<i>Illustration of plants where R. palmarum is found.</i>	<b>9</b>
<b>Figure 4.</b>	<i>Life cycle of the Rhynchophorus palmarum</i>	<b>11</b>
<b>Figure 5.</b>	<i>Rhynchophorus palmarum eggs</i>	<b>11</b>
<b>Figure 6.</b>	<i>Rhynchophorus palmarum larvae</i>	<b>12</b>
<b>Figure 7.</b>	<i>Final stages of R. palmarum.</i>	<b>13</b>
<b>Figure 8.</b>	<i>Adult male Rhynchophorus palmarum</i>	<b>14</b>
<b>Figure 9.</b>	<i>Bursaphelenchus cocophilus</i>	<b>15</b>
<b>Figure 10.</b>	<i>Chontacuro skewers, a traditional dish from the Ecuadorian Amazon</i>	<b>16</b>
<b>Figure 11.</b>	<i>Different ways of representing fatty acids.</i>	<b>18</b>
<b>Figure 12.</b>	<i>Saturated and unsaturated fatty acids</i>	<b>20</b>
<b>Figure 13.</b>	<i>Structures of some monounsaturated and polyunsaturated</i>	<b>21</b>
<b>Figure 14.</b>	<i>Different roles of C18 unsaturated fatty acids in plants</i>	<b>22</b>
<b>Scheme 1.</b>	<i>Acetyl- Coenzyme A Shuttle</i>	<b>23</b>
<b>Figure 15.</b>	<i>Metabolic steps in the synthesis of fatty acids</i>	<b>24</b>
<b>Scheme 2.</b>	<i>Fatty Acid Polymerization Initiation</i>	<b>25</b>
<b>Figure 16.</b>	<i>Elongation of fatty acid chains</i>	<b>26</b>
<b>Scheme 3.</b>	<i><math>\beta</math> – Carbonyl Reduction</i>	<b>27</b>
<b>Scheme 4.</b>	<i>Elongation Cycle</i>	<b>27</b>
<b>Scheme 5.</b>	<i>Triglyceride synthesis</i>	<b>28</b>
<b>Figure 17.</b>	<i>Assembly of a triglyceride</i>	<b>29</b>
<b>Scheme 6.</b>	<i>Importance of moisture content in food processing.</i>	<b>30</b>
<b>Scheme 7.</b>	<i>Methods to obtain ashes</i>	<b>31</b>

<b>Scheme 8.</b>	<i>The general classification of lipids</i>	<b>33</b>
<b>Scheme 9.</b>	<i>Importance of Protein Analysis</i>	<b>35</b>
<b>Scheme 10.</b>	<i>Sample preparation and extraction of mono- and disaccharides</i>	<b>37</b>
<b>Figure 18.</b>	<i>Caprylic acid, PubChem CID: 379</i>	<b>41</b>
<b>Figure 19.</b>	<i>Capric acid, PubChem CID: 2969</i>	<b>42</b>
<b>Figure 20.</b>	<i>Lauric acid, PubChem CID: 3893</i>	<b>43</b>
<b>Figure 21.</b>	<i>Myristic acid, PubChem CID: 11005</i>	<b>44</b>
<b>Figure 22.</b>	<i>Palmitic acid, PubChem CID: 985</i>	<b>45</b>
<b>Figure 23.</b>	<i>Palmitic Acid, PubChem CID: 445638</i>	<b>46</b>
<b>Figure 24.</b>	<i>Margaric acid, PubChem CID: 10465</i>	<b>47</b>
<b>Figure 25.</b>	<i>Stearic acid, PubChem CID: 5281</i>	<b>48</b>
<b>Figure 26.</b>	<i>Oleic acid, PubChem CID: 445639</i>	<b>49</b>
<b>Figure 27.</b>	<i>Linoleic acid, PubChem CID: 5280450</i>	<b>50</b>
<b>Figure 28.</b>	<i>Alpha-Linolenic acid, PubChem CID: 184021992</i>	<b>51</b>
<b>Figure 29.</b>	<i>Arachidonic acid, PubChem CID: 444899</i>	<b>52</b>
<b>Figure 30.</b>	<i>Heneicosanic acid, PubChem CID: 16898</i>	<b>53</b>
<b>Figure 31.</b>	<i>Behenic acid, PubChem CID: 8215</i>	<b>54</b>
<b>Figure 32.</b>	<i>Tricosanoic acid, PubChem CID: 17085</i>	<b>55</b>
<b>Figure 33.</b>	<i>Structure of the SARS-CoV-2 virus</i>	<b>56</b>
<b>Figure 34.</b>	<i>Main membrane receptors that interact with the Spike (S) protein trimer</i>	<b>57</b>
<b>Figure 35.</b>	<i>Union between the spike of the SARS-CoV-2 virus and the ACE2 enzyme in membrane cell</i>	<b>59</b>
<b>Figure 36.</b>	<i>Construction of linoleic acid in Avogadro</i>	<b>61</b>
<b>Figure 37.</b>	<i>Protonation state of linoleic acid in Avogadro</i>	<b>61</b>
<b>Figure 38.</b>	<i>Optimization of linoleic acid in Avogadro</i>	<b>62</b>

<b>Figure 39.</b>	<i>Structure of the SARS-CoV-2 spike receptor binding domain bounding to the ACE2 receptor.</i>	<b>63</b>
<b>Figure 40.</b>	<i>Experimental Data Snapshot of Crystal structure of SARS-CoV-2 spike receptor-binding domain bound with ACE2</i>	<b>64</b>
<b>Figure 41.</b>	<i>Overall quality of Crystal structure of SARS-CoV-2 spike receptor-binding domain bound with ACE2</i>	<b>65</b>
<b>Figure 42.</b>	<i>UCSF chimera visualization of the 6MOJ crystal structure</i>	<b>66</b>
<b>Figure 43.</b>	<i>Visualization of the receptor for angiotensin converting enzyme 2 - ACE2</i>	<b>66</b>
<b>Figure 44.</b>	<i>ACE2 protein uploaded in the MolProbity online program</i>	<b>67</b>
<b>Figure 45.</b>	<i>Validation of the crystal with the ACE2 protein with the online program MolProbity</i>	<b>68</b>
<b>Figure 46.</b>	<i>Overall structure of SARS-CoV-2 RBD bound to ACE2</i>	<b>69</b>
<b>Figure 47.</b>	<i>Summary topology of the SARS-CoV-2 spike monomer</i>	<b>69</b>
<b>Figure 48.</b>	<i>ACE2 protein observed from the DoGSiteScorer program</i>	<b>70</b>
<b>Figure 49.</b>	<i>ACE2 protein binding site predicted by DoGSiteScorer software.</i>	<b>70</b>
<b>Figure 50.</b>	<i>Ligand and protein visualization using UCSF Chimera software</i>	<b>72</b>
<b>Figure 51.</b>	<i>Preparation of ACE2 protein in USCF Chimera software for Docking</i>	<b>73</b>
<b>Figure 52.</b>	<i>Preparation of the ligand for docking in Autodock Vina</i>	<b>74</b>
<b>Figure 53.</b>	<i>Protein and ligand configuration in AutoDock Vina and USCF Chimera</i>	<b>75</b>
<b>Figure 54.</b>	<i>Visualization of a ligand conformation obtained by Autodock Vina and visualized in USCF Chimera</i>	<b>77</b>
<b>Figure 55.</b>	<i>Results obtained from the Docking performed by Autodock Vina</i>	<b>77</b>
<b>Figure 56.</b>	<i>Representation of the conformation of the fatty acids identified in R. palmarum larvae bound to the ACE2 protein</i>	<b>78</b>

## CHAPTER 1: Introduction and literature review

### 1.1. Introduction

Since ancient times for different cultures, insects have been used as medicinal resources, in the form of ointments or infusions, despite being commonly considered disgusting or repugnant animals (Costa Neto E. , 2002). The use of insects in medicine is called entomotherapy and it is used from an ancestral knowledge perspective (Vilharva et al., 2021), therefore it must be considered from a cultural point of view, the knowledge of insects and their use in medicine (Costa Neto, 1999).

Background information pointing to insects as a benefit for humans can be found in the book *Insectotheology*, published in 1699 (Berembaum, 1995). However, there are even older references, one of which is an Egyptian medical treatise from the 16th century BC called the Ebers papyrus, which contains accounts of medicinal ointments obtained from insects and arachnids (Weiss, 1946). Another recorded medicinal use of insects is silkworms, which have been used for more than three thousand years in traditional Chinese medicine to dissolve phlegm and relieve spasms (Zimian et al., 1997). In addition, Pliny the Elder, in his book *Naturalis Historiae*, recounted some insect-based ointments and infusions (entomoterapeutics) that were used in the Roman Empire in the 1st century AD for the treatment of various viral diseases (Carrera, 1993). It is also recorded by Dioscorides Anazarbeus, a roman greek physician, pharmacologist, and botanist, who in his second book of his *Materia Medica*, indicates several entomotherapeutic remedies (insect-derived medicines); one of them is the use of bedbugs to treat quartan fever or the use of fried cicadas for bladder pains. Another remedy recorded in his book is the use of cockroaches ground with oil for earache (Morge, 1973).

In our American continent some records indicate insects or insect derivatives as therapeutic sources; royal jelly, which the bee-eaters use to feed their queen, was used by the Mexican inhabitants to combat cases of anemia (Conconi & Pino, 1988). A total of 210 insect species have been recorded, which are actively used in mexican traditional medicine; the most commonly used orders are *Hymenoptera*, *Homoptera*, *Coleoptera*, and *Orthoptera* (Ramos Elorduy et al., 2001). In 13 states of Brazil, there are reports from colonial times of the use of insects for therapeutic purposes (Costa Neto E. , 2003); one of them is the use of a tea made from the roasted exoskeleton of

a grasshopper to treat people who have suffered a cardiovascular accident or to treat skin diseases (Costa Neto E. , 2002). Also, grasshopper powder, which is obtained by leaving it to dry in the sun, is used to make tea for the treatment of asthma (Costa Neto E. , 2002); as well as tea made from the roasted legs of a spider wasp (*Pompilidae*) (Costa Neto & Melo, 1998). In Colombia, culonas ants (*Atta laevigata*) are used for analgesic and aphrodisiac purposes (Césard et al., 2003). In addition, there are records from South America, Europe, and India, indicating the use of the mandibles of ants of the genus *Atta* for stitching wounds (Gudger, 1925). Currently, about a thousand species of insects used for therapeutic purposes have been recorded; China, in the lead, has recorded about 300 species of insects for medicinal use, which are distributed in 14 orders, 63 families, and 70 genera (Meyer-Rochow, 2017).

In Ecuador, the different indigenous communities located in the Amazon have included the larvae of the weevil *Rhynchophorus palmarum* L. (Coleoptera: Curculionidae) (Linnaeus, 1758), both in their diet (Trujillo-Gonzalez et al., 2011) and in treatment of respiratory diseases of viral origin (Cartay et al., 2020), through their ancestral knowledge; which can be defined as the result of experiences over time by indigenous communities to be directly linked to the environment, which has learned to use the local biodiversity of the different species of plant and animal origin for their benefit (Njoroge et al., 2010; Robinson et al., 2017). It is important to emphasize that *R. palmarum* is considered a pest (Hoddle et al., 2021) of great economic importance (De La Mora et al., 2022) because it is the main vector of the nematode *B. Cocophilus*, which is the cause of the Red Ring (López-Luján et al., 2022), which causes rotting of the bud of different species of palm trees and subsequently the death of the palm (Gómez-Marco et al., 2021). Despite being considered a pest, the larva of *R. palmarum* is a critical source of active agents for modern medicine, since it has been reported to have antimicrobial and antioxidant activity (Vilharva et al., 2021; Vera & Brand, 2014).

There are still no antiviral reports on the larva of *R. palmarum*, where tests have been conducted to show its effectiveness against viral agents in vivo or in silico, as has happened with its antimicrobial and antioxidant activity (Vilharva et al., 2021) (Cerdeira et al., 2001), even though, by ancestral or traditional knowledge, respiratory diseases are treated with this insect, using its fat as a topical applied in the thorax area; and also, its fat is used as an oral emulsion (Delgado et al., 2019). Despite this, there are research records of the characterization of the internal components of the

chontacuro insect (Batalha et al., 2020). Currently, there is evidence indicating, for example, that some of the components of chontacuro serve to cause stress and block the antiviral activity against the hepatitis C virus in cell cultures (Gunduz et al., 2012). In addition, there is research indicating that palmitic and oleic acid, major components of chontacuro, not only combat cardiovascular diseases (Palomer et al., 2018), but also serve to inhibit infection caused by SARS-CoV-2 Omicron and other variants (Lan et al., 2022). Similarly, unsaturated fatty acids found in *R. palmarum* larvae have been shown to block viral outbreaks (Lindwasser & Resh, 2002). It is important to highlight that the internal components of the chontacuro depend on the type of palm from which the insect feeds (Ahipo Dué et al., 200; Espinosa et al., 2020). In addition, since the larvae of *R. palmarum* are herbivorous, and far from the pollution of large cities, it makes them cleaner than other insects that have fatty acids, such as snails and oysters (Viesca & Romero, 2009).

Therefore, in order to carry out this research it will start with the biological cycle of *Rhynchophorus Palmarum* (Linnaeus, 1758), its morphology, the types of palms from which these larvae are obtained, its economic impact on agriculture and its benefits as a food source. Secondly, a bibliographic investigation of the internal components of the *R. palmarum* larvae will be carried out, explaining the variables used by the researchers to determine its internal composition. In addition, the medical benefits of the fatty acids identified in *R. palmarum* larvae will be briefly explained; this explanation of medical benefits is done in order to have a context of the possible benefits of *R. palmarum* larvae associated with viral diseases, infections or anti-immune responses. Third, the role of the ACE2 enzyme, a metallopeptidase, in viral infection caused by the SARS-CoV-2 virus will be explained. Fourthly, a molecular docking will be performed; where the intensity of attraction (score) between the ligand, which will be the fatty acids identified in the *R. palmarum* larvae, and the ACE2 enzyme will be measured. Finally, the data obtained will be analyzed and compared with the available literature; in order to answer the question: do the internal components identified in the *R. palmarum* larva have antiviral activity?

## **1.2. Statement of the problem**

Insects have been the focus of attention throughout human history, for both negative and positive reasons. The negative reasons are related to the economic



impacts, due to the damage caused to crops (Iannacone & Alvarino, 2006); thus, in turn, causing human losses, because some insects are transmitters of diseases such as dengue, malaria, chikungunya and Chagas disease (Stephenson et al., 2022; Chico-Avelino et al., 2022). The positive reasons, as we have observed, related to health, using them as medicines to relieve infections or diseases (Serrano-González et al., 2013; Srivastava et al., 2009); In addition, insects serve as a source of human food, due to their high amount of protein and essential amino acids (Hermans et al., 2021).

Unfortunately, the scientific community only focuses on the analysis of insect-derived foods for introduction into the human diet. In 2008, a workshop sponsored by the Food and Agriculture Organization of the United Nations was held on the subject, which had the title: "Forest Insects as Food: Humans Bite Back" (Yen, 2009) , where they focused on three main themes:

1. Edible forest insects should be considered a natural resource.
2. Presentation of models of sustainable management of insects to obtain food and other products.
3. Bioprospecting of edible forest insects.

In addition, the Food and Agriculture Organization of the United Nations, in 2013, established insects as an alternative source for obtaining food, because they are present in traditional diets in Asia, Africa, America, and Australia. In at least 2 billion people (Food And Agriculture Organization Of The United Nations, 2013) .

However, there is a need to find new sources for drug discovery, because there are records of populations of pathogens resistant to the current drug selection available (Giske et al., 2008). This evolution of resistance makes it difficult to control important diseases, causing economic and human loss; thus, affecting the cost of public health (Paladino et al., 2002). Resistance can be caused by spontaneous mutations that pathogens develop to survive, an example is the RNA virus that causes AIDS, HIV; which has a rate of  $10^4$  and  $10^5$  spontaneous mutations per nucleotide per genome replication (Abram et al., 2010; Mansky & Temin, 1995). Without forgetting the current pandemic caused by the SARS-CoV-2 virus, which has an evolution rate due to spontaneous mutations of  $1.3 \times 10^{-6} \pm 0.2 \times 10^{-6}$  (Amicone et al., 2022). In addition, it is a zoonotic disease, which means that it is a disease of natural origin,

which evolved, breaking the Darwinian division to be able to affect human beings (Brussel & Holmes, 2022).

Consequently, insects have co-existed with all currently known bacteria and viruses; therefore, they have developed defensive chemicals due to their co-evolution with plants and predators (Choudhary et al., 2022), making them a source of abundant resources for pharmacological research (Costa-Neto, 2005). Additionally, at present, molecular coupling simulations can be carried out to identify if there are objective targets that can indicate the antiviral activity of the internal components of different insects toward viruses.

### **1.3. Formulation of the problem**

Do internal components identified in *R. palmarum* larvae possess antiviral activity?

#### **1.3.1. Questions for guidance**

- What is the life cycle of *R. palmarum*?
- What is the effect of the *R. palmarum* beetle on the ecosystem?
- Are the larvae of *R. palmarum* just a harmful pest?
- Do *R. palmarum* larvae serve as a reliable food source?
- How was it determined that *R. palmarum* larvae were a reliable source of food?
- What are the internal components of *R. palmarum* larvae?
- Are there any records indicating any pharmacological potential of the internal components of chontacuro?
- Is there a link between viruses and lipid metabolism of fatty acids?
- What is the role of ACE2 enzyme in viral infection caused by SARS-CoV-2 virus?
- What are the in-silico tools that allow us to observe existing interactions between fatty acids and viruses?

### **1.4. General and Specific Objectives**

#### **1.4.1. General Objective**

To determine the potential antiviral activity of *R. palmarum* larvae within the human organism by in silico molecular docking against the ACE2 protein.

#### **1.4.2. Specific Objectives**

- Identify the role of both the beetle and the larvae in the ecosystem of *R. palmarum*.
- To understand the variables used to determine the nutritional analysis of *R. palmarum* in order to try to classify it as a beneficial and non-toxic food product.
- To understand the possible pharmacological effects of the identified fatty acids in *R. palmarum* larvae.
- Performing molecular docking simulations in order to understand the possible relationships between viral proteins, fatty acids from *R. palmarum* and, the mechanism given by ACE2 protein during a SARS-CoV-2 infection.

## CHAPTER 2: Rhynchophorus Palmarum: Biology

In the tenth edition of Systema Naturae (1758), Carl Linnaeus classified *Rhynchophorus palmarum* in his class "Insecta"; Table 1 provides taxonomic information of *R. palmarum*.

**Table 1.** *Rhynchophorus palmarum* Taxonomy

<b>Taxonomic Classification of <i>Rhynchophorus palmarum</i></b>	
<b>Kingdom</b>	Animalia
<b>Phylum</b>	Arthropoda
<b>Class</b>	Insecta
<b>Order</b>	Colcoptera
<b>Family</b>	Curculionidae
<b>Genus</b>	Rhynchophorus
<b>Species</b>	R. palmarum
<b>Binomial name</b>	Rhynchophorus palmarum (Linnaeus,1758)
<b>Synonyms</b>	South American palm weevil
<b>EPPO code</b>	RHYCPA

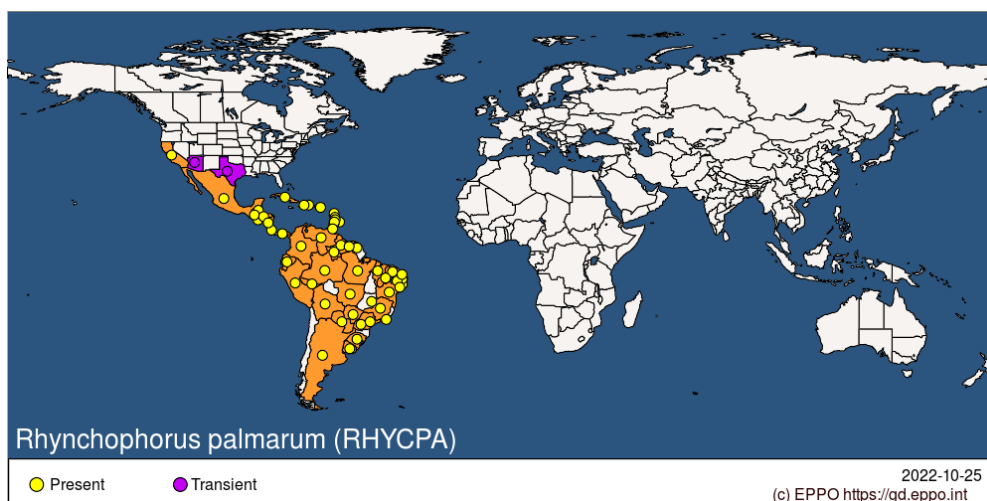
Distributed widely around the world, the South American palm weevil is mainly concentrated in the tropics (see Table 2) (Wattanapongsiri, 1966) in virgin forests and in agro-ecosystems where oil palm is planted (see Figure 1) (EPPO, 2020).

**Table 2.** *Rhynchophorus palmarum* distribution in America continent

<b><i>Rhynchophorus palmarum</i> distribution in America continent</b>	
<b>North America</b>	United States of America (Arizona, California, Texas)
<b>Central America and Caribbean</b>	Barbados, Belize, Costa Rica, Cuba, Dominican Republic, El Salvador, Guatemala, Haití, Honduras, Nicaragua, Panamá, Puerto Rico, Trinidad and Tobago.
<b>South America</b>	Argentina, Bolivia, Brazil, Colombia, Ecuador, French Guiana, Guyana, Paraguay, Peru, Suriname, Uruguay, Venezuela.

**Figure 1.**

*Geographical Distribution of R. palmarum*



Note. Retrieved from: *Rhynchophorus palmarum*. EPPO datasheets on pests recommended for regulation [Photography], EPPO, 2022 (<https://gd.eppo.int>). Copyright by EPPO. CC BY-NC-ND 4.0.

The South American palm weevil has been recorded in at least twelve families of thirty-five different plant species, found especially in palms (*Arecaceae*) (Esser & Meredith, 1987; Sánchez & Cerda, 1993). *R. palmarum* is considered a pest for different palm species, because it is the main vector of the red ring disease, which causes the rotting of the palm bud and its possible death (see Figure 2) (Dalbon et al., 2021); using these palm species both as feeding and reproductive hosts (EPPO, 2020).

**Figure 2.**

*Palm infected by Bursaphelenchus cocophilus*



Note. Cross-section of a palm tree, showing that the palm is infected by *Bursaphelenchus cocophilus*, the red ring nematode. Retrieved from: *Rhadinaphelenchus cocophilus* (red ring nematode) - The

Invasive Species Compendium (ISC) [Photography]. Society of Nematologists, 2020 ([https://entnemdept.ufl.edu/creatures/nematode/red\\_ring\\_nematode.htm](https://entnemdept.ufl.edu/creatures/nematode/red_ring_nematode.htm)). Copyright by Institute of Food and Agricultural Science – University of Florida. CC BY-NC-SA 4.0.

In the Ecuadorian Amazon, the palm weevil is found in two species: the Chonta palm (*Bactris gasipaes*) (see Figure 3A) and the Morete palm (*Mauritia flexuosa*) (see Figure 3B) (Espinosa *et al.*, 2020). There are also records of *R. palmarum* using *Saccharum officinarum* (sugar cane) (see Figure 3C), which is not a palm species, for reproductive reasons, but rather for alimentary purposes (EPPO, 2020).

### Figure 3.

Illustration of plants where *R. palmarum* is found.



Note. Different types of palms where *R. palmarum* feeds and reproduces. **A.** Chonta palm, *Bactris gasipaes* for reproductive and feeding purposes. **B.** Morete palm, *Mauritia flexuosa* for reproductive and feeding purposes. **C.** Sugar cane, *Saccharum officinarum* for feeding purposes only. Retrieved from: **A.** Freepik Company - arttrongphap, 2020 (<https://www.freepik.es/fotos-premium/ilustracion-3d-arbol-bactris-gasipaes-aislado-blanco-su-mascara32754700.htm>) – Copyright by Freepik Company S.L. CC BY-NC-ND 4.0. **B.** HiClipart – Anonymous, n.d. (<https://www.hiclipart.com/free-transparent-background-png-clipart-idkig>) – Copyright by HiClipart. CC BY-SA 2.0. **C.** Francisco Manuel Blanco, 1980 ([https://commons.wikimedia.org/wiki/File:Saccharum\\_officinarum\\_Blanco1.18-cropped.jpg](https://commons.wikimedia.org/wiki/File:Saccharum_officinarum_Blanco1.18-cropped.jpg)). Public Domain Copyright.

According to records in the global database of the European and Mediterranean Plant Protection Organization: *R. palmarum* feeds on a variety of ripe fruits, such as avocado (*Persea americana* [Lauraceae]), banana (*Musa spp.* [Musaceae]), Citrus

spp. (*Rutaceae*), cocoa (*Theobroma cacao* [*Malvaceae*]), guayabo (*Psidium guajava* [*Myrtaceae*]), mango (*Mangifera indica* [*Anacardiaceae*]), and papaya (*Carica papaya* [*Caricaceae*]).

In addition, artificial diets have been developed for laboratory rearing of *R. palmarum* eggs and larvae (López-Luján et al., 2022), using a mixed diet based on sugar cane and pineapple (Giblin-Davis et al., 1989). Laboratory rearing of *R. palmarum* eggs and larvae is developed for use in laboratory bioassays (Santana et al., 2014), because they are considered pests, no ethics committee was needed for their study in laboratories.

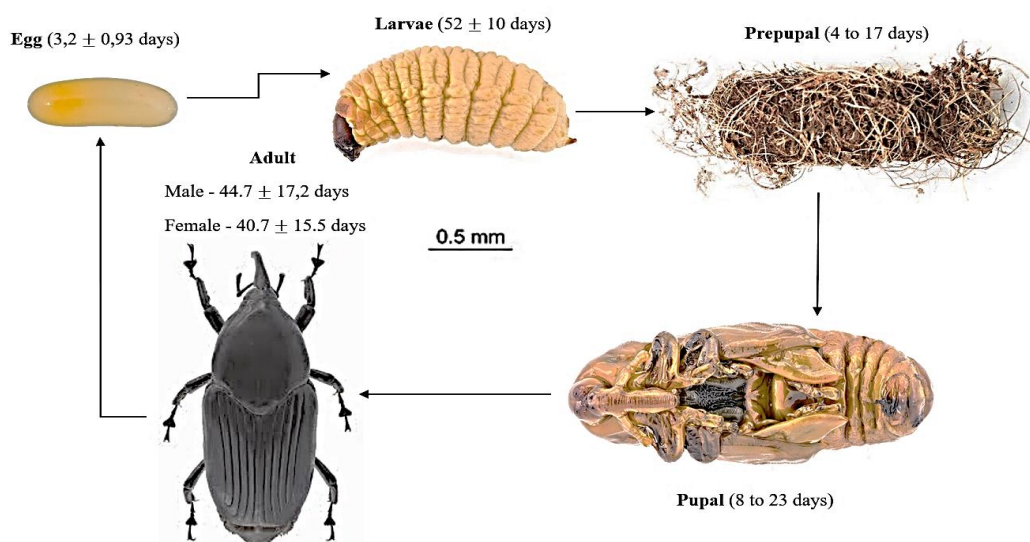
### **2.1. Life Cycle**

The normal life cycle of the South American palm weevil (*Rhynchophorus palmarum*) (see Figure 4) lasts about 120 days (Restrepo et al., 1982), although there are records that under controlled laboratory conditions (20 - 35 C and 62 - 92% relative humidity), its life cycle extends to about 170 days. A female can lay an average of 254 +/- 155 eggs during a period of 30.7 +/- 14.3 days (EPPO, 2020).

In the global database of the European and Mediterranean Plant Protection Organization, the incubation period of *R. palmarum* is 3.2 +/- 0.93 days. The larvae of *R. palmarum* then develop over a period of 52.0 +/- 10.0 days, during which time they have six to ten instars. The larvae then make cocoons using palm fibers, called the prepupal stage, which lasts 4 to 17 days. The pupal stage lasts 8 to 23 days, with the adults remaining in the cocoons for 7.8 +/- 3.4 days before complete metamorphosis. Furthermore, it is reported that female *R. palmarum* live for 40.7 +/- 15.5 days, while males live for 44.7 +/- 17.2 days (Mexzón et al., 1994; Schlickmann-Tank et al., 2020).

**Figure 4.**

*Life cycle of the Rhynchophorus palmarum*



Note. Life cycle of the *Rhynchophorus palmarum* from being an egg to forming into a mature weevil.

**2.2. Morphology**

The eggs (see Figure 5) are pale white, with a wrinkled surface and ovoid in shape, averaging 2.40 mm in length and 0.8 mm in width, until they reach the first instar, where their diameter increases slightly (Hagley, 1965). In addition, the eggs, which are protected by a brown waxy secretion, are individually located within the palm tissue 1 to 2 mm apart (Wattanapongsiri, 1966).

**Figure 5.**

*Rhynchophorus palmarum* eggs



Note. Retrieved from: *Rhynchophorus palmarum* egg, *Rhynchophorus palmarum* (RHYCPA) [Photography], EPPO Global Database – Hoddle, 2022 (<https://gd.eppo.int/taxon/RHYCPA/photos>). Copyright by EPPO Global Database. CC BY-NC-ND 4.0.

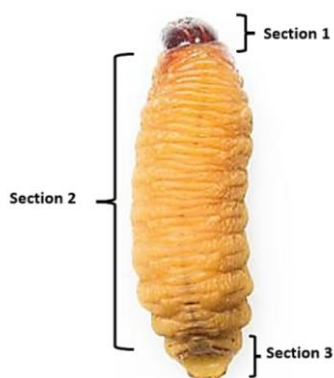


The larvae of *R. palmarum* are cannibalistic, legless and eruciform in shape. Initially, larvae may measure 2.40 - 2.65 mm in length, 0.94 mm in width and 1.9 mg in weight (Restrepo et al., 1982); they may reach 5 - 6 centimeters in length after 6 to 10 larval stages of maturation (Mexzón et al., 1994). The larvae have a dark brown head (see Figure 6), very chitinous; they have sclerotized mouthparts with strong mandibles (EPPO, 2020).

The thorax of *R. palmarum* larvae is divided into three sections. The aft terminal section is rigid and flat. The abdominal section is muscular, with folds that allow locomotion in the larva. Finally, the first section is surrounded by a semi-rigid ring behind the head (see Figure 6).

**Figure 6.**

*Rhynchophorus palmarum* larvae

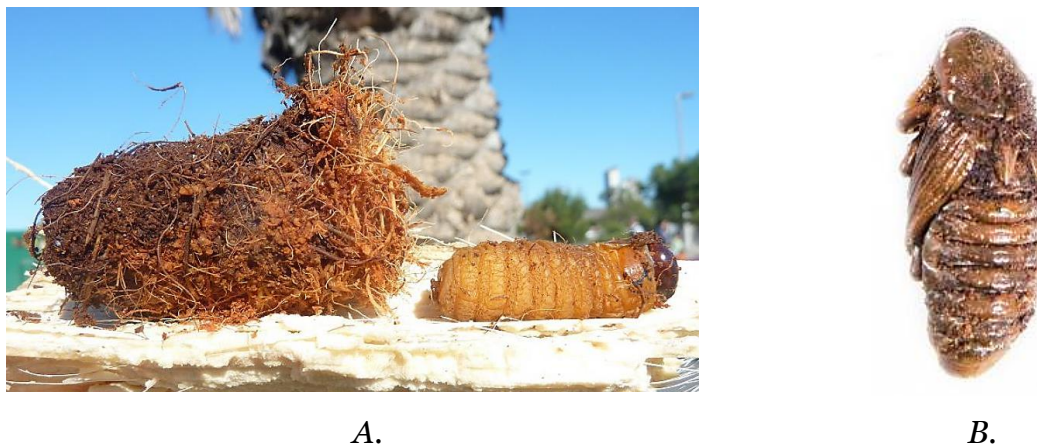


Note. Adapted from: *Rhynchophorus palmarum* life stages, *Rhynchophorus palmarum* (RHYCPA) [Photography], EPPO Global Database – Hoddle, 2022 (<https://gd.eppo.int/taxon/RHYCPA/photos>). Copyright by EPPO Global Database. CC BY-NC-ND 4.0.

Before pupation begins, larvae move to the periphery of the trunk, leaf stalk or flower rachis where they decrease their feeding activity and begin to form their cocoons from interwoven plant fibers (see Figure 7A); pupation begins when the larva is completely enclosed in a closed, cylindrical-ovoid cocoon (see Figure 7B) 7-9 cm long and 3-4 cm in diameter (EPPO, 2020).

**Figure 7.**

*Final stages of R. palmarum.*



Note. The last two adult stages of *R. palmarum* can be observed. **A.** *Rhynchophorus palmarum* cocoon. **B.** *Rhynchophorus palmarum* pupa. Retrieved from: **A.** prepupal *Rhynchophorus palmarum* larvae extracted from its fibrous cocoon. This cocoon was found on the ground under a heavily infested *P. canariensis* in Tijuana Mexico [Photography], EPPO Global Database – Hoddle, 2022 (<https://gd.eppo.int/taxon/RHYCPA/photos>). Copyright by EPPO Global Database. CC BY-NC-ND 4.0. Adapted from **B.** *Rhynchophorus palmarum* life stages. *Rhynchophorus palmarum* (RHYCPA) [Photography], EPPO Global Database – Hoddle, 2022 (<https://gd.eppo.int/taxon/RHYCPA/photos>). Copyright by EPPO Global Database. CC BY-NC-ND 4.0.

Adults of *R. palmarum* are large, robust beetles (see Figure 8), mostly black, although small populations with orange marks have been reported, similar in appearance to *R. ferrugineus* (Löhr et al., 2015). Adult beetles can measure 3 - 5 cm in length and 1.2 - 1.4 cm in width, with an average weight of 1.6 - 2 grams. In addition, *R. palmarum* beetles exhibit sexual dimorphism, where males have hairs on the antero-central dorsal region, while females lack rostral setae (EPPO, 2020; Giblin-Davis et al., 2013).

**Figure 8.**

*Adult male Rhynchophorus palmarum*



**Note.** Retrieved from: an adult male *Rhynchophorus palmarum* [Photography], EPPO Global Database – Hoddle, 2022 (<https://gd.eppo.int/taxon/RHYCPA/photos>). Copyright by EPPO Global Database. CC BY-NC-ND 4.0.

**2.3. Rhynchophorus Palmarum as a plague.**

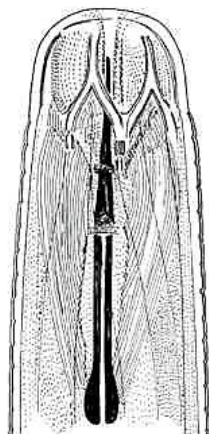
*Rhynchophorus palmarum* is considered an economically important pest, because it not only affects commercial plantations such as oil and coconut palms, but also Amazonian palms such as chonta and morete palms, which are very useful for indigenous communities (Cartay, 2016) (Ponce-Méndez et al., 2022). The adult *Rhynchophorus palmarum* are attracted by wounds and rotting in the buds and stems of the palms (De La Mora Castañeda et al., 2022), where in the soft tissues, *Rhynchophorus palmarum* deposit their eggs (Solines Reyes, 2022). When the eggs are deposited, the palm becomes infected with the nematode *Bursaphelenchus cocophilus* (see Figure 9), which is the main cause of the red ring disease (see Figure 2) (Flores-Pacheco et al., 2022).

*Bursaphelenchus cocophilus* is an obligate migratory endoparasitic nematode, which causes red ring disease (Torres, 2021) and affects species of the *Arecaceae* family; these nematode lives all its life inside the palm, but does not multiply when it is inside the disseminating insect (Aldana de la Torre et al., 2015). The larva of *Rhynchophorus palmarum* acquires the nematode, and maintains it throughout its moults until it reaches its adult stage (Chinchilla & Escobar, 2007); then, when the adult *R. palmarum* leaves the palm, it can infect three or four healthy palms with the nematode (Sarria et al., 2020). At present, there are campaigns to combat and control

this pest, using traps, where natural and synthetic pheromones are placed to attract the insects (De la Mora-Castañeda et al., 2022).

**Figure 9.**

*Bursaphelenchus cocophilus*



Note. Adapted from: remarques sur les genres des sous-familles *Bursaphelenchinae* Paramonov [Graphical Representation], Nematoda: Aphelenchoididae. *Revue de Nematologie* – Baujard, 1989 (<http://nemaplex.ucdavis.edu/Taxadata/G145S3.aspx>). Copyright by Howard Ferris. CC BY-ND 4.0.

**2.4. Rhynchophorus Palmarum as a food.**

The larvae of *Rhynchophorus palmarum*, collected from palm trees, are a great source of protein and fat for Amazonian Indians, who supplement their diet with them (Araujo & Beserra, 2007). There are records indicating low protein malnutrition in Amazonian communities, due to the high consumption of mushrooms, drupes, almonds and insects (Paucar-Cabrera, 2005; Smith, 1996). Amazonian villagers consume these fresh larvae, called chontacuros (chonta worms) either alive or dead, fried or roasted (see Figure 10) (Cartay et al., 2020). Furthermore, in the Ecuadorian Amazon, these larvae are marketed, either for consumption or breeding (Quinteros et al., 2022).

The nutritional value of chontacuro has been recorded in numerous laboratory studies (Cartay et al., 2020; Vilharva et al., 2021; Espinosa et al., 2020). It has been found that the protein value of choncacuro is 76%, much higher than the protein content of beef, which is 50-57% (Cartay et al., 2020). In addition, its total caloric value ranges between 560 kcal/100 grams, which is higher than that of beef, which is 430 kcal/100 grams (Neto & Ramos-Elorduy, 2006). As for the fat content of protein

sources, *Rhynchophorus palmarum* larvae have a percentage ranging from 21 to 54%, which is much higher than meat (17%) and fish (21%) (Cartay et al., 2020), and also have a better composition.

**Figure 10.**

*Chontacuro skewers, a traditional dish from the Ecuadorian Amazon*



Note. Retrieved from: CHONTACURO, the best Amazonian food [Photography], Origenes EC – Ortega, 2022 (<https://origenesec.com/amazonia/chontacuro/>). Copyright by Origenes EC. CC BY-ND 2.0.

### **CHAPTER 3: *Rhynchophorus Palmarum*: Fatty acid composition and potential medical properties.**

In the present chapter, the variables used by Sancho et al., Espinosa et al., Maceda & Chiñi, Cerda et al., Vargas et al., Batalha et al., Vilharva et al. and Ahipo Dué et al. for food analysis and the characterization of the internal composition of *R. palmarum* larvae will be described. First, the definition of fatty acids, their classification (see table 3), ionization, saturation and metabolism within the human organism will be explained, as well as the most important fatty acids found in mammalian tissues (see table 4). Then, saturated, unsaturated, monounsaturated and polyunsaturated fatty acids will be described, because they are variables used to determine the degree of saturation of the fatty acids found in the larvae of *R. palmarum* (see table 5). Afterwards, the variables used to determine the proximal percentage composition of *R. palmarum* will be explained (see table 6), which are: humidity, ash, protein, total fat and carbohydrates; these obtained values serve to reveal the nutritional value of *R. palmarum*. In addition, the content in 100 grams of fat of the fatty acids identified in *R. palmarum* larvae by the aforementioned authors is presented (see Table 7). Finally, the potential medical properties of the different fatty acids identified in *R. palmarum* larvae by the aforementioned authors, whether antimicrobial, antioxidant and antiviral activity, will be explained. This is done in order to clarify the benefits that *R. palmarum* larvae possess and their potential harm to the human body.

#### **3.1.1. Fatty Acids**

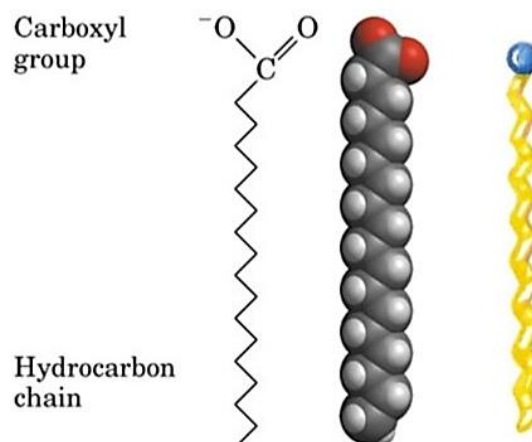
The chemical formula representing the compounds known as fatty acids is as follows (Montgomery et al., 1999) and the different forms in which the fatty acids are represented can be seen in Figure 11:



where R is an alkyl chain consisting of hydrogen and carbon atoms

**Figure 11.**

*Different ways of representing fatty acids.*



Note. Retrieved from: Fatty Acid Structure | Examples | Types | Physical & Chemical Properties [Graphical Representation], iBiologia – Yaqoob, 2022 (<https://ibiologia.com/fatty-acid-structure/>). Copyright by iBiologia. CC-BY 4.0

There is a diverse range of fatty acids of natural origin, more than 1000, these fatty acids with different structures and functional groups (see Figure 11), constitute the main components of waxes, oils, fats and other materials that are made up of lipids (Gunstone et al., 2007). In addition, the vast majority of naturally occurring fatty acids contain pair of carbon atom number.

The main function of fatty acids is to serve as a source of metabolic energy; in addition, to act as structural elements for another class of lipids. The length of the carbon atom chain is usually the most accepted method for classifying fatty acids, as can be seen in Table 3, where human tissues and blood have the highest abundance of long-chain fatty acids (Montgomery et al., 1999). Besides, Table 4 shows the most important structural properties of the fatty acids in mammals, as well as their respective names.

**Table 3.** *Classification of fatty acids according to chain length*

<b>Type</b>	<b>Number of carbon atoms</b>
Short chain	2-4
Medium chain	6-10
Long chain	12-26



**Table 4.** *Important fatty acids in mammalian tissues*

<b><i>Descriptive name</i></b>	<b><i>Systematic name</i></b>	<b><i>Carbon atoms</i></b>	<b><i>Double bonds</i></b>
Acetic		2	0
Lauric	Dodecanoic	12	0
Myristic	Tetradecanoic	14	0
Palmitic	Hexadecanoic	16	0
Palmitoleic	Hexadecenoic	16	1
Stearic	Octadecanoic	18	0
Oleic	Octadecenoic	18	1
Linoleic	Octadecadienoic	18	2
Linolenic	Octadecatrienoic	18	3
$\gamma$ -Homolinolenic	Eicosatrienoic	20	3
Arachidonic acid	Eicosatetraenoic	20	4
EPA*	Eicosapentaenoic	20	5
DHA*	Docosahexaenoic	22	6

\*The descriptive name commonly used is in abbreviated form.

### 3.1.2. Ionization

Under normal conditions, the pH of the intracellular fluid is 7.0 and plasma 7.4 (Hayata et al., 2014). Meanwhile, the  $pK_a$  of the carboxyl group of the fatty acid is approximately 4.8 (Quast, 2016). Therefore, almost all free fatty acid molecules (99%) present in body fluids are ionized, i.e., the fatty acid is in the form of an anion. (Rawling et al., 2020), possessing properties very similar to detergents to long-chain fatty acids; because the hydrocarbon end seeks a non-polarized environment and the ionized carboxyl group interacts with the aqueous medium (Murphy, 2015).



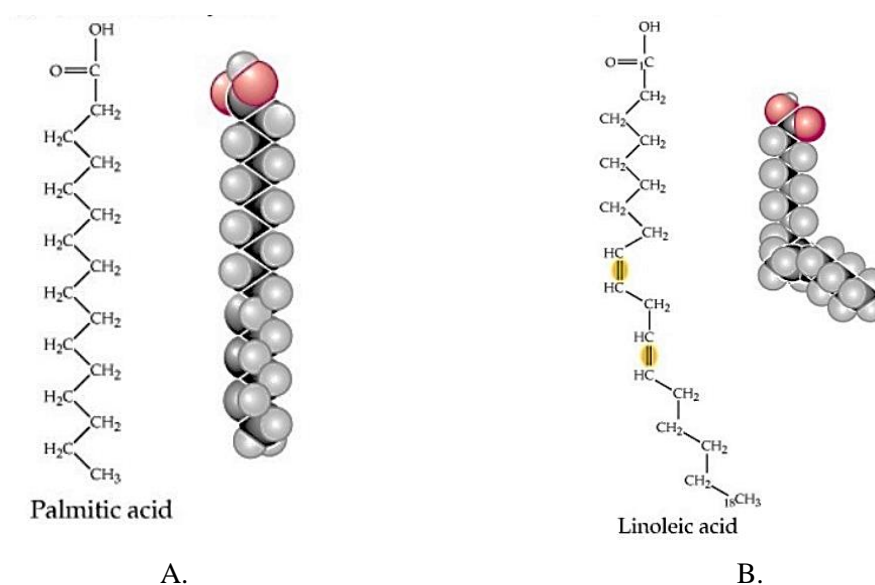


### 3.1.3. Saturation

Fatty acids can be classified as saturated or unsaturated. A saturated fatty acid can be defined as a fatty acid when the alkyl chain does not contain any double bonds (see Figure 12A). In contrast, unsaturated fatty acids are those with one or more double bonds (see Figure 12B) (Kenar et al., 2017). The structure of unsaturated fatty acids was reported in the 1890s. Although fatty acid cycling was discovered in the 1920s, fatty acids did not receive attention until the 1940s, when polymer chemistry and its understanding were in their infancy (List et al., 2017).

**Figure 12.**

*Saturated and unsaturated fatty acids*

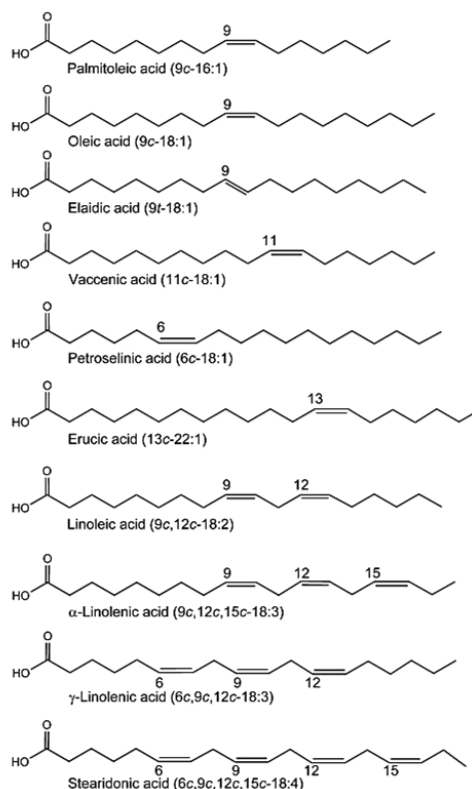


Note. **A.** Saturated fatty acids. **B.** Unsaturated fatty acids. Retrieved from: Fatty Acid Structure | Examples | Types | Physical & Chemical Properties [Graphical Representation], iBiologia – Yaqoob, 2022 (<https://ibiologia.com/fatty-acid-structure/>). Copyright by iBiologia. CC-BY 4.0.

Those naturally occurring fatty acids that have carbon-carbon double bonds along the backbone are known as unsaturated. If they contain one double bond, they are called monounsaturated (monoenoic) and if they have multiple double bonds along the alkyl chain, they are called polyunsaturated (polyenoic) (see Figure 13) (Kenar et al., 2017). In addition, unsaturated fatty acids having double bonds limits the rotation of the alkyl chain, causing isomerism around the double bond, manifesting a cis- or trans-configuration (Park et al., 2023). Naturally occurring unsaturated fatty acids in mammals have the cis-configuration (Antwi-Boasiako & Sander, 2020).

**Figure 13.**

*Structures of some monounsaturated and polyunsaturated*



Note. Retrieved from: Fatty Acids Chemistry, Synthesis, and Applications - Chapter 2 - Naturally Occurring Fatty Acids: Source, Chemistry, and Uses [Graphical Representation], Academic Press and AOCS Press - Kenar et al., 2017 ([doi:10.1016/b978-0-12-809521-8.00002-7](https://doi.org/10.1016/b978-0-12-809521-8.00002-7)). Copyright by Elsevier Inc. CC BY-NC-SA 4.0.

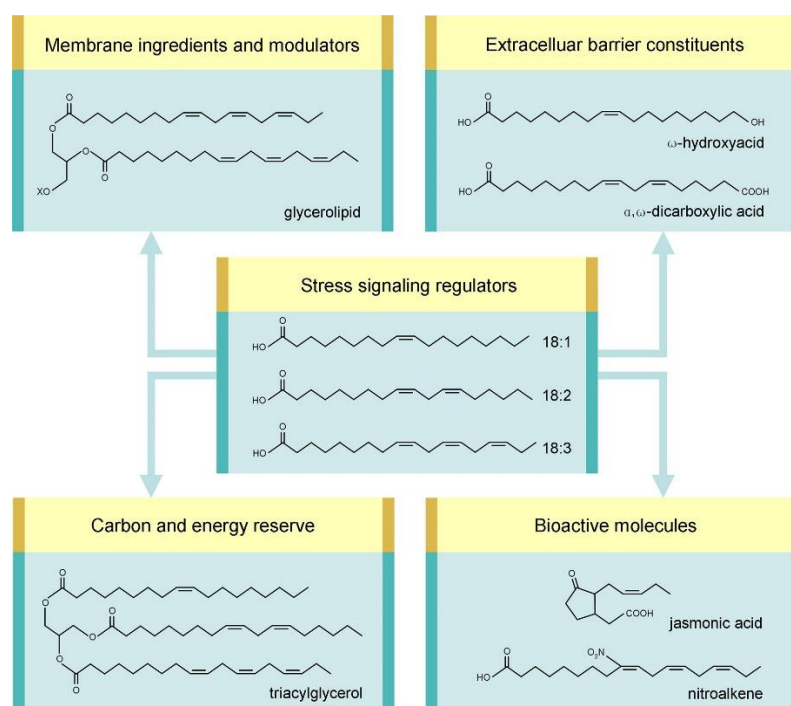
The definition of both polyunsaturated and monounsaturated fatty acids has been explained, but how are these fatty acids distributed within the kingdoms of nature? Bacteria possess unsaturated fatty acids, which are monounsaturated (Keweloh & Heipieper, 1996). Whereas, plants and mammals have both monounsaturated and polyunsaturated fatty acids. It is noteworthy that both fish and plants have higher amounts of polyunsaturated fatty acids than terrestrial mammals (Hulbert, 2021). Insects have monounsaturated and polyunsaturated fatty acids (Mori & Yoshinaga, 2011), but unlike terrestrial animals, they have higher concentrations of polyunsaturated fatty acids (Arrese & Soulages, 2010).

In addition, it is important to mention that unsaturated fatty acids (UFAs) in plants (see Figure 14) and insects are considered general defense systems against different abiotic and biotic stresses (He et al., 2018), because insects when feeding on

different plants capture these unsaturated fatty acids, metabolizing them in their digestive tract and adopting this antioxidant, antibacterial and antiviral defense mechanism coming from plants, serving as a vector, but not for disease transmission, but to adhere new defense mechanisms (Feng et al., 2020). Furthermore, in both plants and animals, unsaturated fatty acids are essential membrane components (Wu et al., 2009).

**Figure 14.**

*Different roles of C18 unsaturated fatty acids in plants*



Note. The stress responses of polyunsaturated fatty acids in plants caused by viruses, bacteria, fungi, nematodes and arthropods can be observed. This ability to fight against these agents is captured by the insects that feed on these plants; in the case of *R. palmarum* larvae, they metabolize these polyunsaturated fatty acids and express them in their fat content as well as in their skin. Different roles of C18 unsaturated fatty acids in plants as a response to stress. Retrieved from: Plant Unsaturated Fatty Acids: Multiple Roles in Stress Response [Graphical Representation], Front. Plant Sci. – He & Ding, 2020 (doi: 10.3389/fpls.2020.562785). Copyright by He & Ding. CC-BY 4.0.

### 3.1.4. Fatty Acid Metabolism (Pelley, 2012)

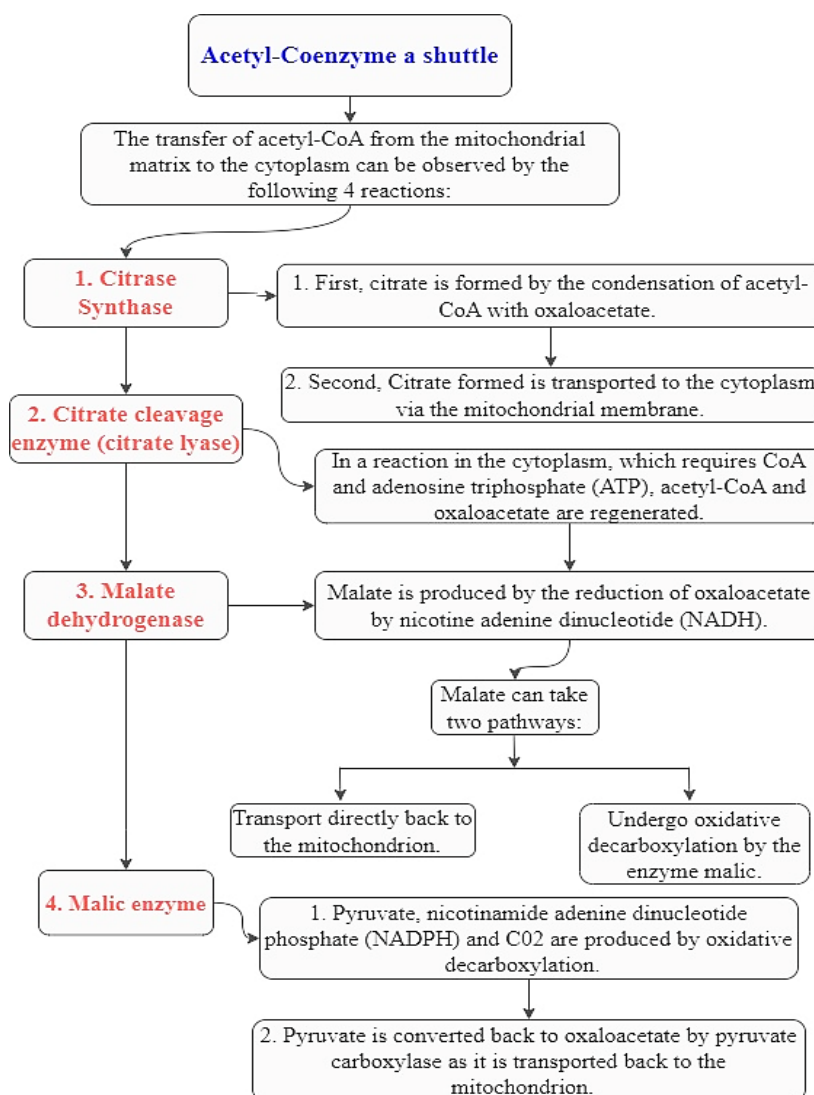
One of the objectives of this research work is to know the interaction that exists between the fatty acids registered in *R. palmarum* and the human organism, that is why it is important to know which is the metabolism that fatty acids follow in our

organism; because, as mentioned in the previous chapter, the route of administration used for the consumption of *R. palmarum* oils is the oral route.

A transport process must precede each fatty acid metabolic pathway. This is because fatty acid chains are oxidized in the mitochondrial matrix and polymerized in the cytoplasm. In addition, it allows separate regulation of each pathway, as well as preventing pathway intermediates from carrying out competitive side reactions. Likewise, free fatty acids must be transported to the mitochondria for further oxidation. However, in order for acetyl-coenzyme A (CoA), which is the precursor of fat synthase, to bind to a fatty acid, it must be transported to the cytoplasm, because acetyl-CoA it originates in the matrix. Reaction steps of the fatty acid synthesis pathway Acetyl-Coenzyme A to Palmitate:

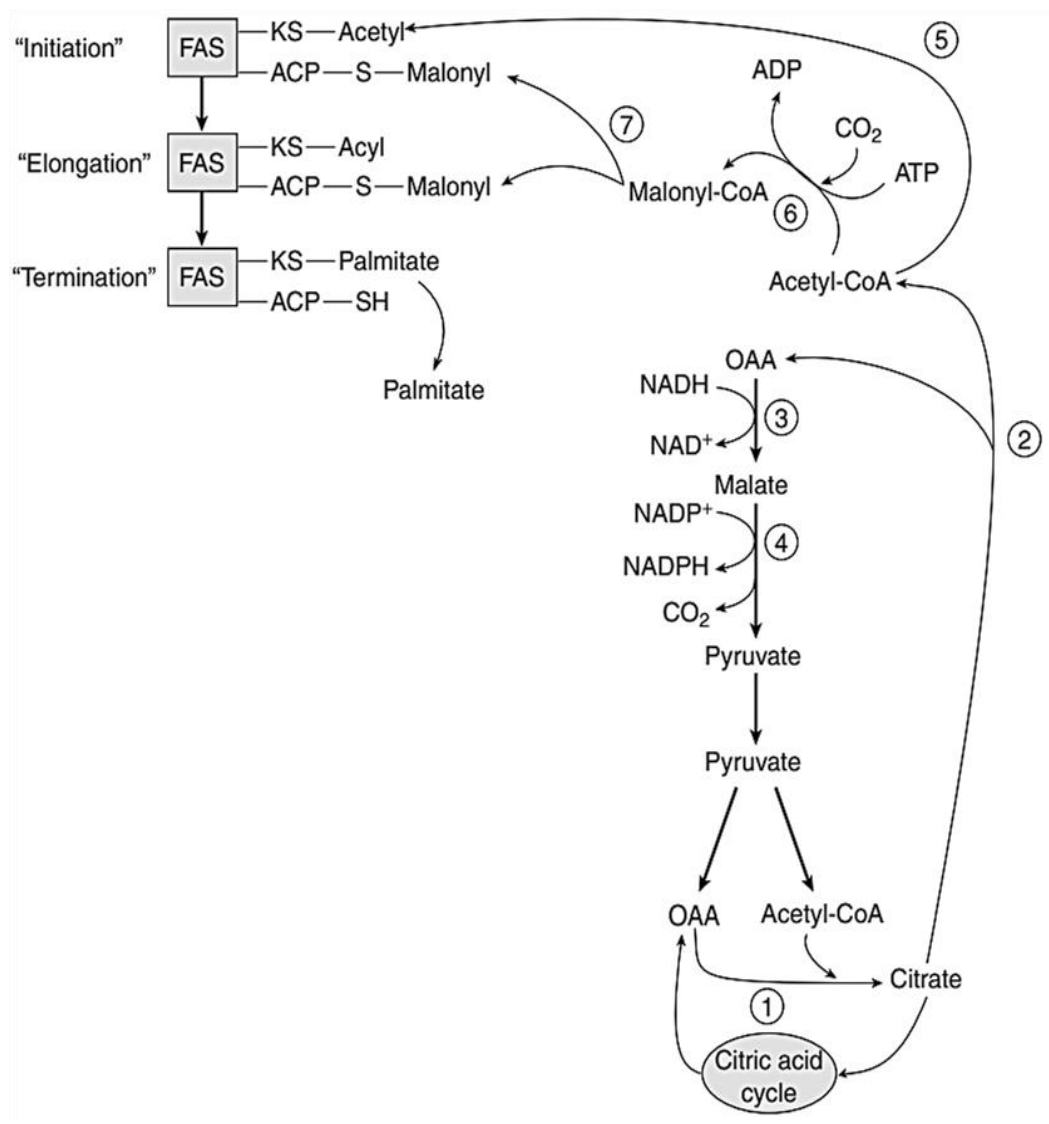
**Scheme 1.**

*Acetyl- Coenzyme A Shuttle*



Note. Adapted from: Fatty Acid and Triglyceride Metabolism [Book], Elsevier's Integrated Review Biochemistry – Pelley, 2012 ([doi:10.1016/b978-0-323-07446-9.00010-6](https://doi.org/10.1016/b978-0-323-07446-9.00010-6)). Copyright by Elsevier Inc. CC BY-NC-SA 4.0.

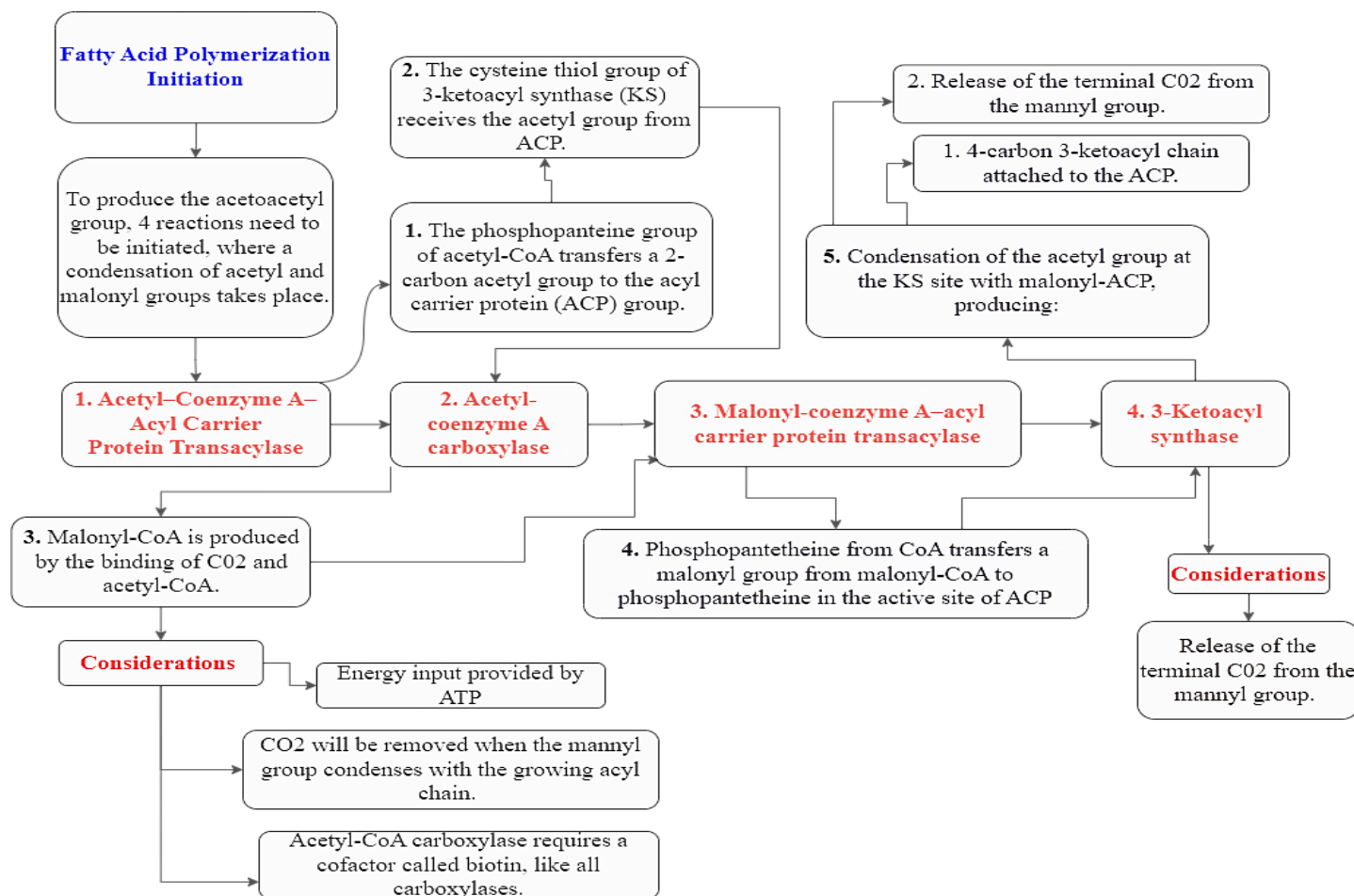
**Figure 15.**  
*Metabolic steps in the synthesis of fatty acids*



Note. Ketoacyl site contains an acetyl group during initiation, an acyl group during elongation, and palmitate before release as free palmitate. **Step 1**, citrate synthase; **Step 2**, citrate cleavage enzyme (citratelase); **Step 3**, malate dehydrogenase; **Step 4**, malic enzyme; **Step 5**, acetyl-coenzyme A (CoA)–acyl carrier protein (ACP) transacylase; **Step 6**, acetyl-CoA carboxylase; **Step 7**, malonyl-CoA-ACP transacylase. FAS, fatty acid synthesis. KS, 3-ketoacyl synthase; ADP adenosine diphosphate; ATP, adenosin triphosphate. Retrieved from: Fatty Acid and Triglyceride Metabolism [Book], Elsevier's Integrated Review Biochemistry – Pelley, 2012 ([doi:10.1016/b978-0-323-07446-9.00010-6](https://doi.org/10.1016/b978-0-323-07446-9.00010-6)). Copyright by Elsevier Inc. CC BY-NC-SA 4.0.

**Scheme 2.**

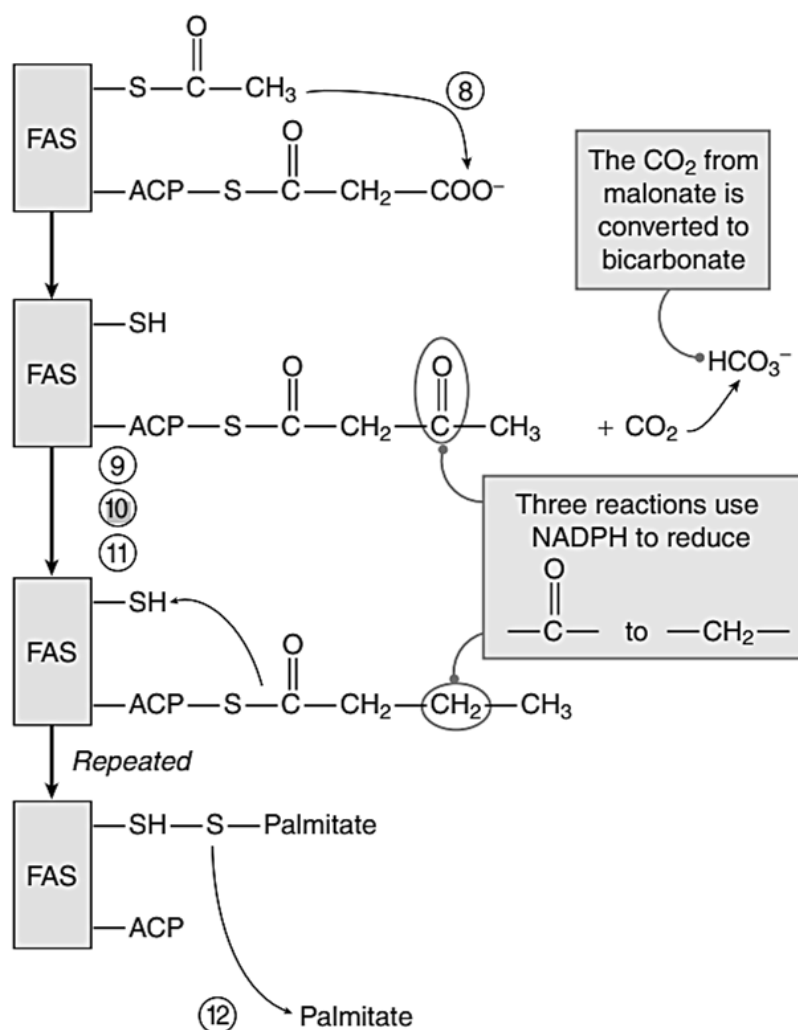
*Fatty Acid Polymerization Initiation*



Note. Adapted from: Fatty Acid and Triglyceride Metabolism [Book], Elsevier's Integrated Review Biochemistry – Pelley, 2012 ([doi:10.1016/b978-0-323-07446-9.00010-6](https://doi.org/10.1016/b978-0-323-07446-9.00010-6)). Copyright by Elsevier Inc. CC BY-NC-SA 4.0.

**Figure 16.**

*Elongation of fatty acid chains*

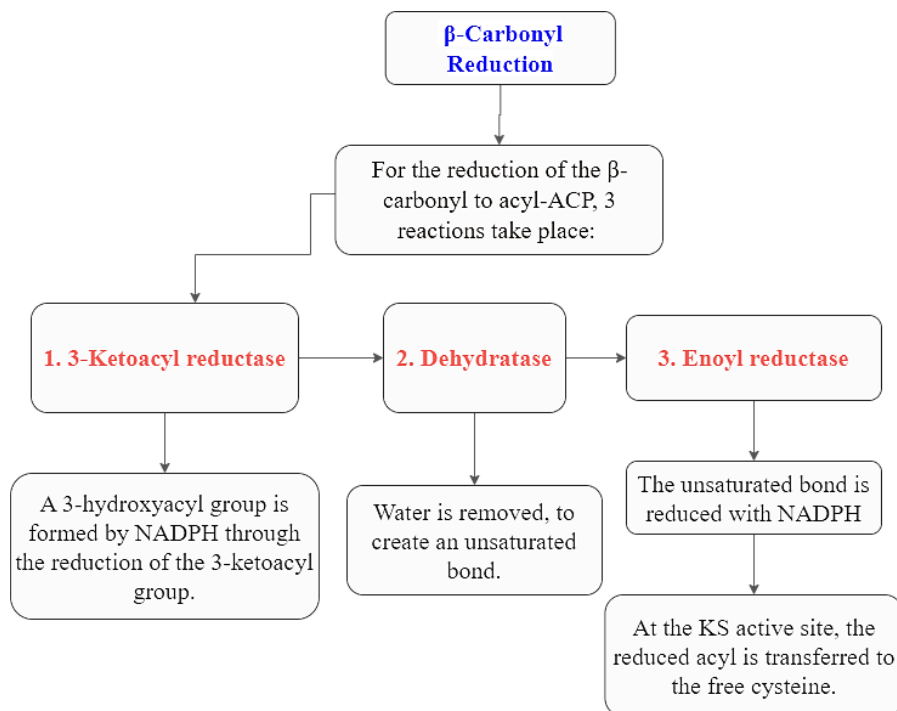


Note. Step 8, 3-ketoacyl synthase; Step 9, 3-ketoacyl reductase; Step 10, dehydratase; Step 11, enoyl reductase; Step 12, thioesterase. NADPH, nicotinamide adenine dinucleotide phosphate. Retrieved from: Fatty Acid and Triglyceride Metabolism [Book], Elsevier's Integrated Review Biochemistry – Pelley, 2012 ([doi:10.1016/b978-0-323-07446-9.00010-6](https://doi.org/10.1016/b978-0-323-07446-9.00010-6)). Copyright by Elsevier Inc. CC BY-NC-SA 4.0.



### Scheme 3.

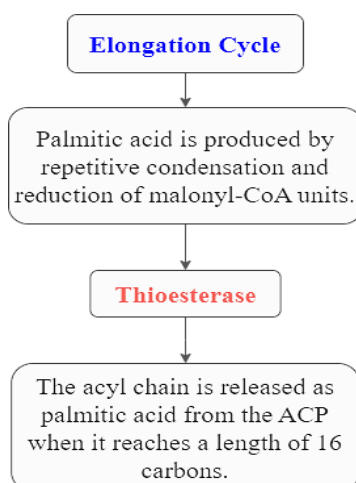
#### $\beta$ – Carbonyl Reduction



Note. Adapted from: Fatty Acid and Triglyceride Metabolism [Book], Elsevier's Integrated Review Biochemistry – Pelley, 2012 ([doi:10.1016/b978-0-323-07446-9.00010-6](https://doi.org/10.1016/b978-0-323-07446-9.00010-6)). Copyright by Elsevier Inc. CC BY-NC-SA 4.0.

### Scheme 4.

#### Elongation Cycle

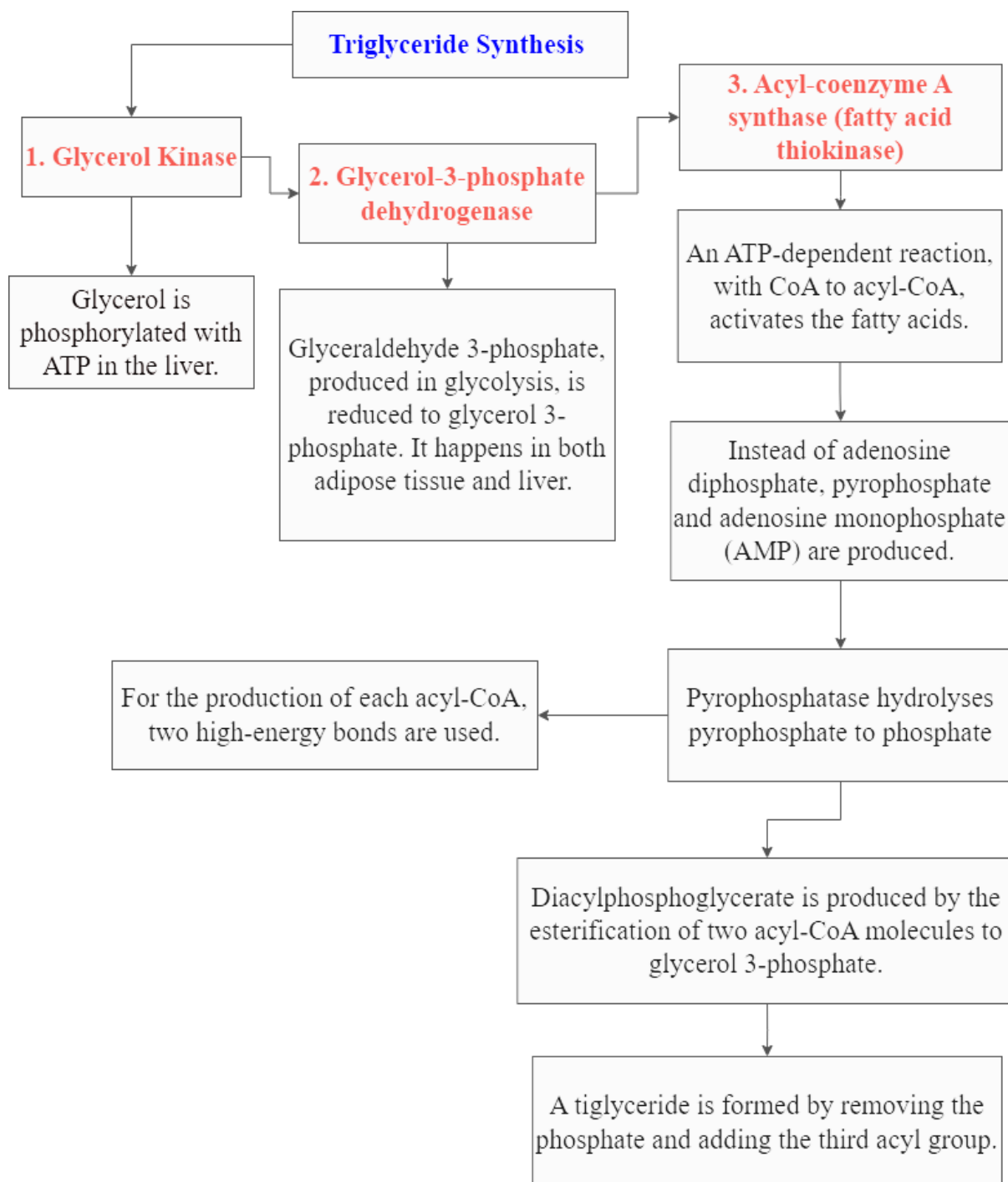


Note. Adapted from: Fatty Acid and Triglyceride Metabolism [Book], Elsevier's Integrated Review Biochemistry – Pelley, 2012 ([doi:10.1016/b978-0-323-07446-9.00010-6](https://doi.org/10.1016/b978-0-323-07446-9.00010-6)). Copyright by Elsevier Inc. CC BY-NC-SA 4.0.



**Scheme 5.**

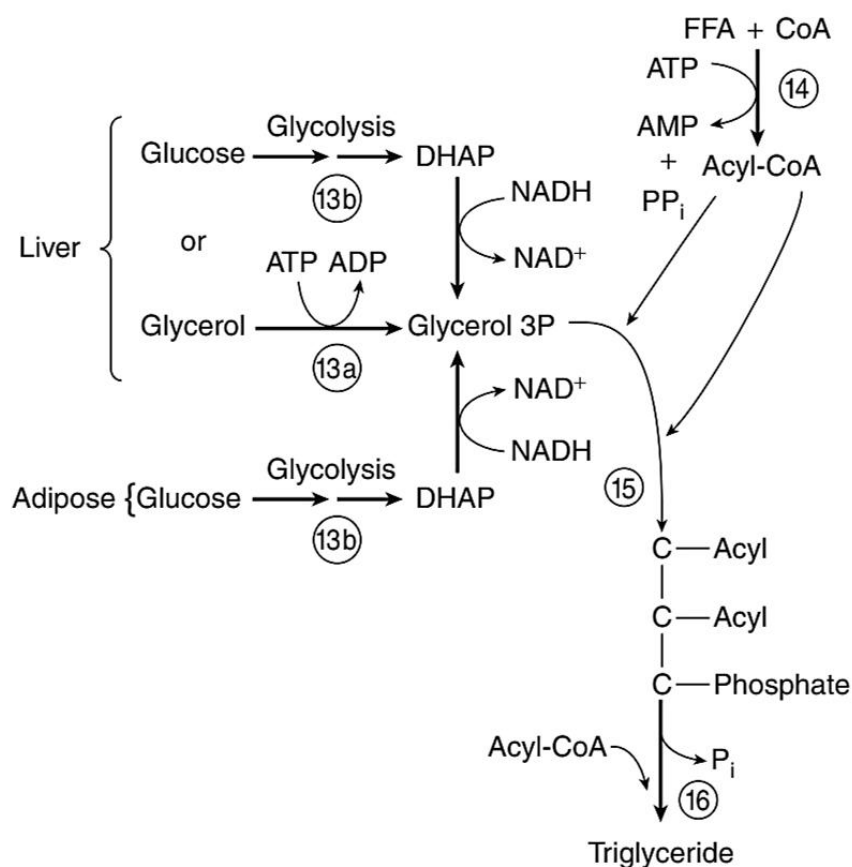
*Triglyceride synthesis*



Note. Adaptated from: Fatty Acid and Triglyceride Metabolism [Book], Elsevier’s Integrated Review Biochemistry – Pelley, 2012 ([doi:10.1016/b978-0-323-07446-9.00010-6](https://doi.org/10.1016/b978-0-323-07446-9.00010-6)). Copyright by Elsevier Inc. CC BY-NC-SA 4.0.

**Figure 17.**

*Assembly of a triglyceride*



Note. Step 13a, glycerol kinase; Step 13b, glycerol-3-phosphate dehydrogenase; Step 14, acetyl-coenzyme A synthase; Step 15 and Step 16, acyltransferase. FFA, free fatty acid; DHAP, dihydroxyacetone phosphate; PP<sub>i</sub>; inorganic pyrophosphate; P<sub>i</sub>, inorganic phosphate. Retrieved from: Fatty Acid and Triglyceride Metabolism [Book], Elsevier's Integrated Review Biochemistry – Pelley, 2012 ([doi:10.1016/b978-0-323-07446-9.00010-6](https://doi.org/10.1016/b978-0-323-07446-9.00010-6)). Copyright by Elsevier Inc. CC BY-NC-SA 4.0.

**3.2. Variables used for food analysis of the proximate composition of *Rhynchophorus palmarum* larvae.**

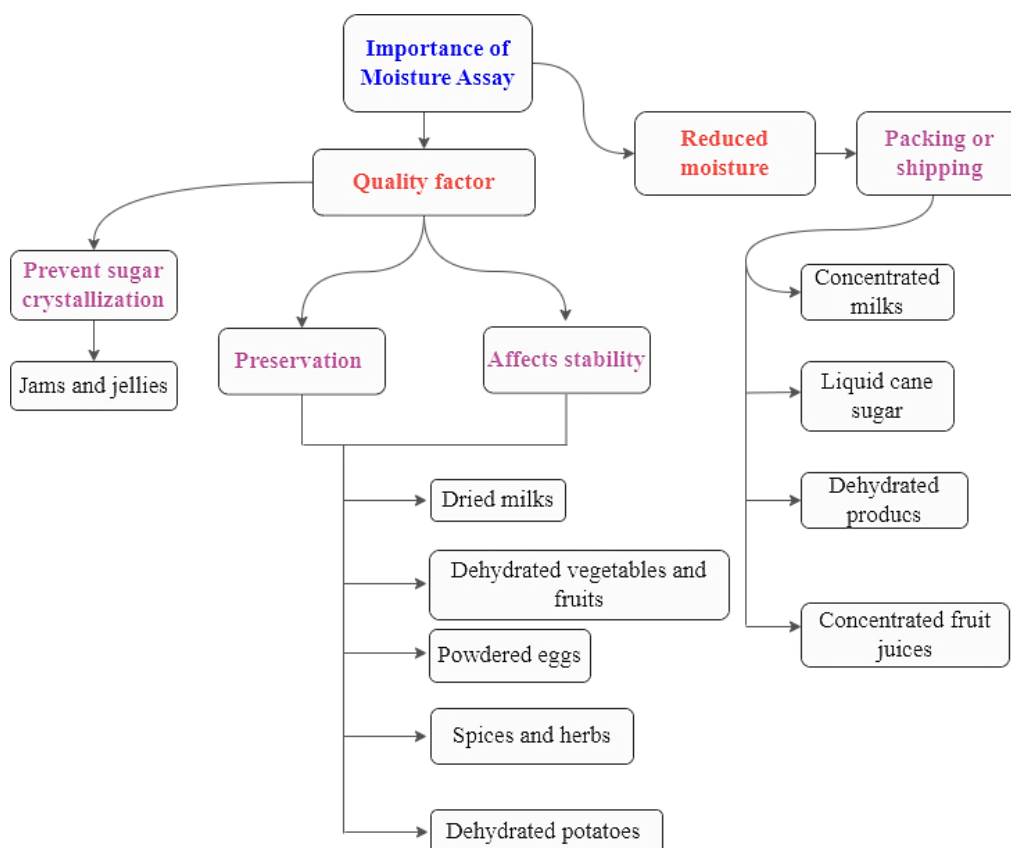
**3.2.1. Moisture**

Moisture allows determining physical properties of materials; as well as powder properties, one of them is flowability (Hwabin et al., 2018). Therefore, moisture quantity testing is considered to be one of the most important and fundamental analytical procedures performed on food products (Bradley, 2010).

The amount of dry matter remaining after the removal of moisture is known as total solids (Ngannikom & Songsermpong, 2011). This value is of utmost importance because water is considered an economic filler (Bradley, 2010). Scheme 6 indicates some of the important factors of moisture in food manufacturing.

**Scheme 6.**

*Importance of moisture content in food processing.*



Note. Adapted from: Food Analysis Fourth Edition - Chapter 6: Moisture and Total Solids [Book], Springer New York – Nielsen Suzanne - Bradley Robert, 2010 (<https://doi.org/10.1007/978-1-4419-1478-1>). Copyright by Springer Science+Business Media, LLC 2010. CC BY-NC-SA 4.0.

The drying method is the most commonly used method to determine moisture content. This method causes the evaporation of water at the boiling point (Kirk et al., 1996). Both the total solids content of the food and the moisture content can be calculated as follows when using the oven drying method (Bradley, 2010):

$$\%Moisture \left( \frac{wt}{wt} \right) = \frac{wt \text{ of wet sample} - wt \text{ of dry sample}}{wt \text{ of wet sample}} \times 100 \quad [1]$$

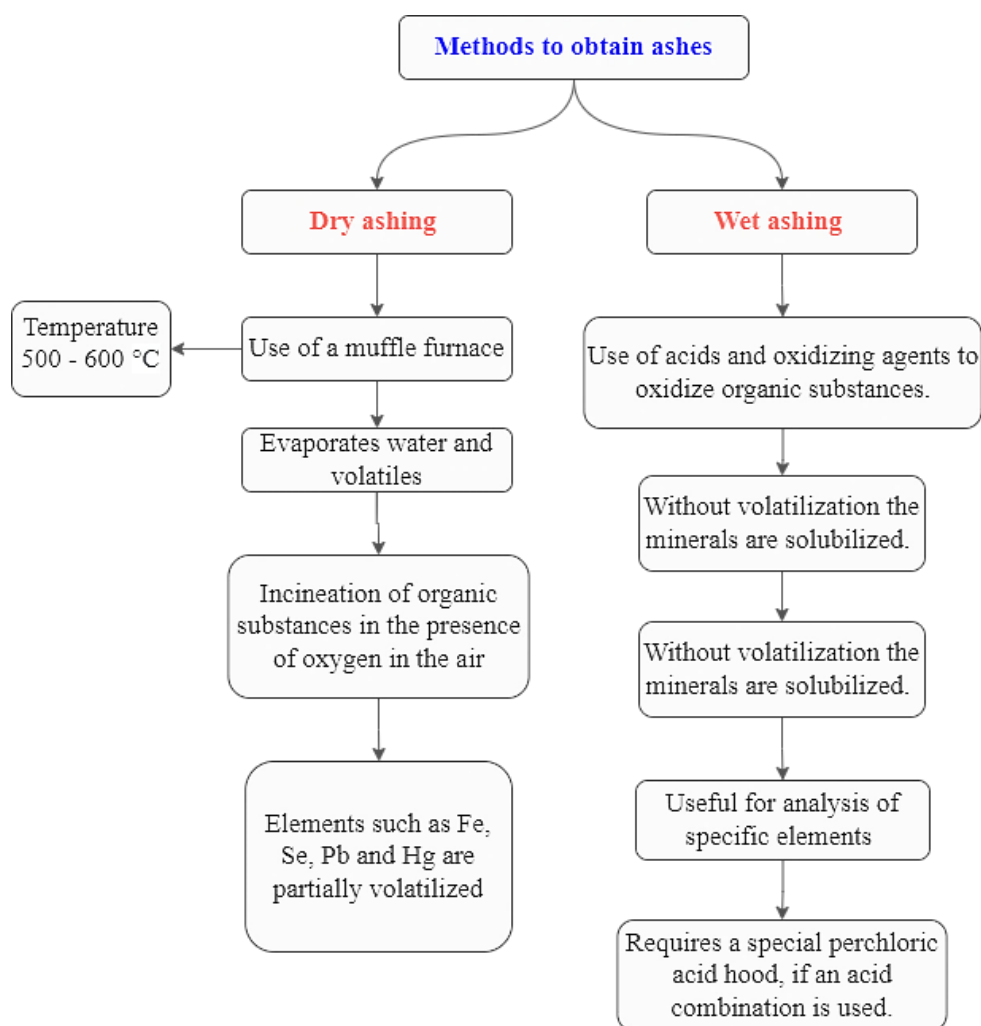
Where: wt Weight

### 3.2.2. Ashes

After the organic matter in a food product undergoes a complete oxidation or ignition process, the remaining inorganic residue is known as ash (AOAC, 2007). The main types used in incineration are two: wet incineration and dry incineration. Wet ashing, or oxidation, is used to analyze certain types of minerals. Dry ashing, on the other hand, is used to know the proximate composition and to analyze specific minerals (Marshall, 2010) (see Scheme 7). The ash content of foods can be expressed in either wet weight or dry weight, depending on the method used (Aurand et al., 1987).

#### Scheme 7.

*Methods to obtain ashes*



Note. Adapted from: Food Analysis Fourth Edition - Chapter 6: Ash Analysis [Book], Springer New York – Nielsen Suzanne – Marshall Maurice, 2010 ([https://doi.org/10.1007/978-1-4419-1478-1\\_7](https://doi.org/10.1007/978-1-4419-1478-1_7)). Copyright by Springer Science+Business Media, LLC 2010. CC BY-NC-SA 4.0.

The importance of ash analysis lies in the fact that it indicates the total mineral content of the food. It is an essential part in determining the proximate analysis for proximate evaluation. The first step for a specific elemental analysis of a food sample is the ash. In products of animal origin, a constant elemental ash content is generally expected, whereas in products of vegetable origin the ash content is variable (Marshall, 2010). The ashes content is calculated as follows (Marshall, 2010):

$$\begin{aligned} \% \text{ ash (dry basis)} \\ = \frac{\text{wt after ashing} - \text{tare wt of crucible}}{\text{original sample wt} \times \text{dry matter coefficient}} \times 100 \quad [2] \end{aligned}$$

Where:

$$\text{dry matter coefficient} = \frac{\% \text{ solids}}{100}$$

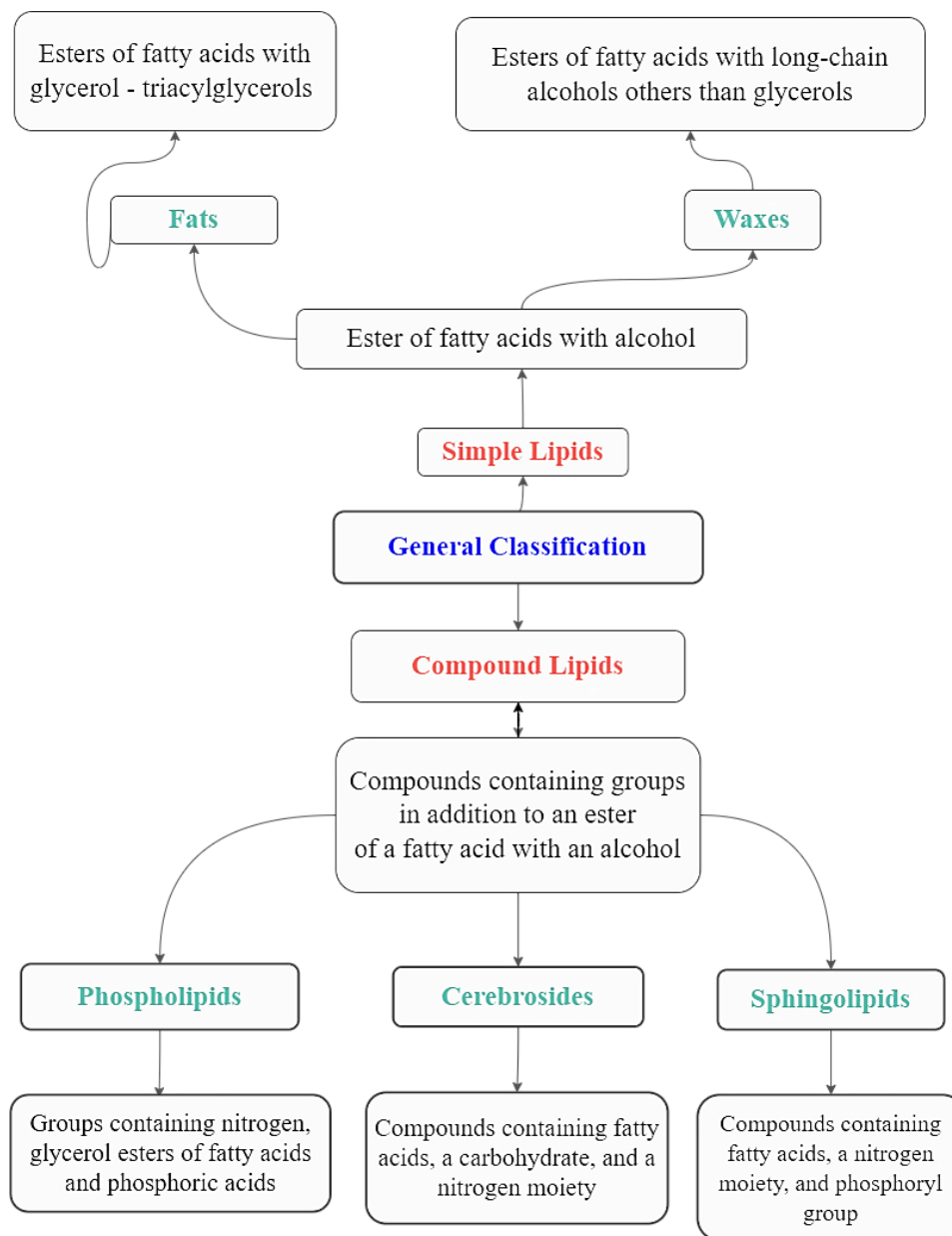
For example, if *R. palmarum* larvae is 87% dry matter, the dry matter coefficient would be 0.87. If ash is calculated on an as-received or wet weight basis (includes moisture), delete the dry matter coefficient from the denominator. If moisture was determined in the same crucible prior to ashing, the denominator becomes (dry sample wt - tared crucible wt).

### 3.2.3. Fat Analysis

The main structural constituents of food are lipids, proteins and carbohydrates (Wijaya et al., 2015). Those substances that are soluble in organic compounds are known as lipids (Senesi & Loffredo, 1998). Some lipids are hydrophobic, such as triacylglycerols; others have hydrophobic and hydrophilic fractions, such as di- and monoacylglycerols, and are therefore soluble in relatively polar solvents (Min & Ellefson, 2010). Lipids are a large group composed of substances of similar composition and common properties (Segré et al., 2001). The most dominant category of lipids are the triacylglycerols, which are composed of fats and oils. Oils refer, in general, to those lipids that are liquid at room temperature; whereas, lipids that are solids at room temperature are referred to as fats (Ellefson, 2017). The U.S. Food and Drug Administration (FDA), to facilitate nutrition labeling, has defined total fat as the sum of fatty acids from C4 to C24, categorizing them as triglycerides. The classification of lipids is specified in scheme 8.

**Scheme 8.**

*The general classification of lipids*



Note. Adaptated from: Food Analysis Fourth Edition - Chapter 8: Fat Analysis [Book], Springer New York – Nielsen Suzanne – Min & Ellefson, 2010 ([https://doi.org/10.1007/978-1-4419-1478-1\\_8](https://doi.org/10.1007/978-1-4419-1478-1_8)). Copyright by Springer Science+Business Media, LLC 2010. CC BY-NC-SA 4.0.

Accurate nutrition labeling depends on accurate and precise quantitative and qualitative analysis of lipids in foods. In addition, they allow us to know whether the food we are about to consume complies with manufacturing and identity standards (Pomeranz, 2013).

To calculate the amount of fats by the Soxhlet method, a semi-continuous extraction method, the following calculation is used (Min & Ellefson, 2010):

$$\% \text{ Fat on dry weight basis} = \left( \frac{\text{g of fat in sample}}{\text{g of dried sample}} \right) \times 100 \quad [3]$$

### 3.2.4. Protein Analysis (Chang, 2010)

An abundant component of cells are proteins, which are fundamental in cell structure and biochemical functions, except for storage proteins. These proteins are very complex and vary in size (from 5000 to more than 1 million Daltons).

Proteins can be classified according to their structure, biological function, composition or solubility properties. The basic building blocks of proteins are the alpha-amino acids; peptide linkages are those that bind these amino acid residues in a protein. In addition, the most distinctive element present in proteins is nitrogen, which makes the analysis of proteins in foods difficult, because the non-protein nitrogen can preferentially come from small peptides, free amino acids, phospholipids, nucleic acids, porphyrin, amino sugars, alkaloids, uric acid, urea, ammonium ions, and some vitamins. The importance of protein analysis in food and guidance on when to perform protein analysis is described in Scheme 9. The calculations for calculating the amount of protein in food are as follows:

$$\text{Moles of HCL} = \text{moles of NH}_3$$

$$\text{Moles of HCL} = \text{moles of N in the sample}$$

Nitrogen must be extracted from the sample in a reagent blank.

$$\% N = N_{HCl} \times \frac{\text{Corrected acid volume}}{\text{g of sample}} \times \frac{14 \text{ g N}}{\text{mol}} \times 100 \quad [4]$$

Where:

NHCL = Normality of HCl

Corrected acid vol. = (ml standard acid for sample) – (ml standard acid for blank)

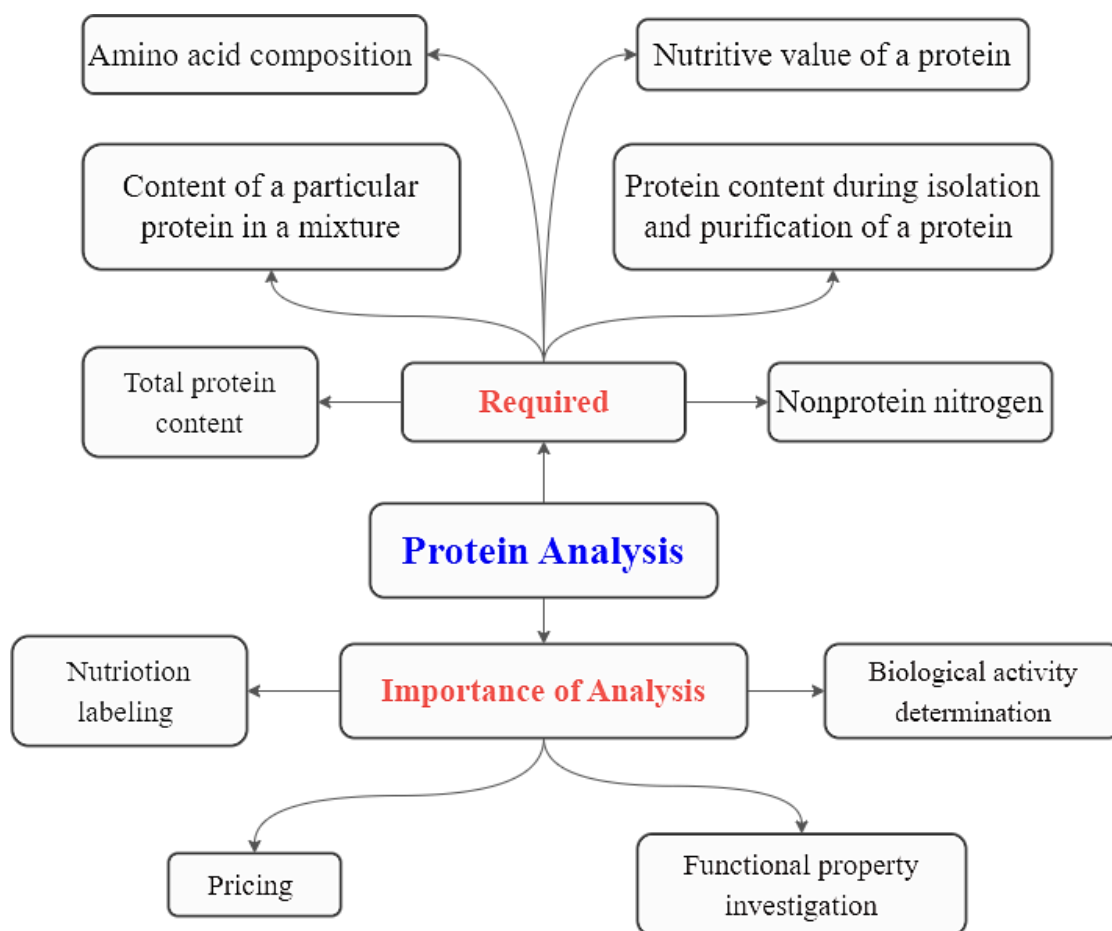
14 = Atomic weight of nitrogen

The percentage of N must be converted into percentage of crude protein, using a factor. Most proteins contain 16% N. The conversion factor is percent N in protein (%N protein) divided by 100 (100 /%N protein = conversion factor).

$$\frac{\% N}{0.16} = \% \text{ protein} \quad [5]$$

$$\% N \times \text{conversion factor} = \% \text{ protein} \quad [6]$$

**Scheme 9. Importance of Protein Analysis**



Note. Adapted from: Food Analysis Fourth Edition - Chapter 9: Protein Analysis [Book], Springer New York – Nielsen Suzanne – Chang Sam, 2010 ([https://doi.org/10.1007/978-1-4419-1478-1\\_9](https://doi.org/10.1007/978-1-4419-1478-1_9)). Copyright by Springer Science+Business Media, LLC 2010. CC BY-NC-SA 4.0.

**3.2.5. Carbohydrate Analysis (BeMiller, 2010)**

One source of energy from food is carbohydrates, which, in order to be digested, must be converted into monosaccharides, which influence physiological processes such as dietary fibers. In the human diet, 70% of the caloric value is carbohydrates. In



addition, excluding lactose, which comes from milk, all carbohydrates are of vegetable origin. Similarly, D-glucose and D-fructose, known as simple sugars (monosaccharides), are found in large quantities.

In alimentary industry, carbohydrates contribute to bulk, viscosity, body, emulsion stability, water-holding capacity, foaming, flavor, freeze-thaw stability, texture and satiety.

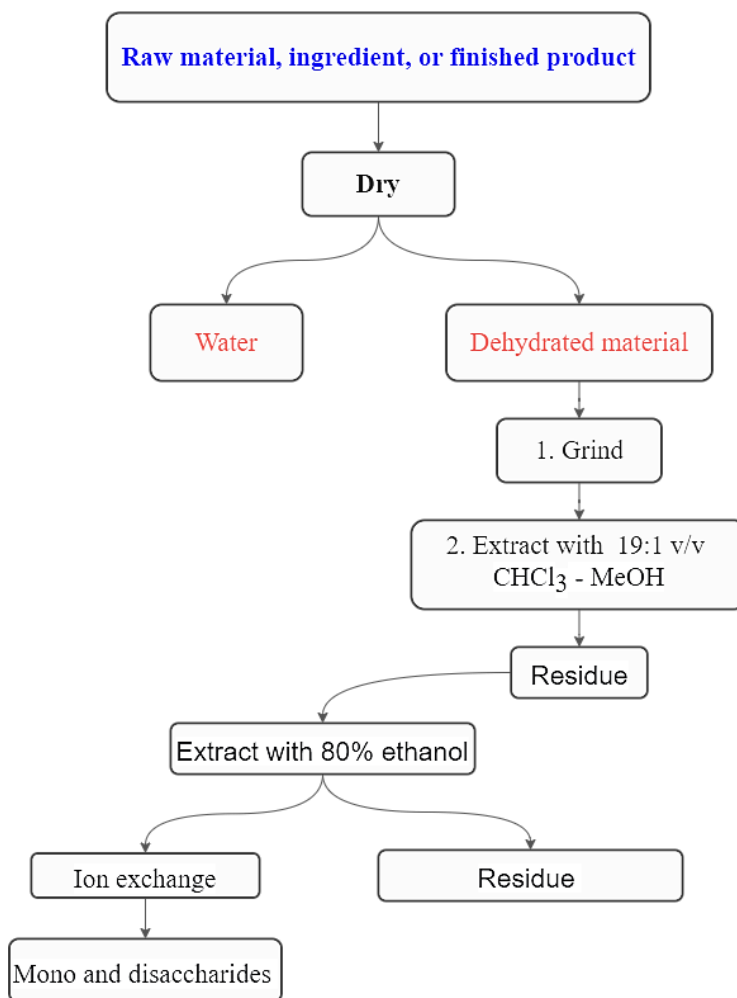
In the small intestine, the only carbohydrates that can be absorbed are monosaccharides. While oligo- and polysaccharides must be hydrolyzed to monosaccharides, so that they can be absorbed and subsequently used. Humans with enzymes found in the small intestine can digest sucrose, lactose, maltooligosaccharides, maltodextrins and starch. In nature, about 90% of carbohydrates are found in the form of polysaccharides.

In carbohydrate analysis, qualitative and quantitative tests are used to determine the composition of ingredients and foods. Qualitative analyses are those that ensure the exact composition of ingredient or food labels. Quantitative analyses are those that ensure that they are listed in the correct order. Both analyses serve as authenticators of ingredients and foods, because they serve to detect if there is any adulteration in the food.

Scheme 10 shows the flow chart for sample preparation and extraction of mono- and disaccharides. In addition, to calculate the total soluble carbohydrate (Kuklinski, 2003) content, a difference is made between the sum total of the values obtained for moisture, ash, protein and fat and the initial weight of the sample (Caravaca et al., 2003).

$$\% \text{ Carbohydrate} = 100 - (\% \text{ moisture} + \% \text{ ash} + \% \text{ fat} + \% \text{ protein}) \quad [7]$$

**Scheme 10.** Sample preparation and extraction of mono- and disaccharides



Note. Adapted from: Food Analysis Fourth Edition - Chapter 9: Protein Analysis [Book], Springer New York – Nielsen Suzanne – BeMiller, 2010 ([https://doi.org/10.1007/978-1-4419-1478-1\\_10](https://doi.org/10.1007/978-1-4419-1478-1_10)). Copyright by Springer Science+Business Media, LLC 2010. CC BY-NC-SA 4.0.

**3.3. Food analysis of *R. palmarum* larvae**

The data obtained for the degree of saturation of skin oils and the digestive fat content of *R. palmarum* larvae (expressed in percentages of g/100 g of total fat) are presented below (see table 5). In addition, the proximal composition (physicochemical parameters) of *R. palmarum* larvae is presented (see table 6). The fatty acid profile found in *R. palmarum* larvae by the authors mentioned at the beginning of the chapter is also presented (see table 7).

It is important to mention that the larvae of *R. palmarum*, used in different investigations carried out by the authors mentioned at the beginning of the chapter,

come from different species of palms; this is due to the fact that the type of palm influences the content of fatty acids found in the *R. palmarum* larvae. As shown in Table 5, the palm species from which the *R. palmarum* larvae were extracted for food analysis were: *Oenocarpus bataua* var. *bataua*, *Jacaratia digitata*, *Mauritia flexuosa*, *Bactris gasipaes* and *Elaeis guineensis*. For the proximate composition analysis, the palm species from which the *R. palmarum* larvae were obtained were *Mauritia flexuosa*, *Bactris gasipaes*, *Oenocarpus bataua* var. *bataua* and *Jacaratia digitata*. For the analysis of the fatty acid profile present in the *R. palmarum* larvae, the chontacurs were extracted from the following palm species: *Elaeis guineensis*, *Mauritia flexuosa*, *Bactris gasipaes*, *Oenocarpus bataua* var. *bataua* and *Jacaratia digitata*. In addition, Batalha et al. cultured the larvae of *R. palmarum* in the laboratory for analysis by sex. Meanwhile, Sancho et al. and Vilharva et al. collected *R. palmarum* larvae in the wild without taking into account the origin of the palm.

### 3.3.1. Fatty acid composition of *R. palmarum* larval oil

As can be seen in Table 5, *R. palmarum* larvae present high amounts of unsaturated and saturated fatty acids. The values vary due to the palm from which the *R. palmarum* larvae were extracted.

**Table 5.**

*Degree of saturation of skin and digestive fat content oils from Rhynchophorus palmarum larvae, expressed in percentages of g/100 g of total fat*

Acid Fatty (%)	Type of Palm										
	<i>O. Bataua</i>		<i>J. Digitata</i>		<i>Mauritia Flexuosa</i>			<i>Bactris gasipaes</i>		<i>Elaeis Guineensis</i>	
	Santivañez & Paucar, 2021			Vargas et al., 2013		Espinosa et al., 2020		Sancho et al., 2015	Ahipo Dué et al., 2009		
				Skin	DFC				Skin	DFC	
TUFA	44,48	45,77	48,08	46,90	45,56	Not reported		No reported	54,90	55,00	
TFSA	55,51	53,03	50,82	53,10	54,44	56,21	55,70	36,8	45,06	44,97	
MUFA	43,40	44,73	44,99	43,85	42,58	41,27	42,05	60,4	47,53	48,77	
PUFA	1,10	1,05	3,10	2,05	2,98	2,88	2,65	1,5	7,37	6,24	

Where:

- DFC** Digestive fat content
- TUFA** Total unsaturated fatty acid
- TFSA** Total saturated fatty acid
- MUFA** Monounsaturated fatty acid
- PUFA** Poly unsaturated fatty acid

### 3.3.2. Proximal composition of *Rhynchophorus palmarum* larvae

As can be seen in Table 6, the amount of total fat presented by *R. palmarum* is relevant, indicating that they are a great source of energy. In addition, insects that are in the larva stage accumulate the greatest amount of fat, in order to use it while they go through their metamorphosis to become beetles (Espinosa et al., 2020).

**Table 6.**

*Proximal chemical composition (100g) of R. palmarum larvae*

Physicochemical parameters	Content 100 g							
	Type of Palm							
	<i>M. Flexuosa</i>					<i>B. Gasipaes</i>	<i>O. Batauta</i>	<i>J. Digitata</i>
	Sancho et al., 2015	Espinosa et al., 2020	Maceda & Chiñi, 2021	Cerda et al., 2001	Vargas et al., 2013	Espinosa et al., 2020	Maceda & Chiñi, 2021	Maceda & Chiñi, 2021
Ash	0,64	0,85	0,5	2,1	1,38	0,76	0,3	1,1
Carbohydrates	1,53	1,44	7,3	8,2	7,81	1,71	6,56	4,4
Moisture	69,88	66	67,2	57,33	71,50	65,20	69,5	94,1
Protein	3,84	8,68	0,6	3,87	13,06	8,72	0,6	0,3
Total fat	24,11	23,02	24,40	28,5	6,31	23,61	23,04	19,42

### 3.3.3. Fatty acid composition of *R. palmarum* larvae sorted by palm type

As can be seen in Table 7, the fatty acid profile depends on the palm species from which the *R. palmarum* larvae were obtained or whether they were cultured in wild or laboratory media. In addition, the fatty acid composition is given as a percentage based on g/100 g of the total fatty acids in the skin oil and digestive fat content of *R. palmarum* larvae.

All the studies that have been carried out show that *R. palmarum* larvae have essential fatty acids for the organism, such as oleic, linolenic and linoleic acids in significant quantities. In addition, since palmitic oil is present in large quantities, it can be used as an energetic food. In industry, palmitic oil is used for the manufacture of margarines and soaps (Vargas et al., 2013)

**Table 7.**

*Fatty acid composition of skin oil and digestive fat content of Rhynchophorus palmarum larvae according to the type of palm of origin (g/100 g of the total fatty acids)*

Fatty Acid (%)	Laboratory		Wild Mode		E. Guineensis	M. Flexuosa				B. Gasipaes	O. Batauta	J. Digitata
	Batalha et al., 2020		Sancho et al., 2015	Vilharva et al., 2021	Ahipo Dué et al., 2009	Espinosa et al., 2020	Vargas et al., 2013		Maceda & Chiñi, 2021	Espinosa et al., 2020	Maceda & Chiñi, 2021	Maceda & Chiñi, 2021
	Skin	DFC	Skin + DFC	Skin + DFC	Skin + DFC	Skin + DFC	Skin	DFC	Skin + DFC	Skin + DFC	Skin + DFC	Skin + DFC
C:8	-----	-----	-----	-----	-----	-----	-----	-----	-----	-----	-----	0,26
C:10	-----	-----	-----	-----	-----	-----	-----	-----	-----	-----	-----	0,29
C:12	-----	-----	0,1	0,1	-----	-----	-----	-----	-----	-----	-----	0,28
C:14	-----	2,47	2,8	5,4	2,54	3,11	1,91	2,27	2,08	3,85	2,11	2,56
C:16	-----	1,90	28,0	42,7	40,44	45,30	41,78	43,65	41,81	45,45	44,56	43,91
C: 16:1	5,35*	37,06	1,2	6,3	-----	1,79	0,75	1,01	1,45	3,10	1,34	1,72
C:17	-----	-----	-----	-----	-----	-----	-----	-----	0,26	-----	-----	-----
C:18	-----	-----	5,9	3,1	1,99	7,80	9,41	8,52	5,95	6,40	8,13	5,16
C: 18:1w-9	11,75*	38,33	59,2	40	46,71	38,70	43,10	41,57	43,54	38,15	42,06	43,01
C 18:2w-6	5,37*	4,77	1,1	1,1	6,24	1,83	2,00	1,93	1,96	1,60	0,67	0,76
C 18:3w-3	-----	-----	0,3	-----	-----	1,05	-----	-----	1,14	1,05	0,43	0,29
C 18:2	-----	-----	-----	-----	-----	-----	1,05	1,05	-----	-----	-----	-----
C:20	0,06	0,73	-----	0,9	-----	0,78	-----	-----	0,72	0,80	0,72	0,58
C:21	0,49	-----	-----	-----	-----	-----	-----	-----	-----	-----	-----	-----
C:22	60,21*	-----	-----	-----	-----	-----	-----	-----	-----	-----	-----	-----
C:23	0,22	-----	-----	-----	-----	-----	-----	-----	-----	-----	-----	-----

\* Fatty acid present only in female *R. palmarum* larvae.

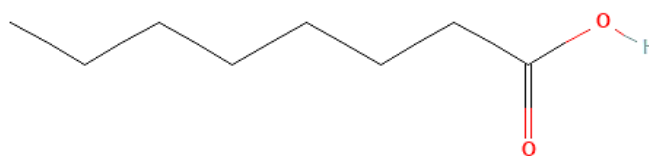
### 3.4. Medical properties of fatty acids identified in *R. palmarum* larvae.

#### 3.4.1. Caprylic acid (Octanoic acid)

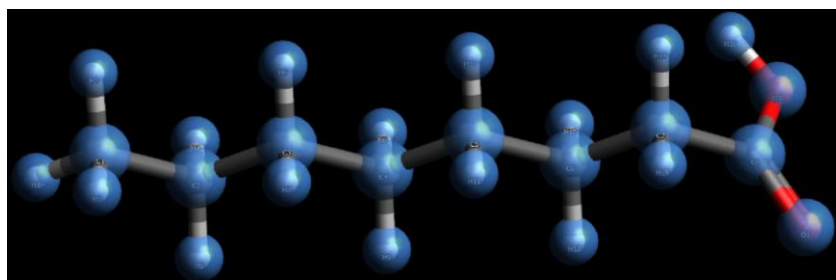
Caprylic fatty acid (see Figure 18) was discovered bound to ghrelin in the stomach of a purified rat (Rioux, 2016). It is a short-chain saturated fatty acid (C:8) (Nair et al., 2005), which is part of the medium-chain saturated fatty acids (MCFAs) (Lemarié et al., 2016). This short-chain fatty acid is found naturally in palm kernel, coconut oil (Lemarié et al., 2016), bovine milk, and breast milk (Jensen et al., 1990). Furthermore, in 1995 a group of scientists, while investigating the antimicrobial activity of lipids present in breast milk, bovine milk and infant formula, discovered that both caprylic fatty acid and monocaprylin, monoglyceride, are effective in disabling infant pathogens. The viruses reported to be disabled by caprylic acid are: respiratory syncytial virus, Group B streptococci, herpes simplex virus and *Haemophilus Influenzae* (Charles et al., 1995).

#### Figure 18.

Caprylic acid, PubChem CID: 379



A.



B.

Note. **A.** 2D structure. **B.** 3D structure is built in the Avogadro program, in order to add the protonation state to the molecule and then optimize it for molecular docking. Retrieved from: **A.** PubChem Compound Summary for CID 379, Octanoic acid [Graphical Representation], PubChem, 2022 (<https://pubchem.ncbi.nlm.nih.gov/compound/Octanoic-acid>). Copyright by National Library of Medicine - National Center for Biotechnology Information - PubChem. CC-BY 4.0.

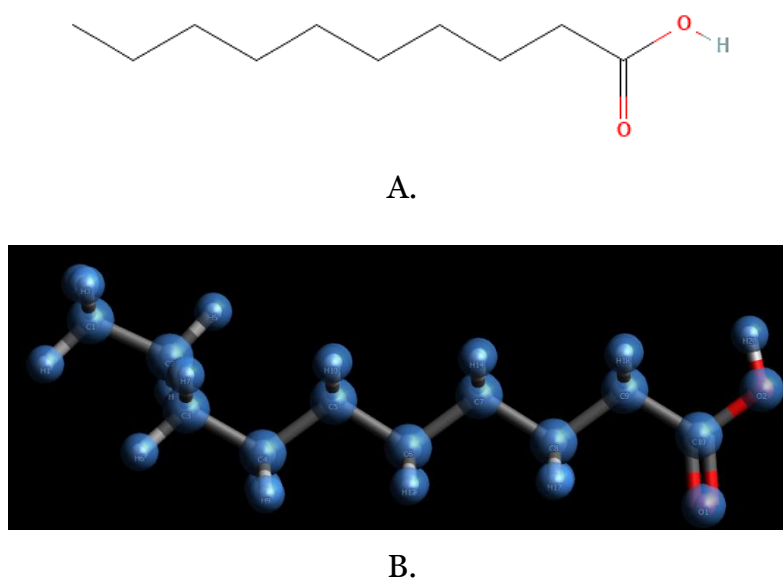
### 3.4.2. Capric Acid (Decanoic acid)

Found naturally in coconut oil and palm oil (Katdare et al., 2019), capric acid (C:10) (see Figure 19) is a saturated straight chain fatty acid belonging to the medium chain fatty acid (MCFA) group. Capric acid is used as an anti-inflammatory and antibacterial agent as well as a plant and human metabolite (National Center for Biotechnology Information, 2022).

Capric oil has been reported to possess divergent immunomodulatory propensities, providing positive regulation of GPR84 and PPAR $\gamma$  (proteins associated with immune responses) (Sam et al., 2021). In addition, it has been reported as a fuel for treating neutrophilic disorders (Gagnon et al., 2018), due to boosting hepatic production of ketone bodies, elevating mitochondrial proton leakage, being involved in metabolic coupling of neurons, astrocytes (Andersen et al., 2021) and in human osteoblastic cells (MG63) (Venugopal et al., 2017). In turn, it has been reported to mitigate properties of porcine epidemic diarrhea virus (PEDV), thus showing an antiviral effect (Gebhardt et al., 2020). In addition, the growth of *Candida albicans* is inhibited when in contact with capric acid (Bergsson et al., 2001).

#### Figure 19.

Capric acid, PubChem CID: 2969



Note. **A.** 2D structure. **B.** 3D structure is built in the Avogadro program, in order to add the protonation state to the molecule and then optimize it for molecular docking. Retrieved from: **A.** PubChem Compound Summary for CID 2969, Decanoic acid [Graphical Representation], PubChem, 2022

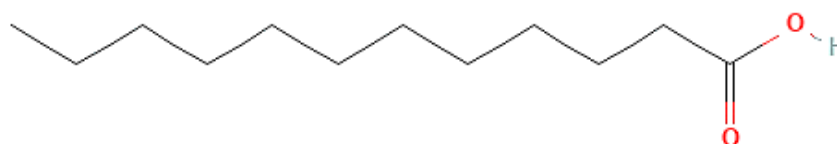
(<https://pubchem.ncbi.nlm.nih.gov/compound/Decanoic-acid>). Copyright by National Library of Medicine - National Center for Biotechnology Information - PubChem. CC-BY 4.0.

### 3.4.3. Lauric Acid (Dodecanoic acid)

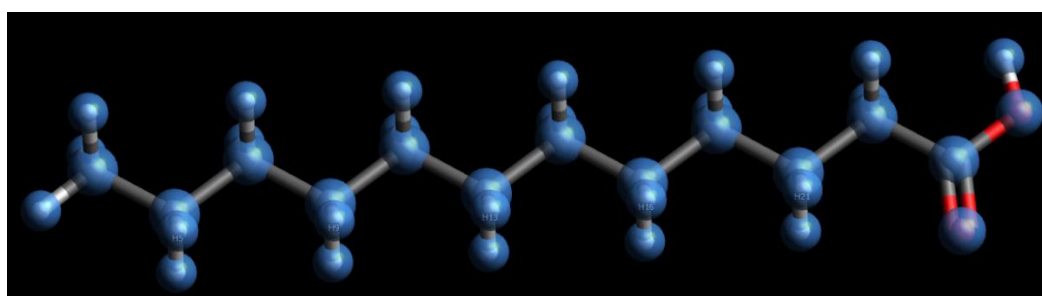
Both coconut oil and palm oil have lauric acid (C:12) (see Figure 20) as their main component (Dayrit, 2015). Which is a fatty acid with a chain of twelve carbon atoms (National Center for Biotechnology Information, 2022), making it a medium chain triglyceride (MCT) (Dayrit, 2015). Lauric acid is used against gram-positive bacteria (*S. aureus*) (Lieberman et al., 2006), viruses (vesicular stomatitis [VSV], herpes simplex [HSV], visna [VV]) and fungi, such as *C. albicans* (Nitbani et al., 2022).

#### Figure 20.

Lauric acid, PubChem CID: 3893



A.



B.

Note. **A.** 2D structure. **B.** 3D structure is built in the Avogadro program, in order to add the protonation state to the molecule and then optimize it for molecular docking. Retrieved from: **A.** PubChem Compound Summary for CID 3893, Lauric acid [Graphical Representation], PubChem, 2022 (<https://pubchem.ncbi.nlm.nih.gov/compound/Lauric-acid>) Copyright by National Library of Medicine - National Center for Biotechnology Information - PubChem. CC-BY 4.0.

### 3.4.4. Myristic Acid (Tetradecanoic acid)

Found in butterfat, coconut and palm oil (Kalaimathi et al., 2022), myristic acid (see Figure 21) (C:14) is a long-chain saturated fatty acid (National Center for Biotechnology Information, 2022). Reports indicate that in liver and blood plasma it increases the concentration of docosahexaenoic acid (DHA) and eicosapentaenoic acid

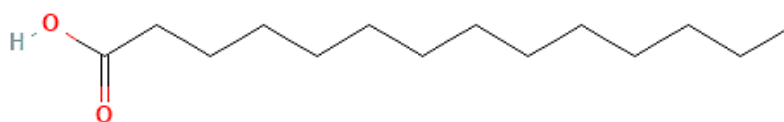


(EPA) with increasing myristic acid intake (Balvers et al., 2010). Also, in brain tissues, it increases DHA and arachidonic acid (AA) concentrations (Kalaimathi et al., 2022). Similarly, myristic acid, along with other long-chain fatty acids, regulate embryonic neural stem cells (eNSCs) (Mahmoudi et al., 2019).

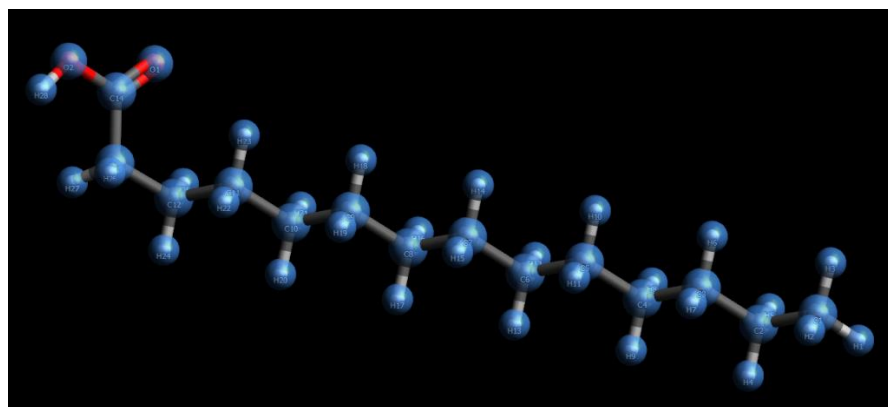
Another activity reported for myristic acid is the inhibition of biofilm formation in bacteria and fungi (Kim et al., 2021), demonstrating antimicrobial and antifungal activity. Antioxidant activity is also reported (Mohd et al., 2021), against oxidative damage produced by diabetes mellitus in the testicles (Henry et al., 2002). In addition, its consumption attenuates hyperglycemia, because it increases glucose uptake in skeletal muscles (Takato et al., 2017).

**Figure 21.**

*Myristic acid, PubChem CID: 11005*



A.



B.

Note. **A.** 2D structure. **B.** 3D structure is built in the Avogadro program, in order to add the protonation state to the molecule and then optimize it for molecular docking. Retrieved from: **A.** PubChem Compound Summary for CID 11005, Myristic acid [Graphical Representation], PubChem, 2022 (<https://pubchem.ncbi.nlm.nih.gov/compound/Myristic-acid>). Copyright by National Library of Medicine - National Center for Biotechnology Information - PubChem. CC-BY 4.0.

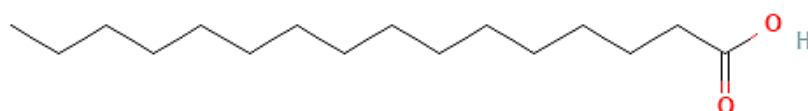
### 3.4.5. Palmitic Acid (Hexadecanoic acid)

Found in meats, cheese, butter, milk, palm oil and palm kernel oil (National Center for Biotechnology Information, 2022), palmitic acid (C:16) is the most common saturated fatty acid found in microorganisms, plants and animals (Gunstone et al., 2007); it is the most common fatty acid found in the human body (Carta et al., 2017).

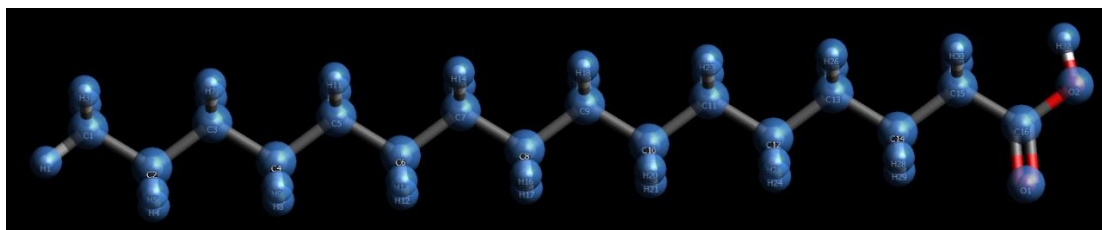
Discovered in saponified palm oil in 1840 (Frémy, 1842), palmitic fatty acid (see Figure 22) is often considered harmful to health because it favors the development of obesity and related diseases, such as insulin resistance, as well as its significant increase in the hypothalamus in mice, altering insulin signaling in neurons (Ávalos et al., 2022). But not all, are disadvantages for palmitic fatty acid, because it is an essential component in cell membranes, as well as in transport and secretory lipids. It also plays indispensable roles in palmitoylated signaling molecules as well as in protein palmitoylation (Agostonia et al., 2016). Furthermore, it has been shown that in human umbilical vein endothelial cells (HUVEC), C:16 increased the expression of ANGPTL4, a protein involved in the regulation of angiogenesis and in the arrest of cardiac diseases (Zhan et al., 2022)

#### Figure 22.

Palmitic acid, PubChem CID: 985



A.



B.

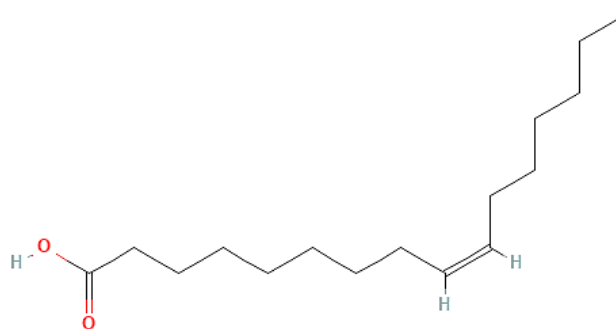
Note. **A.** 2D structure. **B.** 3D structure is built in the Avogadro program, in order to add the protonation state to the molecule and then optimize it for molecular docking. Retrieved from: **A.** PubChem Compound Summary for CID 985, Palmitic Acid [Graphical Representation], PubChem, 2022 (<https://pubchem.ncbi.nlm.nih.gov/compound/Myristic-acid>). Copyright by National Library of Medicine - National Center for Biotechnology Information - PubChem. CC-BY 4.0.

### 3.4.6. Palmitoleic Acid ([Z]-Hexadec-9-enoic-acid)

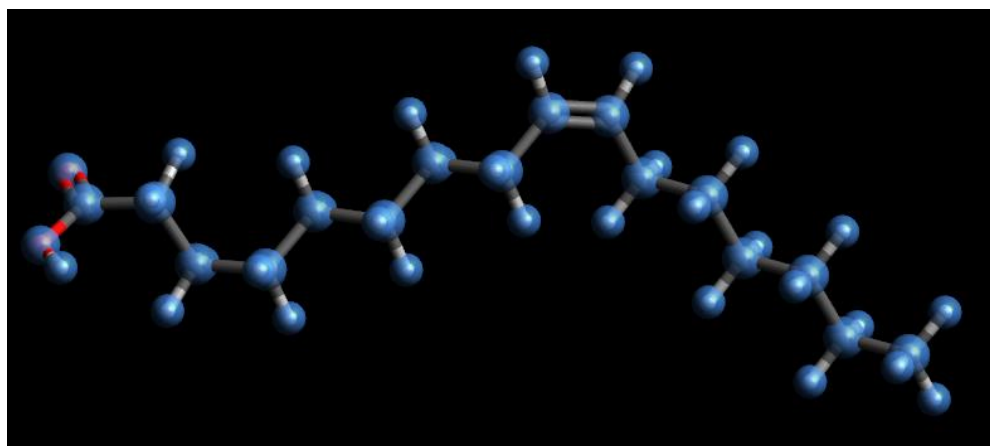
Found in *Pterodon emarginatus* and *Dryopteris assimilis* (National Center for Biotechnology Information, 2022), palmitoleic acid (C<sub>16</sub>:1n-7) (see Figure 23) is a monounsaturated fatty acid, in the human body, it is found in serum, adipose tissue and liver (Frigolet & Gutiérrez-Aguilar, 2017). Palmitoleic acid has been reported to have antimicrobial activity against pathogenic gram-negative bacteria as well as gram-positive bacterial infections (Wille & Kydonieus, 2003).

#### Figure 23.

Palmitic Acid, PubChem CID: 445638



A.



B.

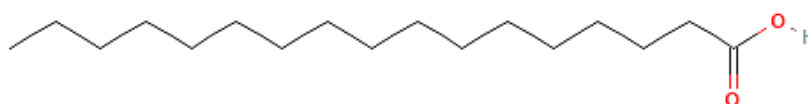
Note. **A.** 2D structure. **B.** 3D structure is built in the Avogadro program, in order to add the protonation state to the molecule and then optimize it for molecular docking. Retrieved from: **A.** PubChem Compound Summary for CID 445638, Palmitoleic acid [Graphical Representation], PubChem, 2022 (<https://pubchem.ncbi.nlm.nih.gov/compound/Palmitoleic-acid>). Copyright by National Library of Medicine - National Center for Biotechnology Information - PubChem. CC-BY 4.0.

### 3.4.7. Margarinic Acid (Heptadecanoic acid)

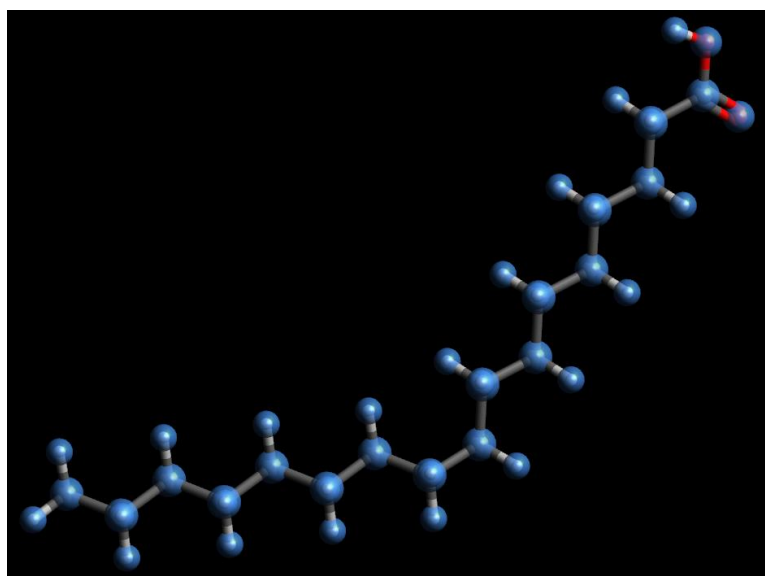
Found in ruminant milk fat (National Center for Biotechnology Information, 2022) and in *M. flexuosa* palm (Maceda & Chiñi, 2021), margarinic acid (see Figure 26), an odd long-chain saturated fatty acid (Xu et al., 2019), serves as a biomarker for milk fat intake (Pfeuffer & Jaudszus, 2016). In addition, margarinic fatty acid has been shown to be an effective agent against non-small cell lung carcinomas (NSCLC), because it prevents cell migration and proliferation; at the same time, it promotes cell apoptosis of PC-9 (derived from a human adenocarcinoma of the lung tissue that remains differentiated) (Xu et al., 2019).

#### Figure 24.

Margarinic acid, PubChem CID: 10465



A.



B.

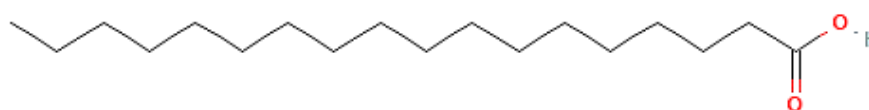
Note. A. 2D structure. B. 3D structure is built in the Avogadro program, in order to add the protonation state to the molecule and then optimize it for molecular docking. Retrieved from: A. PubChem Compound Summary for CID 10465, Heptadecanoic acid [Graphical Representation], PubChem, 2022 (<https://pubchem.ncbi.nlm.nih.gov/compound/Heptadecanoic-acid>). Copyright by National Library of Medicine - National Center for Biotechnology Information - PubChem. CC-BY 4.0.

### 3.4.8. Stearic Acid (Octadecanoic acid)

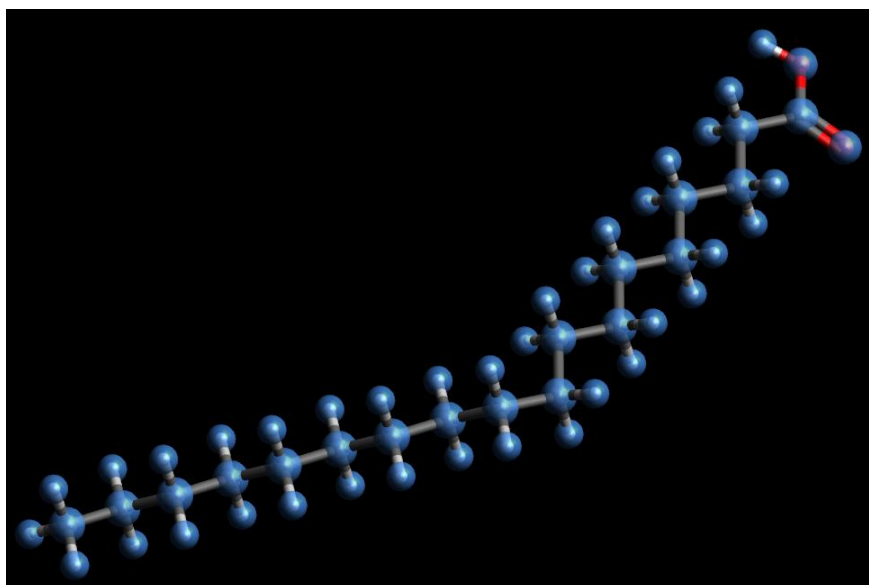
Found in various animals and plants (National Center for Biotechnology Information, 2022), stearic acid (C:18) (see Figure 25) is a saturated fatty acid (Loften et al., 2014), which serves to prevent alcohol-induced liver damage by improving intestinal barrier and regulating intestinal microbiota (GM) (Nie et al., 2022).

#### Figure 25.

Stearic acid, PubChem CID: 5281



A.



B.

Note. **A.** 2D structure. **B.** 3D structure is built in the Avogadro program, in order to add the protonation state to the molecule and then optimize it for molecular docking. Retrieved from: **A.** PubChem Compound Summary for CID 5281, Stearic acid [Graphical Representation], PubChem, 2022 (<https://pubchem.ncbi.nlm.nih.gov/compound/Stearic-Acid>). Copyright by National Library of Medicine - National Center for Biotechnology Information - PubChem. CC-BY 4.0.

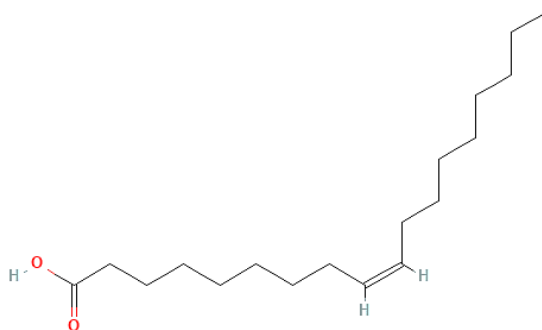
### 3.4.9. Oleic Acid (cis-9-Octadecenoic acid)

Found in *Gladiolus italicus*, *Prunus mume* (National Center for Biotechnology Information, 2022) and other vegetable fats and oils (Liebert, 1987), monounsaturated fatty oleic acid (18:1 cis-9) (see Figure 26) possessing a double bond

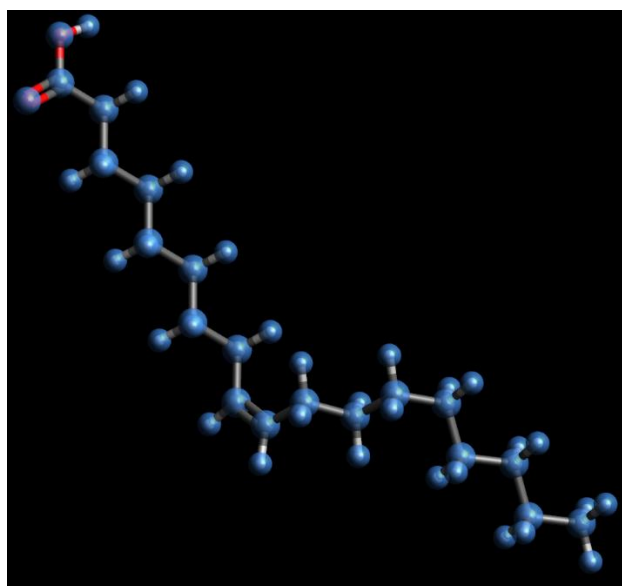
at C-9 (Chaves et al., 2020). It has been reported that oleic acid serves to modulate various biological functions; as well as, in aiding wound healing (Sales-Campos et al., 2013). Oleic acid also has anti-inflammatory potential (Carrillo et al., 2012), lowers systolic blood pressure and myocardial infarction (Karacor & Cam, 2015).

**Figure 26.**

*Oleic acid, PubChem CID: 445639*



A.



B.

Note. **A.** 2D structure. **B.** 3D structure is built in the Avogadro program, in order to add the protonation state to the molecule and then optimize it for molecular docking. Retrieved from: **A.** PubChem Compound Summary for CID 445639, Oleic acid [Graphical Representation], PubChem, 2022 (<https://pubchem.ncbi.nlm.nih.gov/compound/Oleic-acid>). Copyright by National Library of Medicine - National Center for Biotechnology Information - PubChem. CC-BY 4.0.

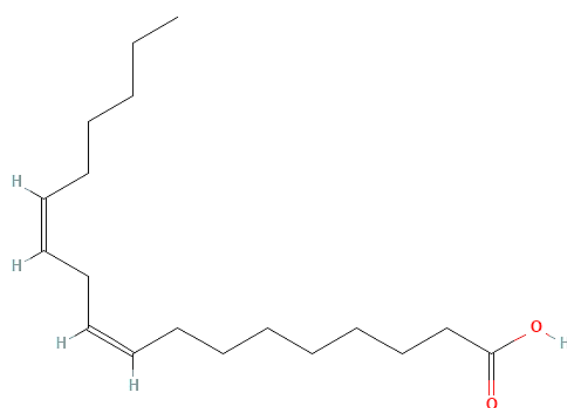
**3.4.10. Linoleic Acid ([9Z-12Z]-octadeca-9,12-dienoic acid)**

Found mainly in vegetable oils, linoleic acid (C<sub>18</sub>:2 Δ<sup>9,12</sup>) (see Figure 27) is an essential polyunsaturated fatty acid (National Center for Biotechnology Information,

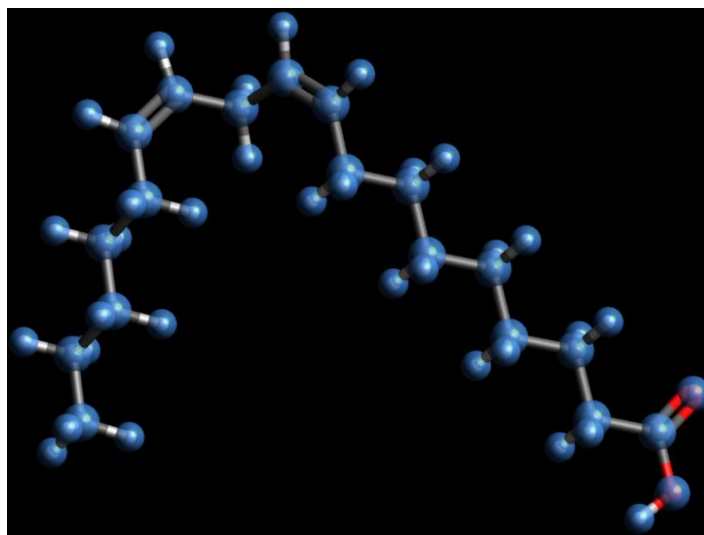
2022), has pro-inflammatory properties (Choque et al., 2014), resulting in adverse health effects (Jandacek, 2017). Despite this, linoleic acid is used to treat skin disorders related to its deficiency. Furthermore, due to the composition of linoleic acid, it confers a certain degree of fluidity to the lipid membrane and in turn participates in cell signaling (Whelan & Fritsche, 2013). It has also been reported that both innate and adaptive immune function is modulated by linoleic acid (O'Shea et al., 2004).

**Figure 27.**

*Linoleic acid, PubChem CID: 5280450*



**A.**



**B.**

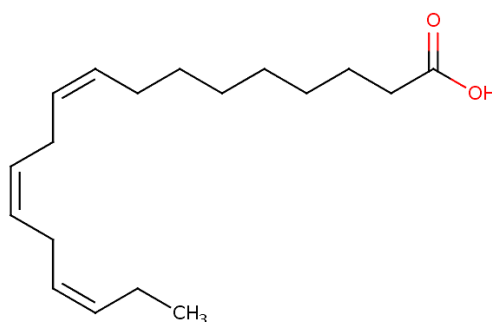
Note. **A.** 2D structure. **B.** 3D structure is built in the Avogadro program, in order to add the protonation state to the molecule and then optimize it for molecular docking. Retrieved from: **A.** PubChem Compound Summary for CID 5280450, Linoleic acid [Graphical Representation], PubChem, 2022 (<https://pubchem.ncbi.nlm.nih.gov/compound/Linoleic-acid>). Copyright by National Library of Medicine - National Center for Biotechnology Information - PubChem. CC-BY 4.0.

### 3.4.11. Alpha-Linolenic Acid

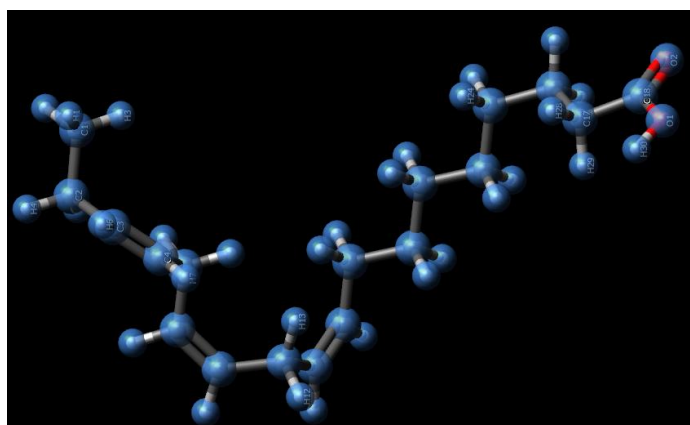
Natural origin, alpha-linolenic acid (C:18) (see Figure 28) is an essential polyunsaturated omega-3 fatty acid (Stark et al., 2008), with 3 cis double bonds; it has anticancer, metabolic anti-syndrome and intestinal flora regulating functions (Yuan et al., 2021). In addition, alpha-linolenic acid serves as a neuroprotector, because it protects the brain from strokes (Blondeau et al., 2015). There are also records that alpha-linolenic acid improves cardiovascular functions, as well as regulates blood pressure (Gogna et al., 2022), preventing and coping with coronary heart disease (Lorgeril & Salen, 2004).

#### Figure 28.

*Alpha-Linolenic acid, PubChem CID: 184021992*



A.



B.

Note. **A.** 2D structure. **B.** 3D structure is built in the Avogadro program, in order to add the protonation state to the molecule and then optimize it for molecular docking. Retrieved from: **A.** PubChem Substance Record for SID 175267648, alpha-linolenic acid [Graphical Representation], PubChem, 2022 (<https://pubchem.ncbi.nlm.nih.gov/substance/175267648>). Copyright by National Library of Medicine - National Center for Biotechnology Information - PubChem. CC-BY 4.0.

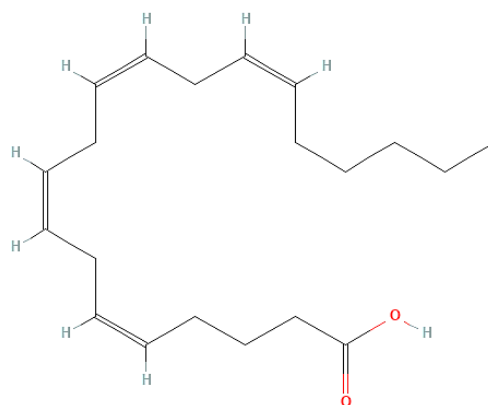


### 3.4.12. Arachidonic acid

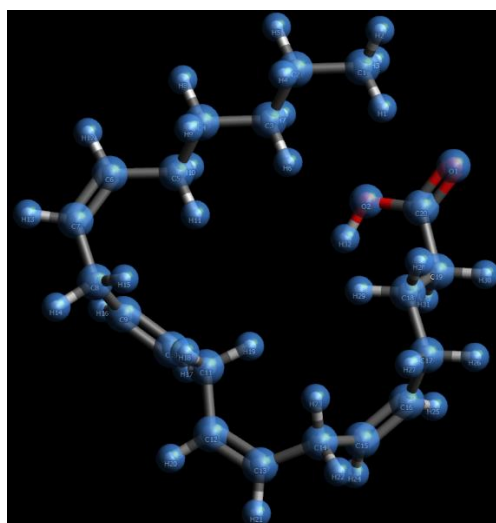
Found in animal and human fat as well as in liver, glandular organs and brain (National Center for Biotechnology Information, 2022), arachidonic acid (C<sub>20</sub>:4(ω-6)) (see Figure 29) is a polyunsaturated fatty acid with four cis double bonds (Tallima & Ridi, 2017); it participates, as a precursor, in the biosynthesis of thromboxanes, Bosetti leukotrienes and prostaglandins, thus participating in the functions of vasodilator, vasoconstrictor and bronchoconstriction (Davies, 2008). In addition, there are records that arachidonic acid participates in cardiovascular diseases and inflammatory diseases, as well as in carcinogenesis, asthma and arthritis (Wang et al., 2021). Also, polyunsaturated fatty acid is involved in cell signaling to regulate TRP channel activities (TRPV1 and TRPV4) (Luo & Hu, 2014)

#### Figure 29.

Arachidonic acid, PubChem CID: 444899



A.



B.

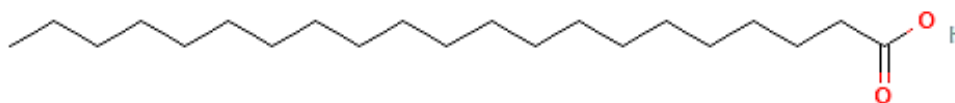
Note. **A.** 2D structure. **B.** 3D structure is built in the Avogadro program, in order to add the protonation state to the molecule and then optimize it for molecular docking. Retrieved from: **A.** PubChem Compound Summary for CID 444899, Arachidonic acid [Graphical Representation], PubChem, 2022 (<https://pubchem.ncbi.nlm.nih.gov/compound/Arachidonic-acid>). Copyright by National Library of Medicine - National Center for Biotechnology Information - PubChem. CC-BY 4.0.

### 3.4.13. Heneicosanoic acid

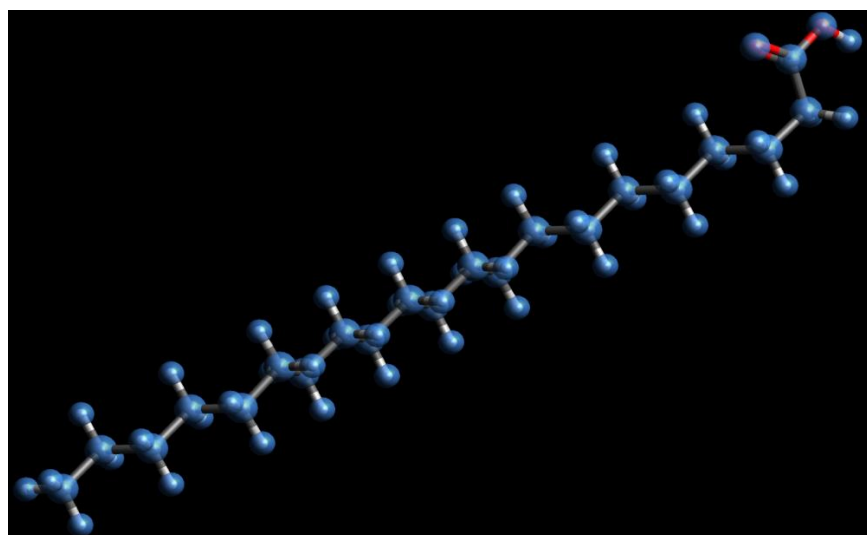
Present in *Rhizophora apiculata*, *Aloe africana* and other plant products (Batalha et al., 2020), heneicosanoic acid (C:21) (see Figure 30) is a long-chain saturated fatty acid (National Center for Biotechnology Information, 2022); it is used as a biomarker because it is unusual in biological systems (Universal Biologicals, 2022). In addition, heneicosanoic acid has been shown to have inhibitory effects on the p53 protein. (Iijima et al., 2006).

#### Figure 30.

Heneicosanoic acid, PubChem CID: 16898



A.



B.

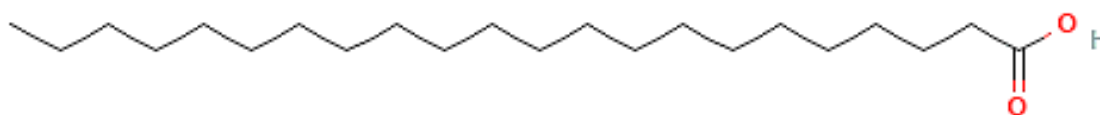
Note. **A.** 2D structure. **B.** 3D structure is built in the Avogadro program, in order to add the protonation state to the molecule and then optimize it for molecular docking. Retrieved from: **A.** PubChem Compound Summary for SID 16898, Heneicosanoic acid [Graphical Representation], PubChem, 2022 (<https://pubchem.ncbi.nlm.nih.gov/compound/Heneicosanoic-acid>). Copyright by National Library of Medicine - National Center for Biotechnology Information - PubChem. CC-BY 4.0.

### 3.4.14. Behenic acid (Docosanoic acid)

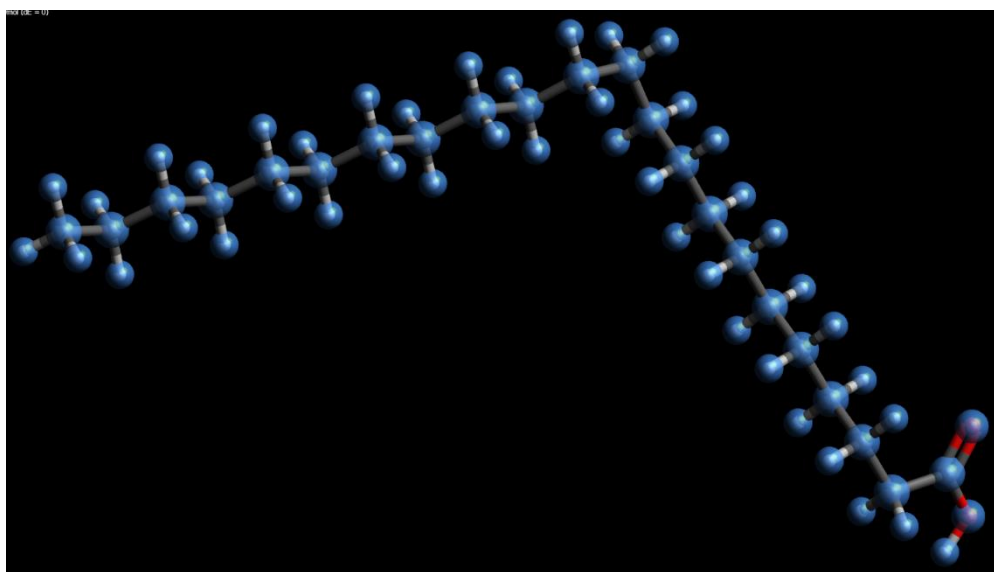
Found in *Staphisagria macrosperma* and *Tripneustes ventricosus*, behenic acid (C:22) (see Figure 31), is a very long chain monounsaturated fatty acid with a cis link at C13 (National Center for Biotechnology Information, 2022), it has properties as an antiviral and antimicrobial agent (Liang et al., 2020). However, it has negative effects against cardiac muscle, thus being considered as a natural toxin (Vetter et al., 2020).

#### Figure 31.

Behenic acid, PubChem CID: 8215



A.



B.

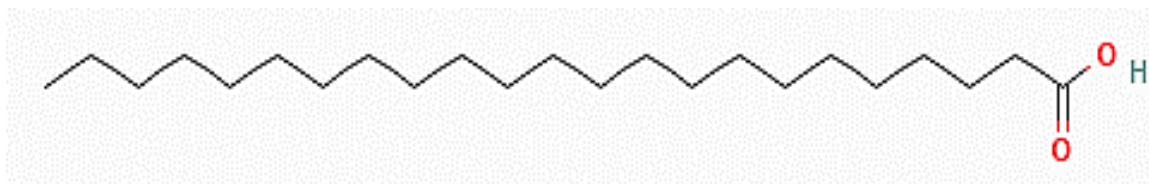
Note. **A.** 2D structure. **B.** 3D structure is built in the Avogadro program, in order to add the protonation state to the molecule and then optimize it for molecular docking. Retrieved from: **A.** PubChem Compound Summary for CID 8215, Docosanoic acid. [Graphical Representation], PubChem, 2022 (<https://pubchem.ncbi.nlm.nih.gov/compound/Docosanoic-acid>). Copyright by National Library of Medicine - National Center for Biotechnology Information - PubChem. CC-BY 4.0.

### 3.4.15. Tricosanoic acid

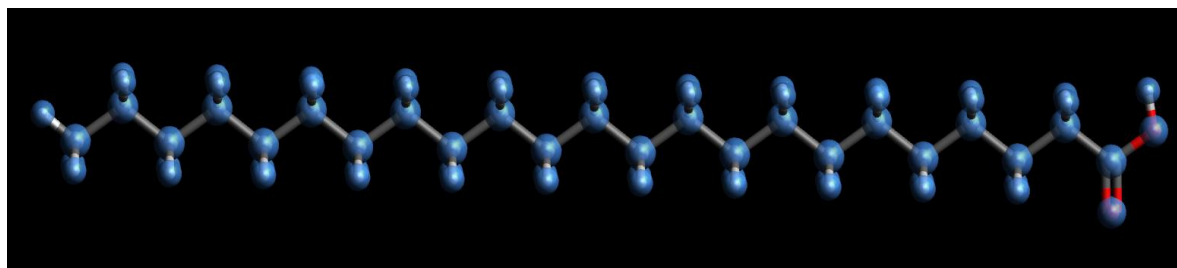
Considered as a plant and human metabolite, tricosanoic fatty (C:23) (see Figure 32) acid is a very long chain saturated fatty acid (National Center for Biotechnology Information, 2022).

#### Figure 32.

Tricosanoic acid, PubChem CID: 17085



A.



B.

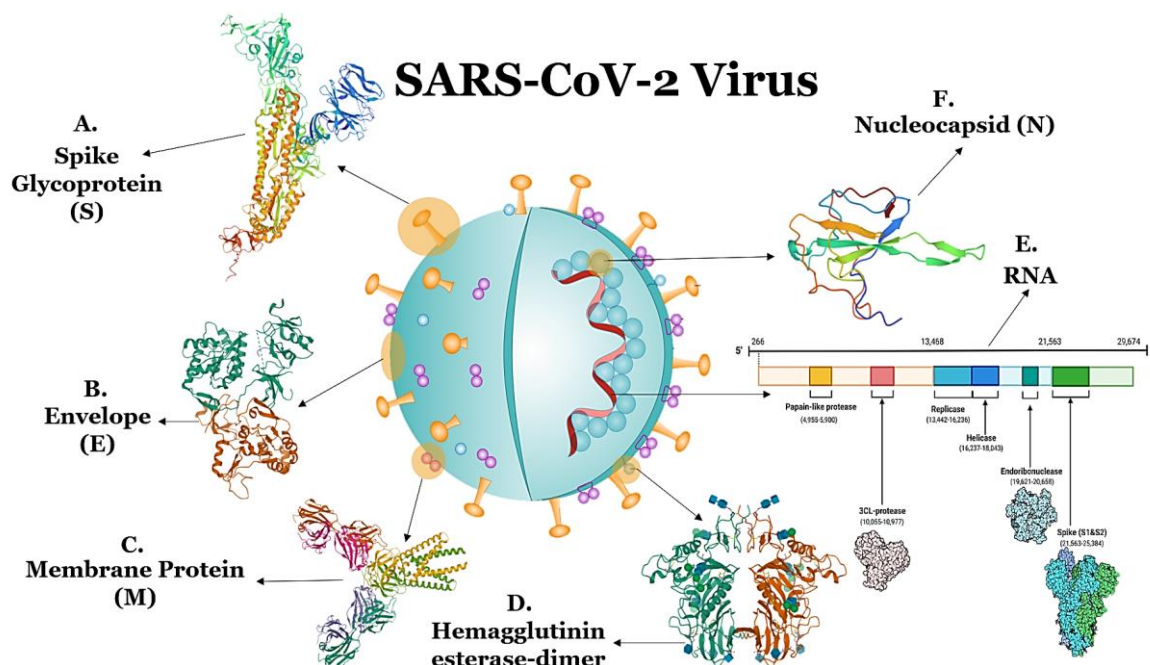
Note. **A.** 2D structure. **B.** 3D structure is built in the Avogadro program, in order to add the protonation state to the molecule and then optimize it for molecular docking. Retrieved from: **A.** PubChem Compound Summary for CID 17085, Tricosanoic acid [Graphical Representation], PubChem, 2022 (<https://pubchem.ncbi.nlm.nih.gov/compound/Tricosanoic-acid>). Copyright by National Library of Medicine - National Center for Biotechnology Information - PubChem. CC-BY 4.0.

## CHAPTER 4: ACE2 Receptor for SARS-CoV-2

In early 2020, the WHO declared pandemic of COVID 19 (World Health Organization, 2022) began, and the SARS-CoV-2 strain was identified as the cause of the pandemic. SARS-CoV-2, in a general way, it is composed of several structural proteins that encapsulate a positive single-stranded genomic RNA. The structural proteins are: nucleocapsid protein (N), envelope protein (E), membrane protein (M), spike protein (S) and hemagglutinin esterase-dimer (showed in Figure 33).

**Figure 33.**

*Structure of the SARS-CoV-2 virus*

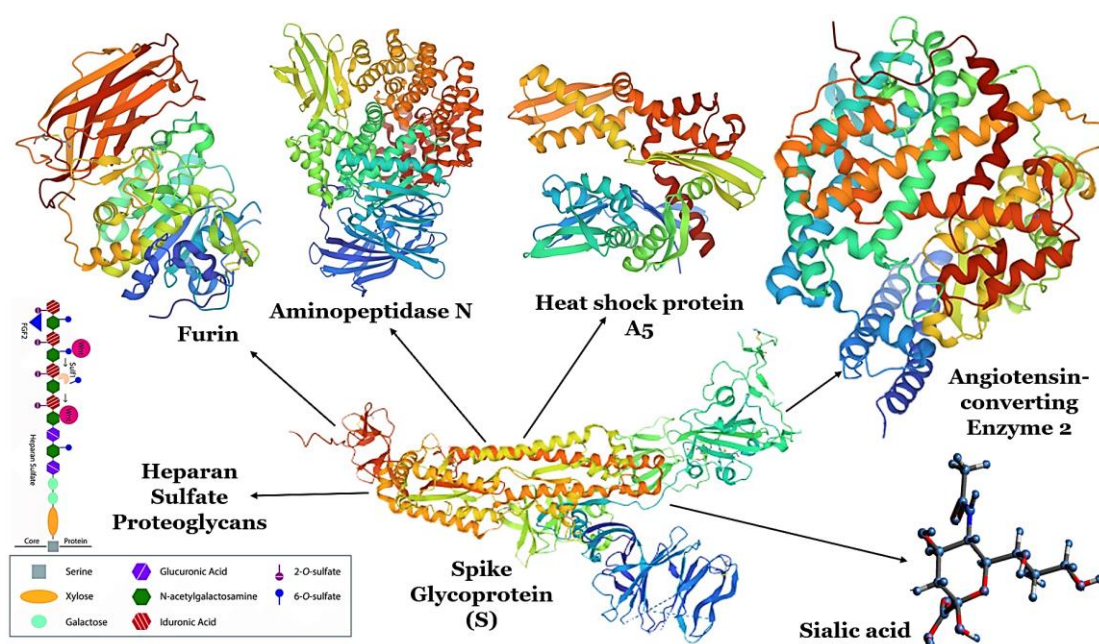


Note. Schematic diagram of the SARS-CoV-2 structure and its several accessory proteins. **A.** Spike Glycoprotein (S), mediates the receptor binding and membrane fusion between the virus and host cell. **B.** Envelope (E), involved in virus assembly. **C.** Membrane Protein (M), is responsible for the transmembrane transport of nutrients, the bud release and the formation of envelope. **D.** Hemagglutinin Esterase-dimer, is used as invading mechanism. **E.** Single-stranded RNA genome of SARS-CoV2. **F.** Nucleocapsid (N), is used to protects the viral RNA. Adapted from: Immune-mediated approaches against COVID-19 [Graphical Representation], Nature Nanotechnology - Florindo et al, 2020 (<https://doi.org/10.1038/s41565-020-0732-3>). Copyright by Springer Nature Limited – Nature Nanotechnology. CC BY-NC 4.0. 3D structures were obtained from the RCSB Protein Data Bank - COVID-19/SARS-CoV-2 Resources, 2023 [Crystal Structure Representation] ([RCSB.org/covid19](https://www.rcsb.org/covid19)). Copyright by RCSB Protein Data Bank. CC BY-SA 4.0.

In the SARS-CoV-2 strain, as with all viruses in the *Coronaviridae* family (Ou et al., 2020), the protein called Spike (S) [ $\sim$ 1300 amino acids], is responsible for host cell recognition and adhesion. (Khan et al., 2020; Li F. , 2016). Six different receptors have been identified in various human cell membranes that are recognized by the Spike (S) protein trimer (see Figure 34), which are: furin (amino acid cleavage convertase proteins)], sialic acid (component of glycoproteins [monosaccharide]), aminopeptidase N (hydrolyze the amino terminus residue of peptides [peptidase enzyme]), heat shock protein A5 (HSPA5) (cause cellular stress [proteins]), heparan sulfate proteoglycans (selective interaction with ligands [proteins]) and angiotensin-converting enzyme 2 (ACE2) (control blood pressure [enzyme]) (Belouzard et al., 2012; Hasan et al., 2020; Hofmann et al., 2005; Huang et al., 2015; Ibrahim et al., 2020).

**Figure 34.**

*Main membrane receptors that interact with the Spike (S) protein trimer*



Note. The crystal structures were obtained from the PDB (Protein Data Bank). **Furin**. Adapted from X-ray structure of furin in complex with the dichlorophenylpyridine-based inhibitor 1 [Crystal Structure Representation], RCSB Protein Data Bank (PDB 7QY0) - Dahms et al., 2022 (DOI: [10.2210/pdb7QY0/pdb](https://doi.org/10.2210/pdb7QY0/pdb)). Copyright by RCSB Protein Data Bank. CC BY-SA 4.0. **Aminopeptidase N**. Adapted from: Crystal Structure of Aminopeptidase N from Escherichia coli [Crystal Structure Representation], RCSB Protein Data Bank (PDB 2DQ6) – Nakajima et al., 2006 (DOI: [10.2210/pdb2DQ6/pdb](https://doi.org/10.2210/pdb2DQ6/pdb)). Copyright by RCSB Protein Data Bank. CC BY-SA 4.0. **Heat shock protein A5**. Adapted from Crystal structure of the human 70kDa heat shock protein 5



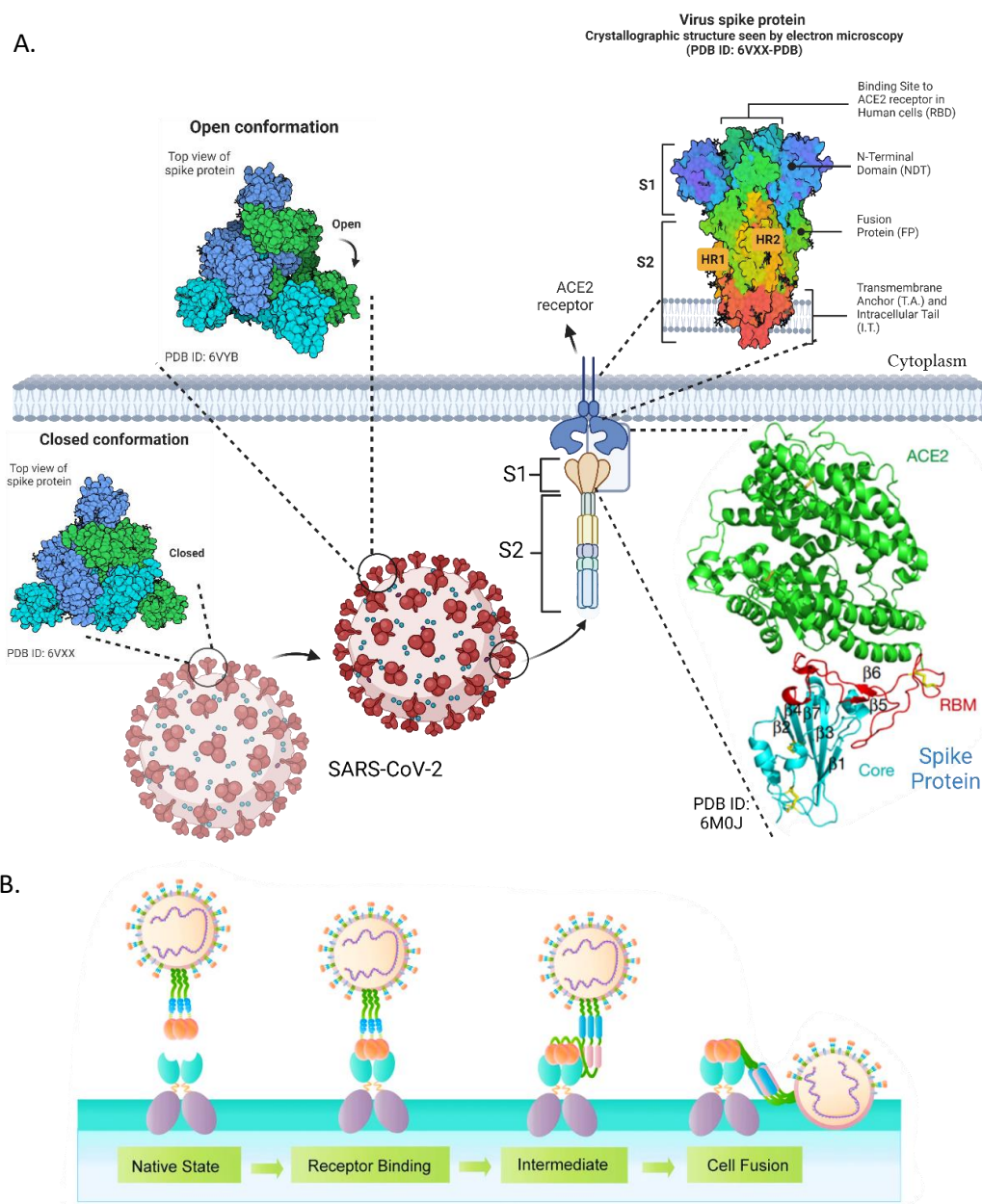
(BiP/GRP78) ATPase domain in complex with ADP [Crystal Structure Representation], RCSB Protein Data Bank (PDB 3IUC) – Wisniewska et al., 2009 ([DOI: 10.2210/pdb3IUC/pdb](https://doi.org/10.2210/pdb3IUC/pdb)). Copyright by RCSB Protein Data Bank. CC BY-SA 4.0. **Angiotensin-converting enzyme 2**. Adapted from Native Human Angiotensin Converting Enzyme-Related Carboxypeptidase (ACE2) [Crystal Structure Representation], RCSB Protein Data Bank (PDB 1R42) – Towler et al., 2004 ([DOI: 10.2210/pdb1R42/pdb](https://doi.org/10.2210/pdb1R42/pdb)). Copyright by RCSB Protein Data Bank. CC BY-SA 4.0. **Spike Glycoprotein (S)**. Structure of SARS-CoV-2 spike at pH 4.0 [Crystal Structure Representation], RCSB Protein Data Bank (PDB 6XLU) – Zhou et al., 2020 ([DOI: 10.2210/pdb6XLU/pdb](https://doi.org/10.2210/pdb6XLU/pdb)). Copyright by RCSB Protein Data Bank. CC BY-SA 4.0. **Sialic acid**. Adapted from SMILE code obtained from PubChem Compound Summary for CID 906, Sialic acid [Graphical Representation], PubChem, 2020 (<https://pubchem.ncbi.nlm.nih.gov/compound/Sialic-acid>). Copyright by National Library of Medicine - National Center for Biotechnology Information - PubChem. CC-BY 4.0. **Heparan Sulfate Proteoglycans**. Adapted from Exploiting Heparan Sulfate Proteoglycans in Human Neurogenesis—Controlling Lineage Specification and Fate [Graphical Representation], Frontiers in Integrative Neuroscience. - Yu et al., 2017 (<https://doi.org/10.3389/fnint.2017.00028>). Copyright by Yu, Griffiths and Haupt. CC-BY 4.0.

The present research focused on the angiotensin-converting enzyme 2 (ACE2) receptor, because by selecting ligands based on the RBD-SARS-CoV-2 sequence (Lan J. et al., 2020), different polyunsaturated (Kothapalli et al., 2020; Rogero et al., 2020) and monounsaturated fatty acids were found to interact (Yaqoob, 2002) and interfere more effectively with binding to the ACE2 receptor – and the SARS-CoV-2 Spike protein (Baral et al., 2022; Hathaway et al., 2020). The union between the spike of the SARS-CoV-2 virus and the ACE2 enzyme causes fusion between the cell membrane and the viral capsid, which allows entry of the virus (see Figure 35A) (Hoffmann et al., 2020; Jaimes et al., 2020; Lippi et al., 2020).

The virus-membrane binding and fusion mediators are S1 and S2, which are the units that make up the transmembrane glycoprotein S (spike protein) (Hathaway et al., 2020). The S1 subunit contains the binding to the ACE2 receptor, in its N-terminal domain (NTD) (Lan J. et al., 2020). When this binding occurs, the S2 subunit undergoes a conformational change, specifically the regions of heptad repeats (HR); which are transformed into an intra-hairpin-helical structure, this structure has six bundles of helices (Bosch et al., 2003; Xu et al., 2020) (see Figure 35B). After the conformational change in the human cell membrane, the fusion peptide is attached, causing the nucleocapsid protein to be delivered into the cell by the virus.

**Figure 35.**

*Union between the spike of the SARS-CoV-2 virus and the ACE2 enzyme in membrane cell*



Note. Schematic of the SARS-CoV-2 S protein binding to the ACE2 enzyme to enter the cell cytoplasm for replication. **A.** The S protein binds to the receptor ACE2. **B.** The binding and virus–cell fusion process mediated by the S protein. The graphical representation A was made in [biorender.com](https://www.biorender.com). **B.** Adapted from: Structural and functional properties of SARS-CoV-2 spike protein: potential antiviral drug development for COVID-19 [Graphical Representation], Acta Pharmacol Sin – Huang et al., 2020 (<https://doi.org/10.1038/s41401-020-0485-4>) Reproduced with permission from Springer Nature.



**CHAPTER 5: Methodology****5.1 Structural retrieval**

The structures of the natural compounds identified by various authors from the larva *R. palmarum*, specified in section 3.4. and identified by composition in Table 7, were retrieved from the PubChem database (Kim et al., 2019), are specified in Table 8, together with their SMILE code, formula and molecular weight. The identification number of each organic compound (CID) is given in section 3.4. The SMILES code is used for the design of the fatty acids identified in *R. palmarum* larvae in the Avogadro software.

**Table 8.** Chemical structures of the fatty acids identified in the larvae of *R. palmarum*

<i>Section</i>	<i>SMILES</i>	<i>Molecular Formula</i>	<i>Molecular Weight (g/mol)</i>
3.4.1.	<chem>CCCCCCCC(=O)O</chem>	C <sub>8</sub> H <sub>16</sub> O <sub>2</sub>	144.21
3.4.2.	<chem>CCCCCCCCC(=O)O</chem>	C <sub>10</sub> H <sub>20</sub> O <sub>2</sub>	172.26
3.4.3.	<chem>CCCCCCCCCCC(=O)O</chem>	C <sub>12</sub> H <sub>24</sub> O <sub>2</sub>	200.32
3.4.4.	<chem>CCCCCCCCCCCC(=O)O</chem>	C <sub>14</sub> H <sub>28</sub> O <sub>2</sub>	228.37
3.4.5.	<chem>CCCCCCCCCCCCC(=O)O</chem>	C <sub>16</sub> H <sub>32</sub> O <sub>2</sub>	256.42
3.4.6.	<chem>CCCCC/C=C\CCCCCCC(=O)O</chem>	C <sub>16</sub> H <sub>30</sub> O <sub>2</sub>	254.41
3.4.7.	<chem>CCCCCCCCCCCCCCCC(=O)O</chem>	C <sub>17</sub> H <sub>34</sub> O <sub>2</sub>	270.5
3.4.8.	<chem>CCCCCCCCCCCCCCCCC(=O)O</chem>	C <sub>18</sub> H <sub>36</sub> O <sub>2</sub>	284.5
3.4.9.	<chem>CCCCCCCC/C=C\CCCCCCC(=O)O</chem>	C <sub>18</sub> H <sub>34</sub> O <sub>2</sub>	282.5
3.4.10.	<chem>CCCCC/C=C\C/C=C\CCCCCCC(=O)O</chem>	C <sub>18</sub> H <sub>32</sub> O <sub>2</sub>	280.4
3.4.11.	<chem>O=C(O)CCCCC/C=C\C/C=C\C/C=C\CC</chem>	C <sub>18</sub> H <sub>30</sub> O <sub>2</sub>	278.43
3.4.12.	<chem>CCCCC/C=C\C/C=C\C/C=C\C/C=C\CCCC(=O)O</chem>	C <sub>20</sub> H <sub>32</sub> O <sub>2</sub>	304.5
3.4.13.	<chem>CCCCCCCCCCCCCCCCCCCC(=O)O</chem>	C <sub>21</sub> H <sub>42</sub> O <sub>2</sub>	326.6
3.4.14.	<chem>CCCCCCCCCCCCCCCCCCCCC(=O)O</chem>	C <sub>22</sub> H <sub>44</sub> O <sub>2</sub>	340.6
3.4.15.	<chem>CCCCCCCCCCCCCCCCCCCCC(=O)O</chem>	C <sub>23</sub> H <sub>46</sub> O <sub>2</sub>	354.6

Note. The column section refers to the fatty acids described in section 3.4.

## 5.2. Molecular Docking Studies

### 5.2.1. Structure of natural compounds

The three-dimensional structures of the different fatty acids were constructed using Avogadro (see Figure 36) (Hanwell et al., 2012), where their protonation state was constructed by adding hydrogens per pH 7.4 [physiological] (see Figure 37). Then, an optimization was executed, performing a molecular mini-dynamics, to determine the coordinates and spacing of the atoms; in these dynamics we used the chemical force field MMFF94, made by Merck research laboratories (Halgren, 1996); where, what is sought, is the lowest energy state of the molecule given by kJ/mol, while the derivative of the energy (energy change that is happening), tends to be zero (see Figure 38). In the end, the molecule is obtained in its proper protonation state and conformation.

#### Figure 36.

*Construction of linoleic acid in Avogadro*

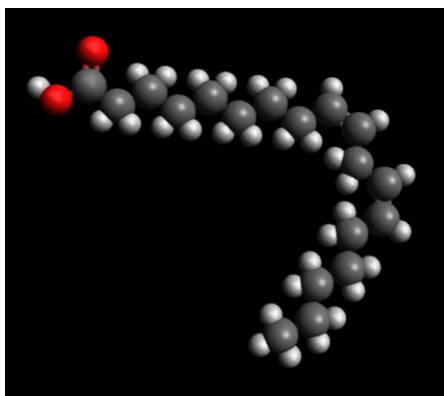


#### Figure 37.

*Protonation state of linoleic acid in Avogadro*

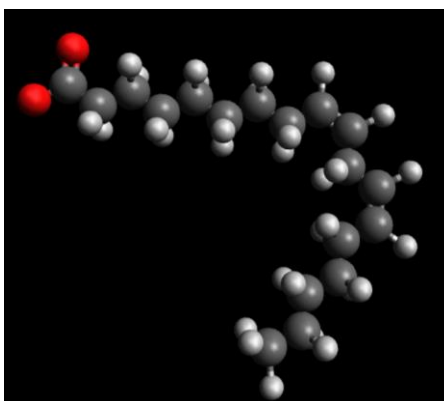
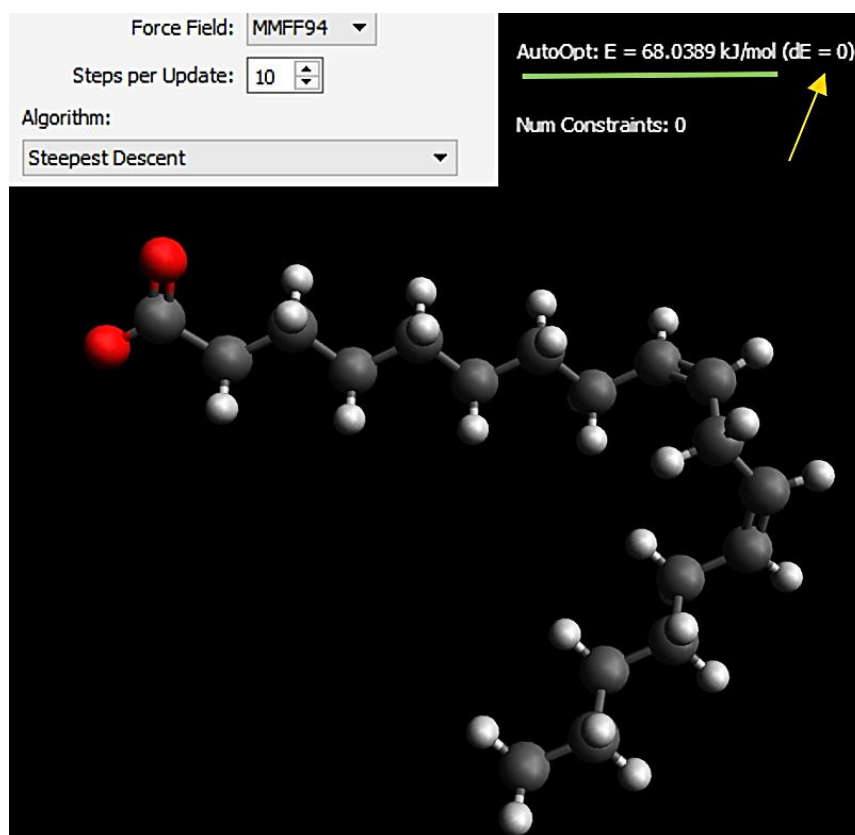


### Figure 38.

#### Optimization of linoleic acid in Avogadro

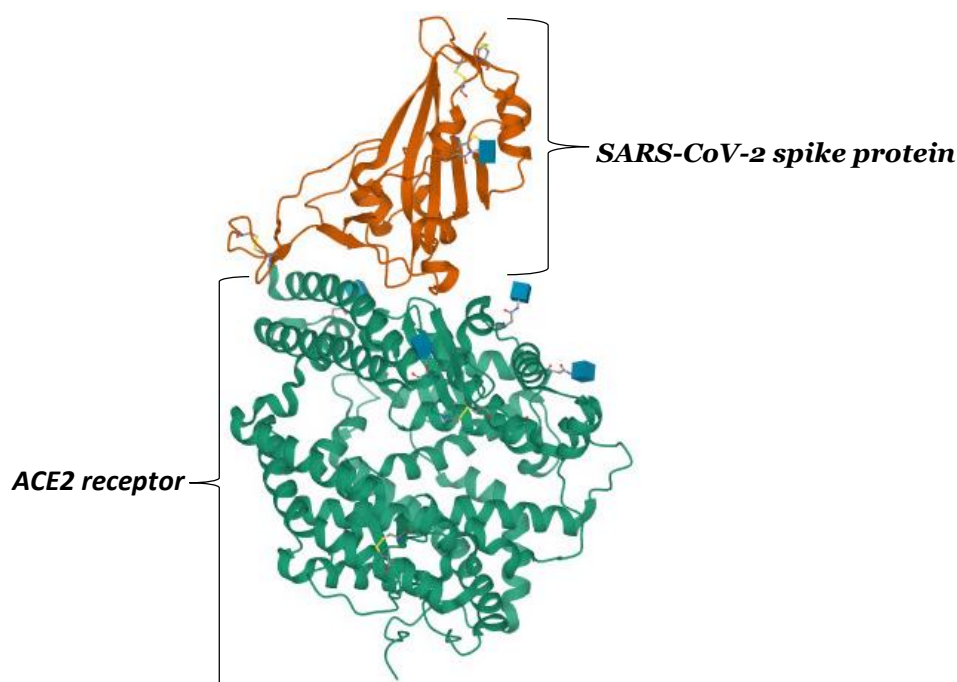


#### 5.2.2. Crystal structure of the SARS-CoV-2 protein spike (S) trimer and angiotensin-converting enzyme receptor 2 (ACE2)

The 3D structures of the organic molecules will interact with the crystal structure of the angiotensin-converting enzyme receptor 2 (ACE2), which is bounding to the SARS-CoV-2 protein spike (S) trimer (PDB code: 6MoJ) (Lan J. et al., 2020) (see Figure 39), this structure was obtained from the Protein Data Bank (Berman et al., 2021).

**Figure 39.**

*Structure of the SARS-CoV-2 spike receptor binding domain bounding to the ACE2 receptor.*



Note. Adapted from: Crystal structure of SARS-CoV-2 spike receptor-binding domain bound with ACE2 [Crystal Structure Representation], RCSB Protein Data Bank (PDB 6MoJ) – Wang et al., 2020 (DOI: [10.2210/pdb6MoJ/pdb](https://doi.org/10.2210/pdb6MoJ/pdb)). Copyright by RCSB Protein Data Bank. CC BY-SA 4.0.

By literature search, six crystal structures of the ACE2 receptor were available. Their PDB codes are: 1R4L - 2AJF - 5E84 - 6ZB5 - 7CAI - 6MoJ respectively. The crystal structure 6MoJ was chosen because of its resolution, which is 2.45 Å, lower than all the structures mentioned above; knowing that the lower the resolution, the better the crystal is for molecular docking. In addition, as shown in the Figure 40 the R-Value Free is 0.227, R-Value Work is 0.192 and R-Value Observed is 0.194.

The R values indicate the quality of the model, tending that an R equal to 0.63, would be the maximum value that can be obtained. In addition, this value would indicate that the model has a totally random distribution, so that something in the crystal would not be distinguishable. On the other hand, an R equal to 0, would be a perfect R; this value is impossible to find because the proteins are still vibrating, therefore, they will have a degree of disorder. The most important value to decide which crystal structure is better to perform a correct

molecular docking is the Free R-value (Atomistic Resolution Model), because this value is calculated. When calculating the crystal structure model, 10 percent of the observed data is removed. While, with the remaining 90 percent a model is constructed, in order to make a prediction of the remaining 10 percent. Finally, it is observed whether the observed and calculated values fit together.

**Figure 40.**

*Experimental Data Snapshot of Crystal structure of SARS-CoV-2 spike receptor-binding domain bound with ACE2*

**Experimental Data Snapshot**

**Method:** X-RAY DIFFRACTION

**Resolution:** 2.45 Å

**R-Value Free:** 0.227

**R-Value Work:** 0.192

**R-Value Observed:** 0.194

Note. The experimental data snapshot is obtained from Crystal structure of SARS-CoV-2 spike receptor-binding domain bound with ACE2 [Crystal Structure Representation], RCSB Protein Data Bank (PDB 6MoJ) – Wang et al., 2020 ([DOI: 10.2210/pdb6MoJ/pdb](https://doi.org/10.2210/pdb6MoJ/pdb)). Copyright by RCSB Protein Data Bank. CC BY-SA 4.0.

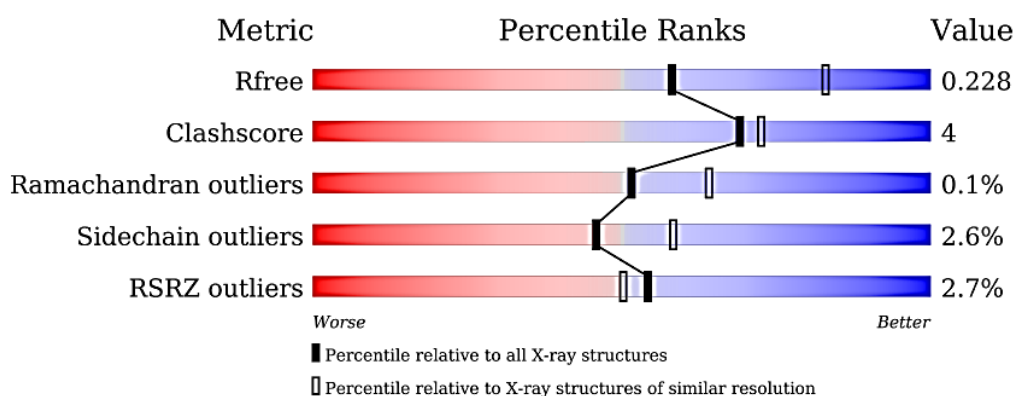
Another parameter to take into account is the Clashscore, which is 4 (see Figure 41). This parameter indicates the number of atom pairs that are unusually close, which is incorrect. Because, there are physical forces, such as Van der Waals and electrostatic forces that maintain an average distance between pairs of atoms, so that they are not overlapping. The lower the Clashscore value, the better the quality of the crystal.

The next parameter is Ramachandran outliers, which is 0.1% and it is a percentage of residues in the favored regions of the Ramachandran plot (see Figure 41). An outlier is something (variable, residual) that deviates from standard conditions or the normal distribution. In an amino acid chain, there is a C-terminus and an N-terminus; at each of these, peptide bonds are forming, which link one amino acid to another amino acid. In this peptide bond a dihedral angle is formed; this angle will be in motion because proteins are not static. Between two peptide bonds two angles are formed,  $\phi$  and  $\psi$ . These angles have an interval in which they are constantly moving. The Ramachandran outliers

refer to these two twisting angles  $\phi$  and  $\psi$ ; where the Ramachandran plot makes a correlation between the two angles, to know which links have the standard or normal angles and which angles do not have a proper conformation, i.e., they may be twisted or very far apart.

**Figure 41.**

*Overall quality of Crystal structure of SARS-CoV-2 spike receptor-binding domain bound with ACE2*



Note. The experimental data snapshot is obtained from Crystal structure of SARS-CoV-2 spike receptor-binding domain bound with ACE2 [Crystal Structure Representation], RCSB Protein Data Bank (PDB 6MoJ) – Wang et al., 2020 (DOI: [10.2210/pdb6MoJ/pdb](https://doi.org/10.2210/pdb6MoJ/pdb)). Copyright by RCSB Protein Data Bank. CC BY-SA 4.0.

**5.2.3. ACE2 protein optimization**

The 6MoJ crystal structure will be visualized in UCSF Chimera, which is a protein database (PDB) file viewer and molecular analysis program (see Figure 42) (Pettersen et al., 2004). The crystalline structure is visualized, where it can be seen that it is made up of several ligands and two molecules, one is the SARS-CoV-2 spike receptor (E chain - red color) (see Figure 42) and the ACE2 enzyme (A chain - blue color) (see Figure 42). The target chain is ACE2, therefore, waters, E-chain and unwanted molecules are removed (see Figure 43).

**Figure 42.**

*UCSF chimera visualization of the 6MoJ crystal structure*

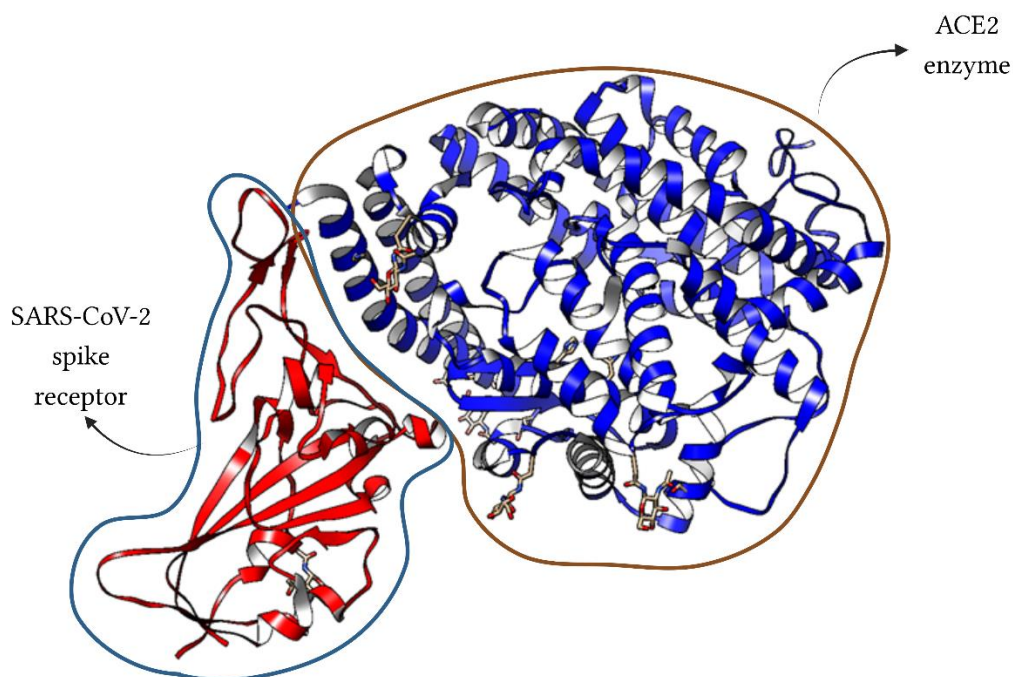
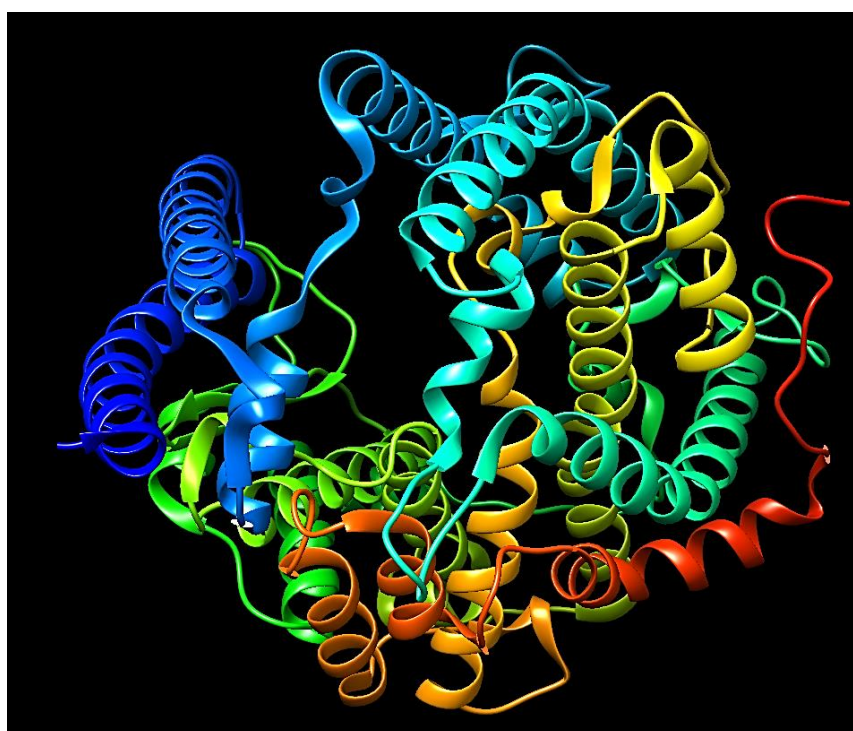


**Figure 43.**

*Visualization of them cell membrane receptor for angiotensin converting enzyme 2 - ACE2*



Note. The structure starts with its C-terminal chain (blue) and ends with its N-terminal chain (red). This crystalline structure is used in molecular docking.



#### 5.2.4. Revalidation of the crystal structure.

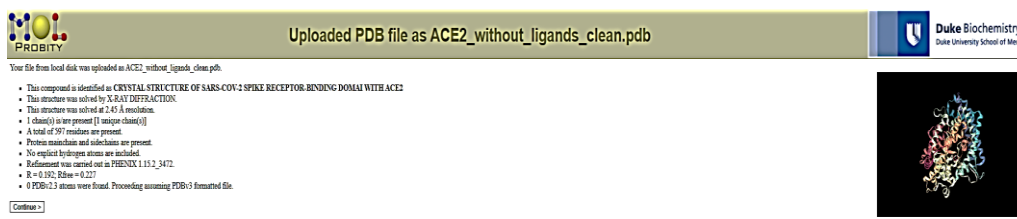
After optimizing the 6MOJ crystal structure, the ACE2 enzyme alone was obtained. Now, the obtained model must be validated. To carry out the validation, MolProbity (see Figure 44) (Williams et al., 2018), an online software, is used, which allows to perform a validation of the new structure, in this case the ACE2 enzyme obtained in the Chimera software (see Figure 43).

The validation performed by the MolProbity (Williams et al., 2018) software is shown in Figure 45, despite having 2 negative variables, while the other parameters are in an acceptable range. Therefore, the ACE2 enzyme, the new structure created, is valid for molecular docking.

The negative variables are due to the crystalline model of the ACE2 enzyme having side chains with high energy, therefore they are in a more rigid state than normal. This causes the angles of some peptide bonds to be outside the normal range (Ramachandran outliers). Nevertheless, the ACE2 enzyme model shows a very good Clashscore and score (see Figure 45).

#### Figure 44.

ACE2 protein uploaded in the MolProbity online program



The screenshot shows the MolProbity web interface. At the top, it says "Uploaded PDB file as ACE2\_without\_ligands\_clean.pdb". Below this, there is a list of statistics and a "Continue >" button. To the right, there is a small 3D molecular model of the ACE2 protein structure.

PROBITY

Uploaded PDB file as ACE2\_without\_ligands\_clean.pdb

Duke Biochemistry  
Duke University School of Medicine

Your file from local disk was uploaded as ACE2\_without\_ligands\_clean.pdb.

- This compound is identified as CRYSTAL STRUCTURE OF SARS-COV-2 SPIKE RECEPTOR-BINDING DOMAIN WITH ACE2
- This structure was solved by X-RAY DIFFRACTION
- This structure was solved at 2.45 Å resolution
- 1 chain(s) is/are present (1 unique chain(s))
- A total of 597 residues are present
- Protein mainchains and sidechains are present
- No explicit hydrogen atoms are included
- Refinement was carried out as PHENIX 1.15.2\_3472
- R = 0.192; Rfree = 0.227
- 0 PDB-1.3 atoms were fixed. Proceeding assuming PDB-3 formatted file.

Continue >

Note. The validation of the model was performed using the open-source online software MolProbity, which has a BSD and Apache license. The operation of the MolProbity program is specified at MolProbity: More and better reference data for improved all-atom structure validation [Scientific Paper], Duke University School of Medicine – Richardson Laboratory - Williams et al., 2018 (doi: [10.1002/pro.3330](https://doi.org/10.1002/pro.3330)). The software can be found at <https://github.com/rlabduke/MolProbity>.



**Figure 45.**

*Validation of the crystal with the ACE2 protein with the online program MolProbity*

**Summary statistics**

All-Atom Contacts	Clashscore, all atoms:	7.24	98 <sup>th</sup> percentile* (N=346, 2.45Å ± 0.25Å)
	Clashscore is the number of serious steric overlaps (> 0.4 Å) per 1000 atoms.		
Protein Geometry	Poor rotamers	14	2.65% Goal: <0.3%
	Favored rotamers	481	91.10% Goal: >98%
	Ramachandran outliers	1	0.17% Goal: <0.05%
	Ramachandran favored	583	97.98% Goal: >98%
	Rama distribution Z-score	-1.43 ± 0.29	Goal: abs(Z score) < 2
	MolProbity score <sup>^</sup>	1.72	98 <sup>th</sup> percentile* (N=8489, 2.45Å ± 0.25Å)
	Cβ deviations >0.25Å	0	0.00% Goal: 0
	Bad bonds:	0 / 5016	0.00% Goal: 0%
Bad angles:	2 / 6817	0.03% Goal: <0.1%	
Peptide Omegas	Cis Prolines:	1 / 27	3.70% Expected: ≤1 per chain, or ≤5%
Additional validations	Chiral volume outliers	0/711	
	Waters with clashes	0/0	0.00% See UnDowser table for details

In the two column results, the left column gives the raw count, right column gives the percentage.

\* 100<sup>th</sup> percentile is the best among structures of comparable resolution; 0<sup>th</sup> percentile is the worst. For clashscore the comparative set of structures was selected in 2004, for MolProbity

<sup>^</sup> MolProbity score combines the clashscore, rotamer, and Ramachandran evaluations into a single score, normalized to be on the same scale as X-ray resolution.

Key to table colors and cutoffs here: ?

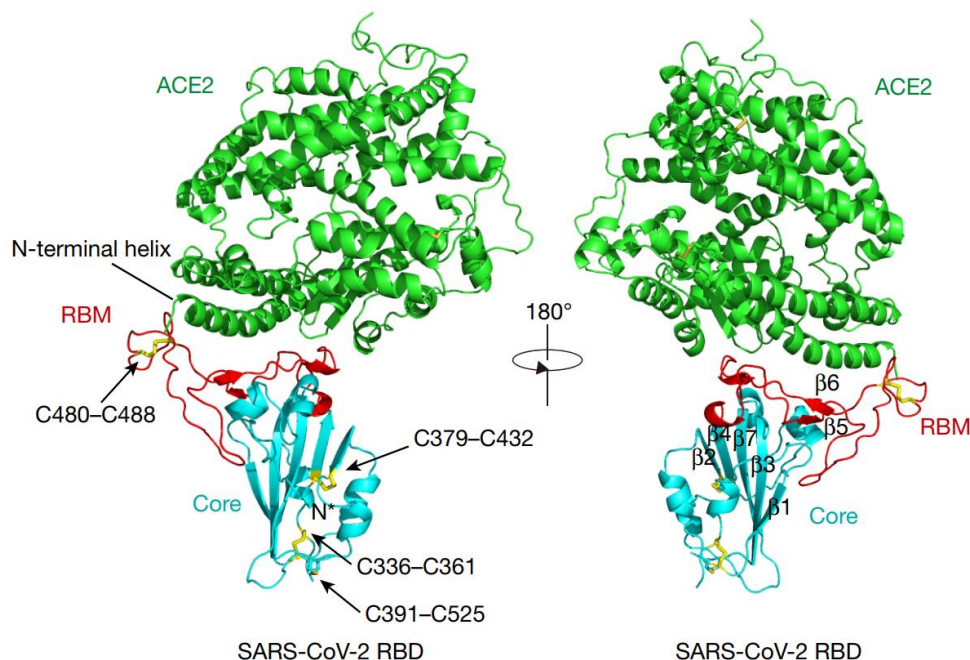
Note. The operation of the MolProbity program is specified at MolProbity: More and better reference data for improved all-atom structure validation [Scientific Paper], Duke University School of Medicine – Richardson Laboratory - Williams et al., 2018 (doi: [10.1002/pro.3330](https://doi.org/10.1002/pro.3330)). The software can be found at <https://github.com/rlabduke/MolProbity>.

### 5.2.5. Evaluate binding sites and pharmacological potential

After validating our ACE2 protein model. We proceeded to carry out an identification of binding sites and the pharmacological potential, to execute a directed docking. In the crystal structure 6MoJ, they indicated the sites where the spike protein of SARS-CoV-2 interacted with the enzyme ACE2 (see Figure 46). The receptor-binding domain (RBD) of the SARS-CoV-2 virus is linked to the ACE2 enzyme receptor, by a receptor-binding motif (RBM) (see Figure 47) which is made up of amino acids 436 to 506 in SARS-CoV-2 and in ACE2 are Q24, T27, F28, D30, K31, H34, E35, E37, D38, Y41, Q42, L79, M82, Y83, N330, K353, G354, D355, R357 and R393 (Lan J. et al., 2020).

**Figure 46.**

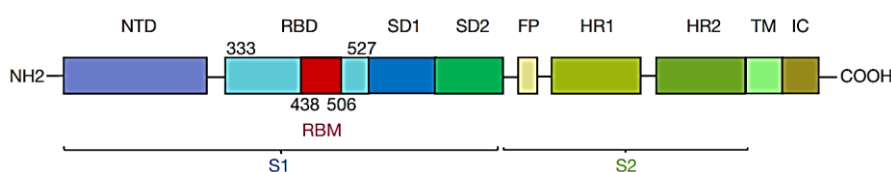
*Overall structure of SARS-CoV-2 RBD bound to ACE2*



Note. SARS-CoV-2RBD core is shown in cyan, RBD is ACE2 is shown in green and the RBM is shown in red. Adapted from: Crystal structure of SARS-CoV-2 spike receptor-binding domain bound with ACE2 [Crystal Structure Representation], RCSB Protein Data Bank (PDB 6MoJ) – Wang et al., 2020 ([DOI: 10.2210/pdb6MoJ/pdb](https://doi.org/10.2210/pdb6MoJ/pdb)). Copyright by RCSB Protein Data Bank. CC BY-SA 4.0.

**Figure 47.**

*Summary topology of the SARS-CoV-2 spike monomer*

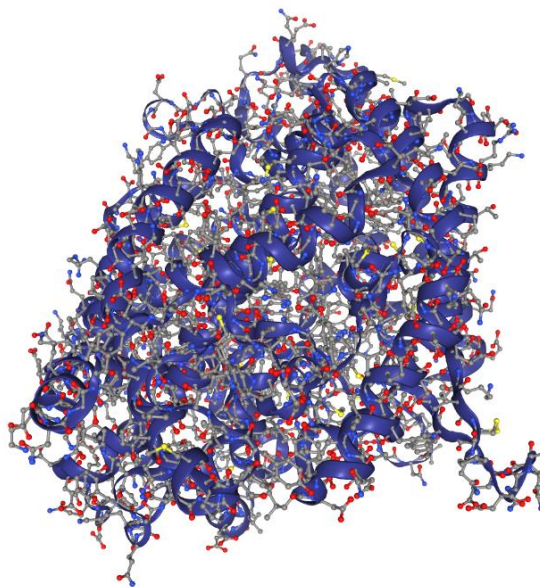


Note. Adapted from: Crystal structure of SARS-CoV-2 spike receptor-binding domain bound with ACE2 [Crystal Structure Representation], RCSB Protein Data Bank (PDB 6MoJ) – Wang et al., 2020 ([DOI: 10.2210/pdb6MoJ/pdb](https://doi.org/10.2210/pdb6MoJ/pdb)). Copyright by RCSB Protein Data Bank. CC BY-SA 4.0.

DoGSiteScorer (Volkamer et al., 2010, 2012), a tool from the Center for Bioinformatics at the University of Hamburg, was used to predict ACE2 protein (see Figure 48) binding sites (Figure 49A). In addition, the properties of the binding site were evaluated, highlighting the pharmacological potential (see Figure 49B).

**Figure 48.**

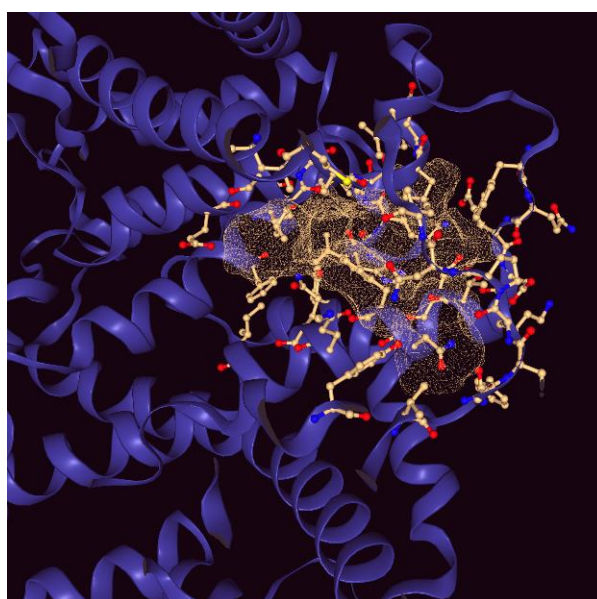
*ACE2 protein observed from the DoGSiteScorer program*



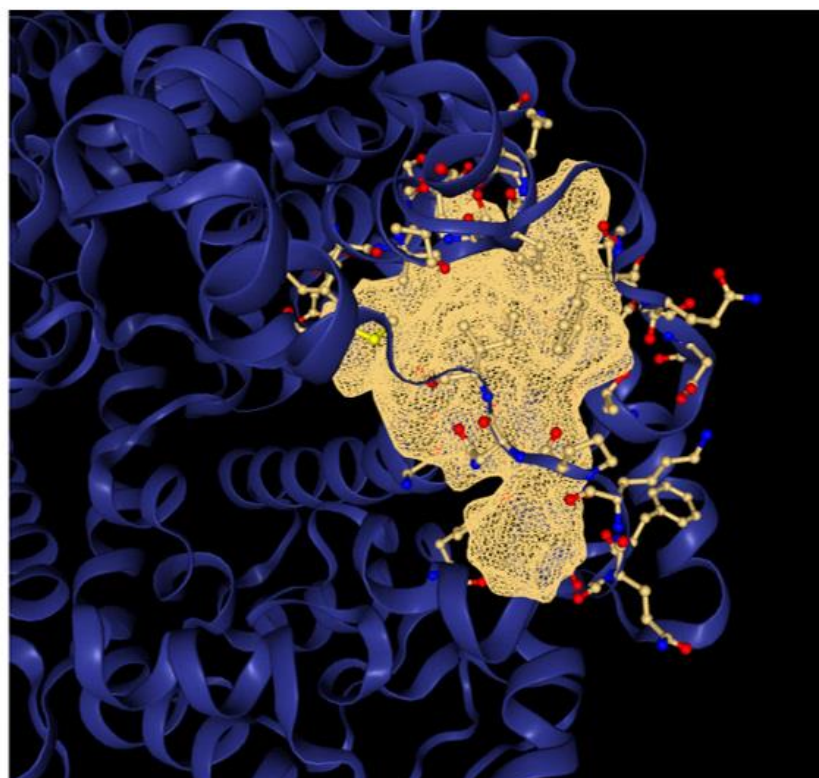
Note. The DoGSiteScorer program is part of the ProteinsPlus program, which is supported by the BMBF as part of the de.NBI - German Bioinformatics Infrastructure Network, which is free for commercial and academic use. This program is responsible for predicting binding sites and estimating their pharmacology between proteins and ligands. The software operation is explained in Analyzing the topology of active sites: on the prediction of pockets and subpockets and in Combining global and local measures for structure-based druggability predictions [Scientific Paper], Chem Inf Model - Volkamer et al. 2010-2012 (DOI: <https://doi.org/10.1021/ci100241y> ; DOI: <https://doi.org/10.1021/ci200454v>).

**Figure 49.**

ACE2 protein binding site predicted by DoGSiteScorer software.



A.



B.

Name	Volume Å <sup>3</sup>	Surface Å <sup>2</sup>	Drug Score	Simple Score
P_0	876.74	1068.47	0.83	0.56

**Size and shape descriptors**

volume [Å <sup>3</sup> ]	876.74
surface [Å <sup>2</sup> ]	1068.47
depth [Å]	23.22
ellipsoid main axis ratio c/a	0.11
ellipsoid main axis ratio b/a	0.58
enclosure	0.11

**Functional group descriptors**

# hydrogen bond donors	21
# hydrogen bond acceptors	49
# metals	0
# hydrophobic interactions	40
hydrophobicity ratio	0.36

**Element descriptors**

# pocket atoms	177
# carbons (C)	122
# nitrogens (N)	23
# oxygens	29
# sulfurs (S)	3
# other elements	0

**Amino acid composition**

apolar amino acid ratio	0.38
polar amino acid ratio	0.38
positive amino acid ratio	0.13
negative amino acid ratio	0.10

C.

Note. A. and B. ACE2 protein binding site predicted by DoGSiteScorer software. C. The pharmacological potential of 0.83 is observed. The DoGSiteScorer program is part of the ProteinsPlus program, which is supported by the BMBF as part of the de.NBI - German Bioinformatics Infrastructure Network, which is free for commercial and academic use. This program is responsible for predicting binding sites and estimating their pharmacology between proteins and ligands. The software operation is explained in Analyzing the topology of active sites: on the prediction of pockets and subpockets and in Combining global and local measures for structure-based druggability predictions [Scientific Paper], Chem Inf Model - Volkamer et al. 2010-2012 (DOI: <https://doi.org/10.1021/ci100241y>; DOI: <https://doi.org/10.1021/ci200454v>).



### 5.2.6. Docking with Autodock Vina and UCSF Chimera

After determining the binding site of the ACE2 enzyme, we proceeded to perform molecular docking using Autodock Vina (Eberhardt et al., 2021) (Trott & Olson, 2010) for calculations and UCSF Chimera (Pettersen et al., 2004) for ligand visualization. It should be noted that the docking process was performed for each of the 15 fatty acids identified in the larvae of *R. palmarum*.

After performing the steps explained in sections 5.2.1. and 5.2.3. we proceed to visualize the ACE2 protein with a ligand (fatty acid explained in section 3.4.) from Table 7 (see Figure 50).

#### Figure 50.

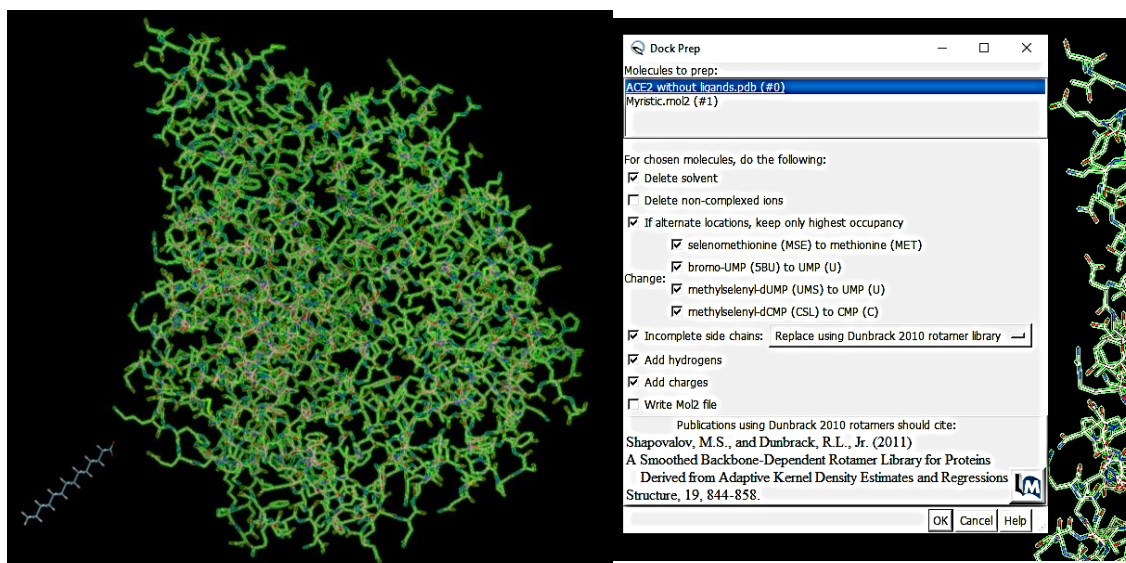
*Ligand and protein visualization using UCSF Chimera software*



In order to perform docking by means of Autodock Vina (Eberhardt et al., 2021; Trott & Olson, 2010), the protein must be prepared. In the *tool's menu* of the UCSF Chimera program (Pettersen et al., 2004), there is an option that allows us to prepare the protein called *Dock Prep* (see Figure 51A). The configuration that was performed is shown in the Figure 51B, then, the hydrogens must be added to the protein (see Figure 51C). Then, the charges must be assigned to the protein (see Figure 51D), where the mechanical force field is chosen for the standard residues AMBER ff14SB and for the other residues AM1-BCC is chosen, which is a database of added charges, but not calculated. The protein ready to interact with the ligand is obtained using the Autodock Vina program (see Figure 51E).

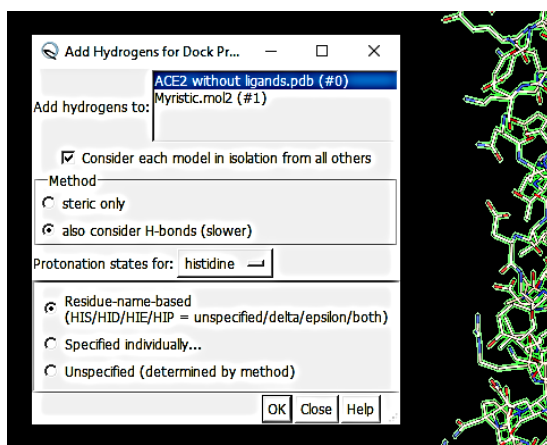
**Figure 51.**

*Preparation of ACE2 protein in USCF Chimera software for Docking*

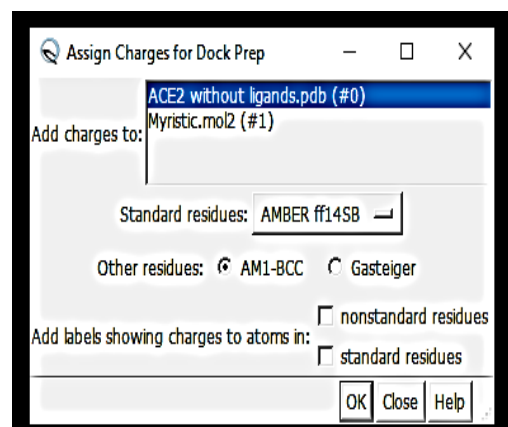


**A. Protein and ligand.**

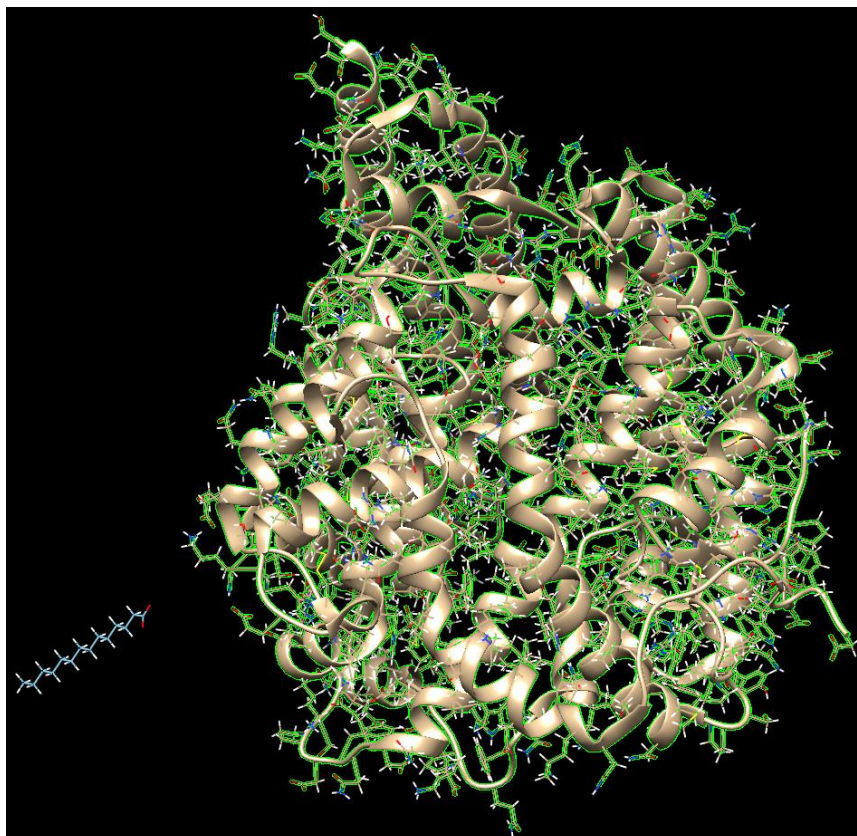
**B. ACE2 protein configuration.**



**C. Addition of hydrogens to ACE2 protein**



**D. Load assignment for ACE2 protein.**

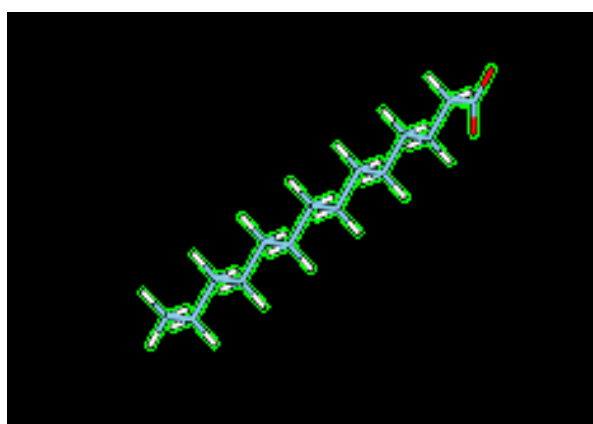


E. ACE2 protein prepared for docking with added hydrogens and fillers.

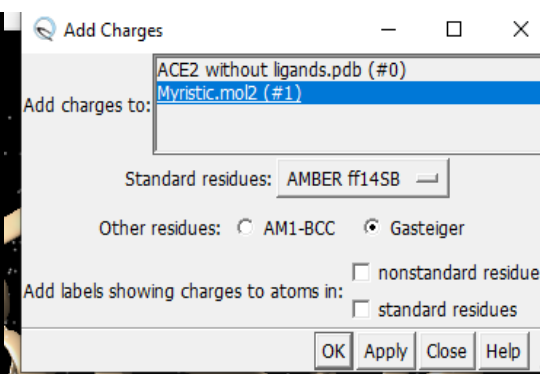
Now, we must prepare the ligand (see Figure 52A), to which the charges must be added using the UCSF Chimera program. The ligand is selected, and in tools, in the Structure Editing option, we proceed to add the charges. The added loads are added using the Gasteiger method, which calculates the loads to be added (see Figure 52B).

**Figure 52.**

*Preparation of the ligand for docking in Autodock Vina*



A. Ligand selected to add loads.

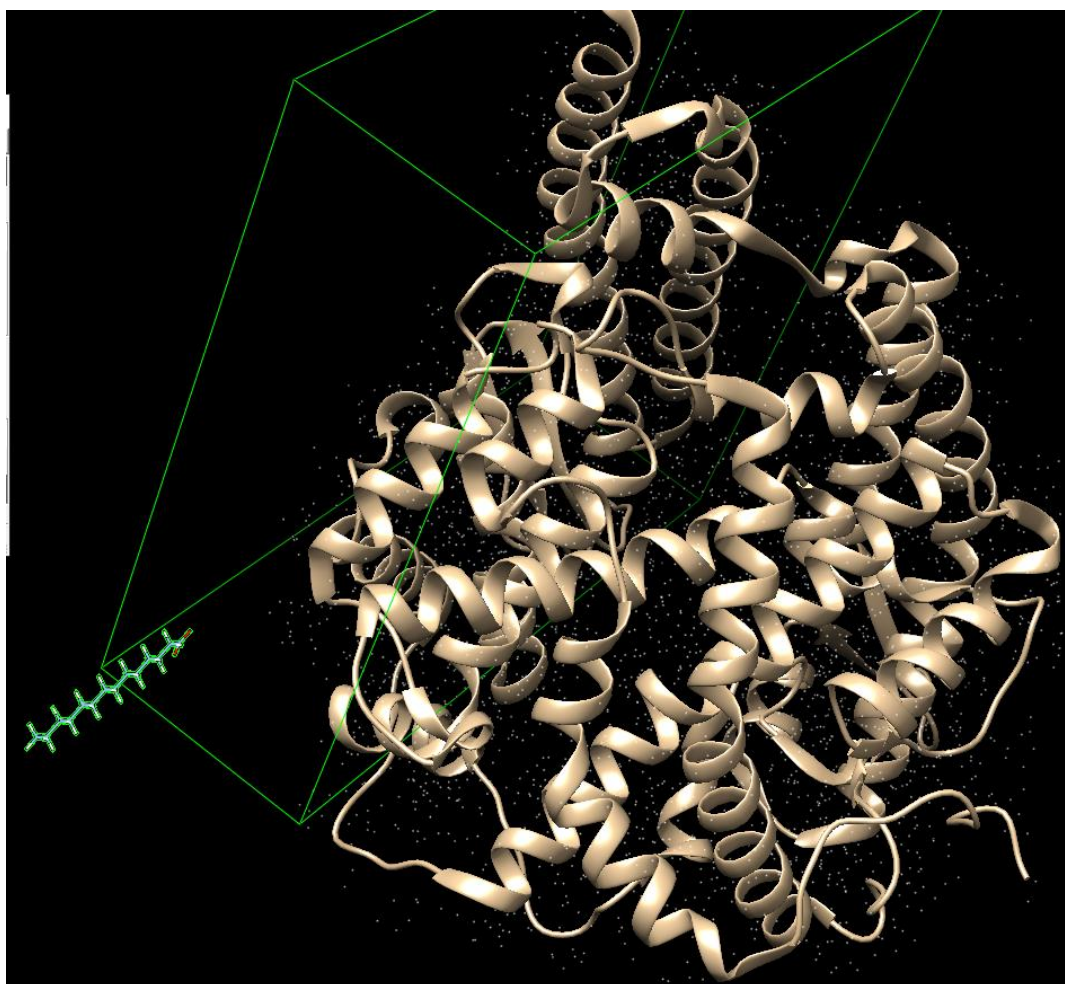


B. Load aggregation process by means of the Gasteiger method.

Finally, we open Autodock Vina. The first thing to do is to find the document saving site. Then, establish which is the receptor and the ligand. Later, the volume in which the protein-ligand interactions will take place must be determined (see Figure 53A; 53B). This interaction box was determined in section 5.2.5. Then, the receptor, ligand and advanced options are established, where 10 binding modes, 8 nuclei in the exhaustivity of the interaction search and a maximum energy difference of 3 kcal/mol (see Figure 53C) were chosen.

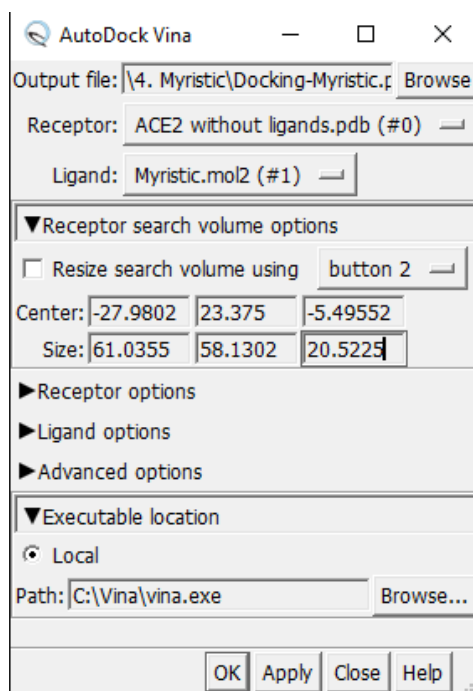
**Figure 53.**

*Protein and ligand configuration in AutoDock Vina and UCSF Chimera*



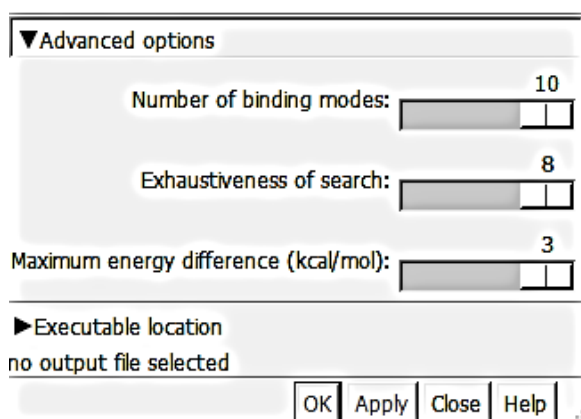
A. Ligand-protein interaction grid





**B.**

Configuration for performing Molecular Docking in Autodock Vina



**C.**

Configuration of the advanced options chosen for docking using the Autodock Vina software.

In UCSF Chimera, each of the 10 ligands interacting with the protein is obtained visually (see Figure 54). In addition, a table indicates the existing interaction strength (SCORE), which the more negative the higher the binding strength between the protein and the ligand. Also, Root mean square deviation (RMSD) values measuring the average distance between atoms of a position relative to the best fitting position, are calculated using only movable heavy atoms. Two variants of RMSD metrics are provided, rmsd/lb (RMSD lower bound) and rmsd/ub (RMSD upper bound), differing in how the atoms are matched in the distance calculation: rmsd/ub matches each atom in one conformation with itself in the other conformation, ignoring any symmetry. rmsd' matches each atom in one conformation with the closest atom of the same element type in the other conformation rmsd/lb is defined as follows:  $\text{rmsd/lb}(c_1, c_2) = \max(\text{rmsd}'(c_1, c_2), \text{rmsd}'(c_2, c_1))$ , with  $c_n$  conformation  $n$ .

**Figure 54.**

*Visualization of a ligand conformation obtained by Autodock Vina and visualized in UCSF Chimera*

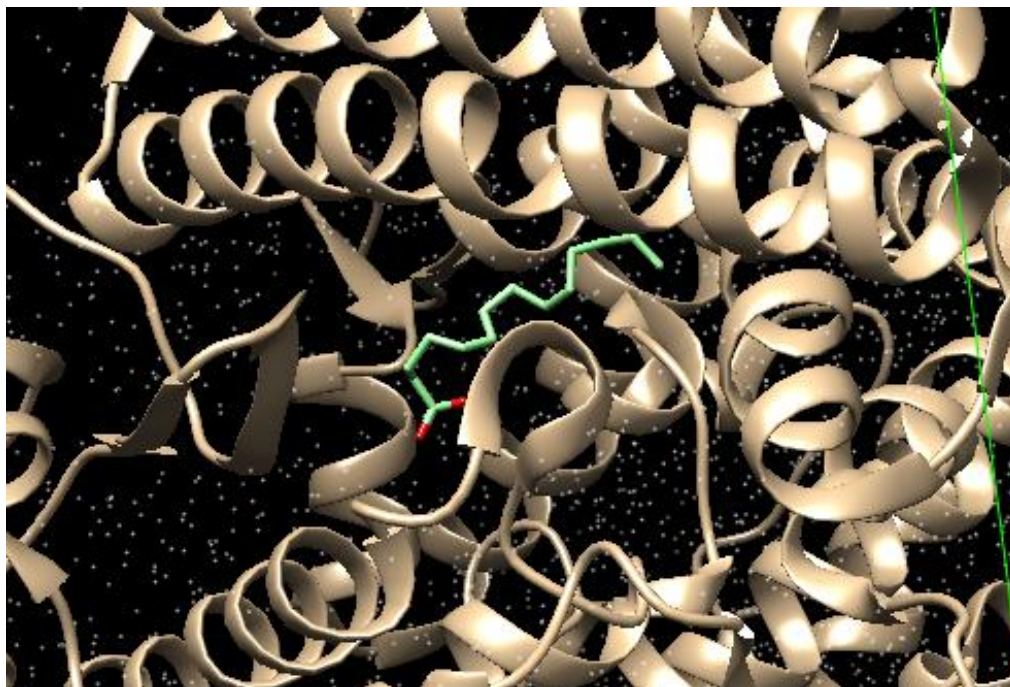


**Figure 55.**

*Results obtained from the Docking performed by Autodock Vina*

ViewDock - C:\Users\Usuario\Downloa

File	Compounds	Column	Selection
S	Score	RMSD l.b.	RMSD u.b.
V	-5.2	0.0	0.0
V	-5.1	5.559	8.318
V	-5.0	2.501	3.191
V	-5.0	2.302	2.988
V	-4.8	3.749	5.393
V	-4.8	2.492	3.39
V	-4.8	3.084	4.998
V	-4.7	6.221	9.256
V	-4.7	5.373	9.582
V	-4.6	4.92	6.899

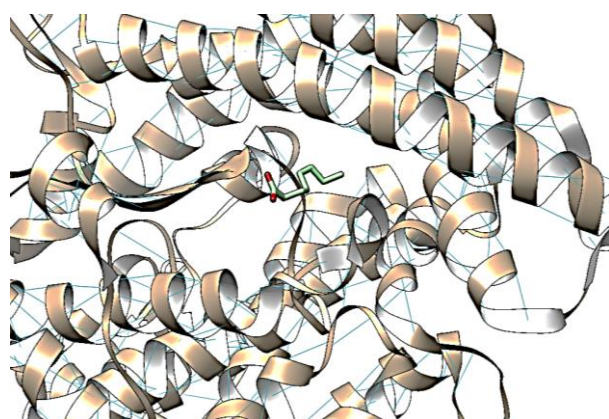
## CHAPTER 6: Results and Analysis

As mentioned in chapter 3, in the section on fatty acids identified inside *R. palmarum* larvae, they have been reported to have pharmacological properties, showing that they influence physiological and biochemical processes. Figure 56 (A to K) shows the representative interactions of various fatty acids in *R. palmarum* larvae. In addition, Table 9 indicates the SCORE of each fatty acid identified in *R. palmarum* larvae, as well as the hydrogen bonds formed with ACE2 enzyme. Also, Table 9 and Figure 57, classify in increasing order, which are the fatty acids that have greater interaction with the ACE2 protein. For the analysis, all those fatty acids with a score less than or equal to 5 are discarded.

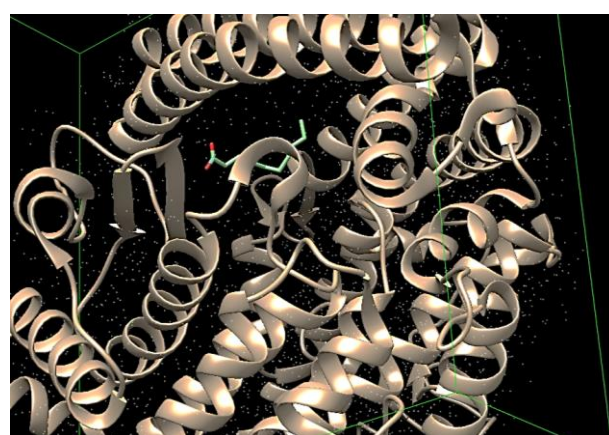
It is observed from Figure 58 that arachidonic acid is the fatty acid identified in *R. palmarum* larvae that has the greatest attraction force with the ACE2 protein, with a score of -6.4. While linoleic (-5.8), oleic (-5.6), caprylic (-5.4), alpha-linoleic (-5.4), behenic (-5.4), palmitic (-5.3), tricosanoic (-5.3), myristic (-5.2), margaric (-5, 2) and palmitoleic (-5.1), indicating that these fatty acids to a greater or lesser extent can counteract the binding of the ACE2 enzyme, exposed in the cell, to the SARS-CoV-2 spike; preventing the recognition of the virus.

### Figure 56.

*Representation of the conformation of the fatty acids identified in R. palmarum larvae bound to the ACE2 protein*

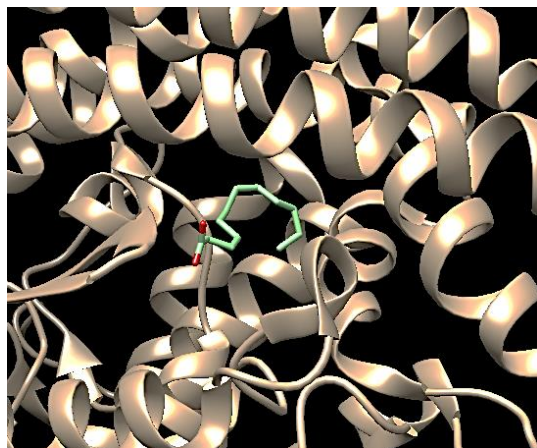


A. Caprylic Acid

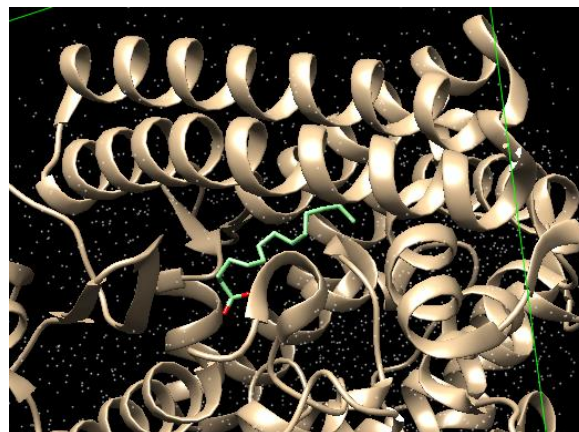


B. Capric Acid





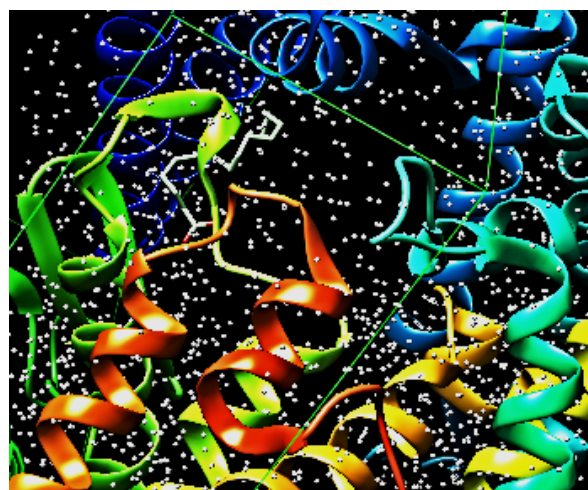
C. Lauric Acid



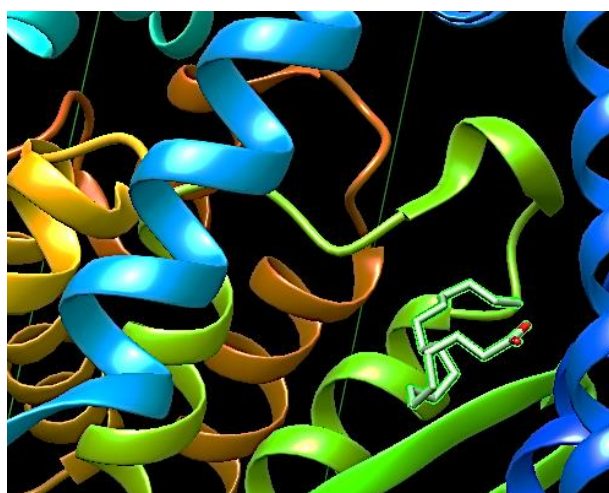
D. Myristic Acid



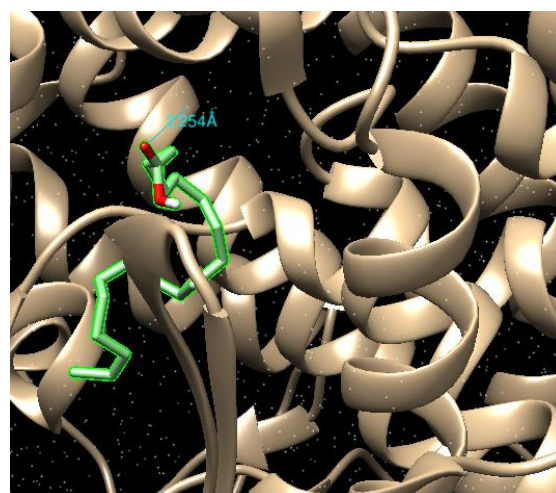
E. Palmitic Acid



F. Palmitoleic

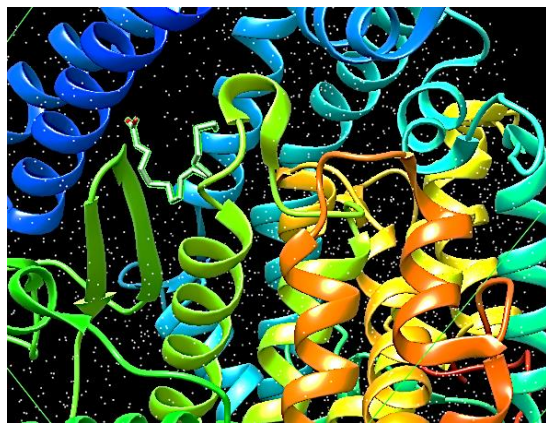


G. Margaric Acid

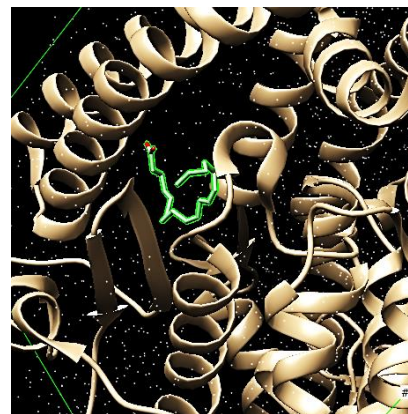


H. Stearic Acid

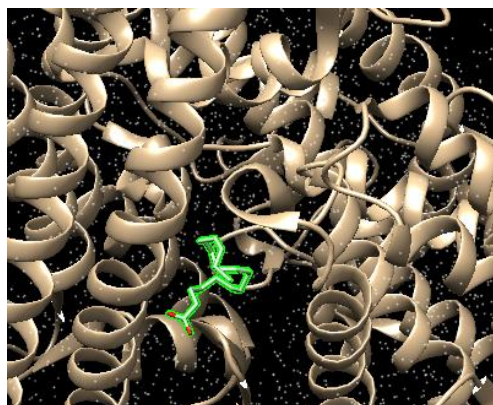




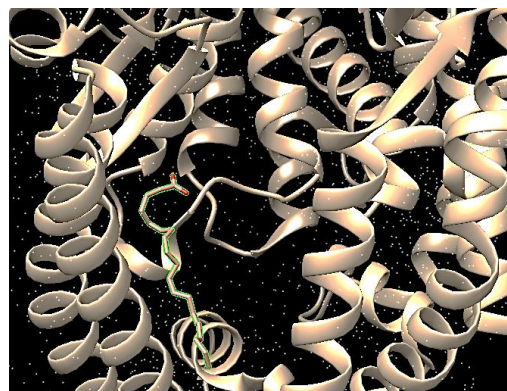
**I.** Oleic Acid



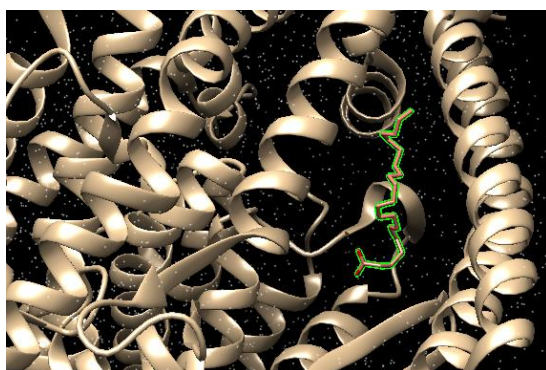
**F.** Linoleic Acid



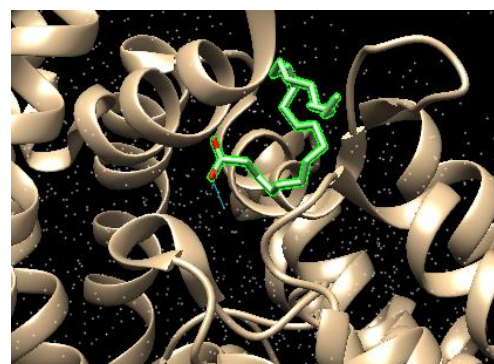
**G.** Alpha-Linoleic Acid



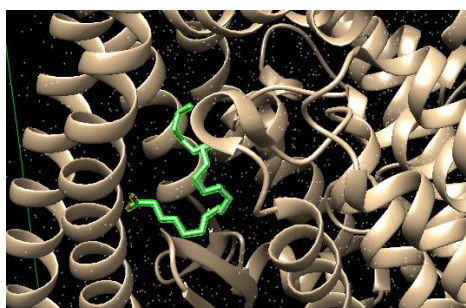
**H.** Arachidonic Acid



**I.** Heneicosanoic Acid



**J.** Behenic Acid



**K.** Tricosanoic Acid

**Table 9.**

Molecular docking results of each fatty acid identified in *R. palmarum* larvae with the ACE2 protein

Compound	AutoDock score (kcal/mol)
Caprylic Acid	-5.4
Capric Acid	-4.9
Lauric	-4.9
Myristic	-5.2
Palmitic	-5.3
Palmitoleic	-5.1
Margaric	-5.2
Stearic	-5.0
Oleic	-5.6
Linoleic	-5.8
Alpha-linoleic	-5.4
<b>Arachidonic</b>	<b>-6.4</b>
Heneicosanoic	-3.8
Behenic	-5.4
Tricosanoic	-5.3

Chapter 4 explained the relationship between the SARS-CoV-2 spike protein and the ACE2 enzyme. In addition, it was mentioned that there is a conformational reorganization in the cell membrane and in the SARS-CoV virus, which causes the S1 and S2 subunits of the spike protein (S) to increase their sensitivity to be degraded or ingested (proteolytic digestion) (Hamming et al., 2004) (Li et al., 2006). In turn, it is important to note that angiotensin converting enzyme 2 (ACE2) is expressed in vascular endothelial cells, in a selected subset of lung cells and in macrophages (Lake, 2020; Tay et al., 2020; Lan J. et al., 2020; Kleinehr et al., 2021).

The highest score value is that of arachidonic acid with -6.4 kcal-mol, which indicates that it has a higher inhibitor binding efficiency in the viral RBD chain, because as mentioned in the Methodology chapter, the docking that was performed to the crystal structure of the ACE2 enzyme was directed to the binding site with a higher pharmacological potential (Figure 51-52), which also coincided with the viral RBD of binding between the Spike protein and the ACE2 enzyme.

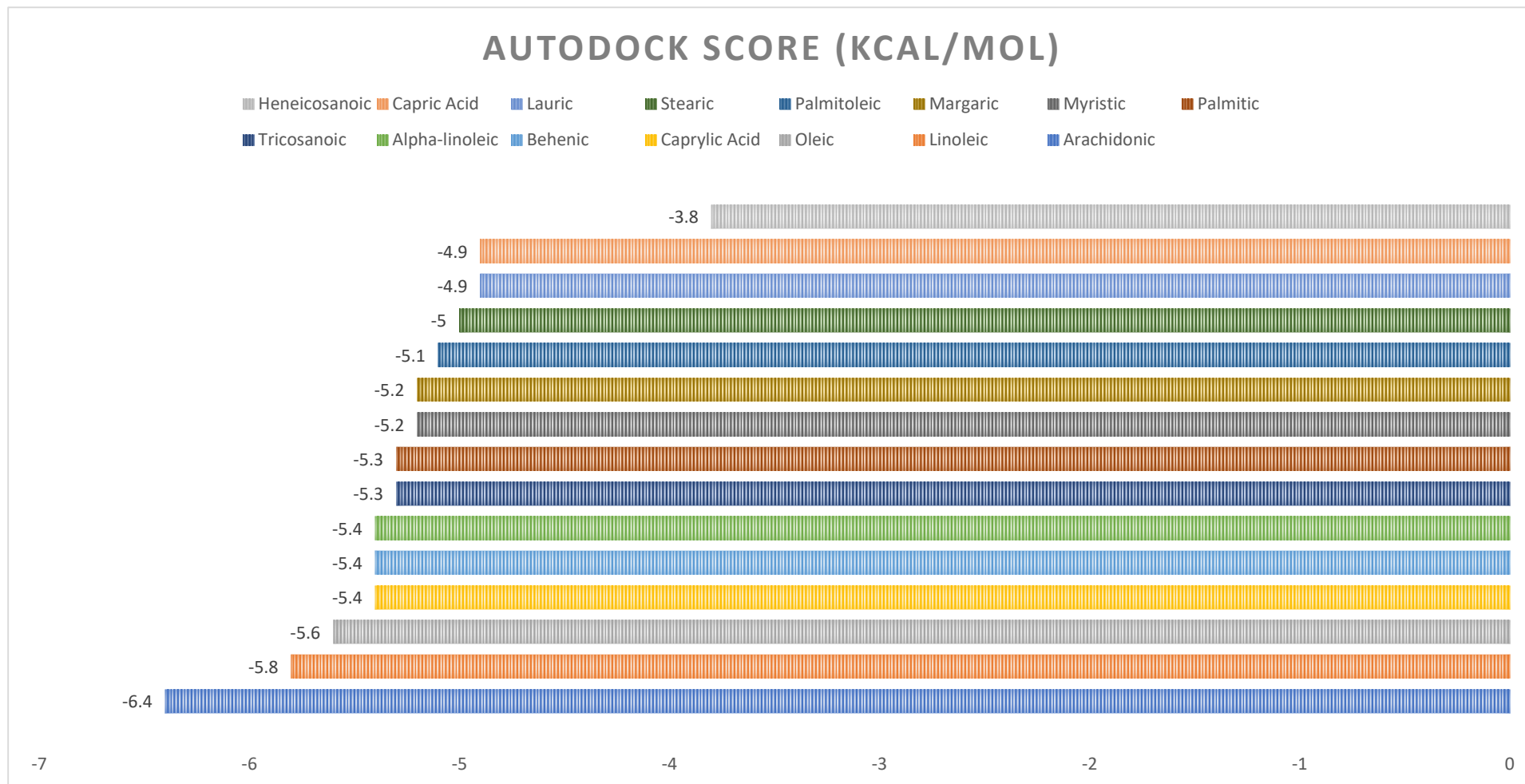


**Figure 58.** Molecular docking results of each fatty acid identified in *R. palmarum* larvae with ACE2 protein from highest interaction to lowest interaction (blue) and hydrogen bonds formed in the protein (ACE2)-ligand (fatty acid) interaction (orange).

Now, as described in section 3.4.12, it is known that omega-6 arachidonic fatty acid participates in inflammatory and immune responses (Natto et al., 2019); due to the fact that in immune cells, the cell membrane contains mostly arachidonic acid (Innes & Calder, 2020). In addition, this fatty acid is a main precursor of the synthesis of eicosanoids, which produce prostaglandins, which in turn regulate inflammation (Dennis & Norris, 2015). In SARS-CoV-2 viral infection, there are records that the use of non-steroidal anti-inflammatory drugs (Mazaleuskaya et al., 2015), increases the expression of ACE2 in the intestine, kidneys and lungs, causing the infection to be more aggressive (Hoffmann et al., 2020). This is caused by the fact that this type of medication selectively or not inhibits COX-1 (cytoprotective enzyme) and COX-2 (participates in the mechanisms of inflammation, inflammation and pain), which in turn block the cascade reactions of arachidonic acid for the formation of prostaglandins (Mazaleuskaya et al., 2015). This influence on viral control is also recorded in other types of viruses such as influenza and herpes (Kohn et al., 1980) (Tormar et al., 1987).

In the case of linoleic fatty acid (score = -5.8 kcal/mol), it also has a decent interaction, although inferior to arachidonic acid (score = -6.4 kcal/mol), with the ACE2 enzyme, coinciding with reports of in vivo experiments indicating inhibitory efficacy in viral binding between the spike protein (S) of SARS-CoV-2 and the ACE2 enzyme (Goc et al., 2021). Oleic acid (score = -5.6 kcal/mol), one of the two most abundant fatty acids in *R. palmarum* larvae (Table 7), indicates that it also has a decent interaction with the ACE2 enzyme, since this fatty acid also has anti-inflammatory potential and modulates biological functions of viruses (section 3.3.9). Behenic, caprylic and alpha-linoleic acids have a score of -5.4 kcal/mol, their interaction with the enzyme is lower than those mentioned above. The alpha-linoleic acid, which is particulate in inflammatory diseases (Pászti-Gere et al., 2016), while caprylic acid is effective against pathogens and viruses as well as behenic acid (section 3.3.1), the latter being considered as a toxin for cardiac muscle (Vetter et al., 2020). Palmitic, tricosanoic, myristic, margaric (-5.3 kcal/mol) and palmitoleic (-5.1 kcal/mol) acids do not have such a pronounced affinity for the ACE2 enzyme, but even so, antiviral properties (Goc et al., 2021) are reported, which suggests that despite not reacting to a great



extent with the ACE2 protein, they interact with pathogens that enter the human body (section 3.4.1 – 3.4.7 - 3.4.6 - 3.4.4.), with the exception of palmitic acid which participates in the regulation of angiogenesis (section 3.4.5.).

Finally, a protocol described in Chapter 5 was developed, in which anyone with basic knowledge of bioinformatics can perform molecular docking to determine protein-ligand interactions.

## CHAPTER 7: Conclusions

In-silico, studies need to have a long context to be accepted by the scientific community, in addition to the verification of the silicon studies themselves. In the present research, a different approach to the in-silico study was proposed, prioritizing the safety of the people who consume the *R. palmarum* larvae to verify their potential pharmaceutical activity. A historical context was established to show how insects have served as a source of medicine throughout the history of mankind, finding that insects have helped to fight bacterial and viral infections. Then, as observed in chapter 2, the biology of the species *Rhynchophorus Palmarum* is presented, thus discovering that the beetle of the Curculionidae family is considered a pest for palm plantations, being a vector of the nematode *Bursaphelenchinae Paramonov*, which causes the red ring disease. However, the larvae of *R. palmarum* are a source of food for the Ecuadorian Amazon populations because they are considered a great source of protein.

Upon learning about these properties, a bibliographic review of the food analysis developed by different authors in chapter 3 was carried out, where it was found that when insects consume plants, they metabolize the fatty acids found in these plants in their digestive tract and adopt the antioxidant, antibacterial and antiviral defense mechanism. Tables 5 and 6 show the food analysis of *R. palmarum* larvae by palm species. Table 7 shows the fatty acid profile found in *R. palmarum* larvae depending on the origin of the larvae; either from wild origin, specific type of palm or from the laboratory. It was concluded that the origin and diet of the *R. palmarum* larvae influence the content in their digestive tract and skin. After knowing the fatty acid content of *R. palmarum* larvae, an analysis of the medical properties (Chapter 3) of each one of them was carried out, finding that they possess antioxidant, antibacterial and antiviral activity. In addition, 3D reconstructions and optimizations of the fatty acids that will be used for molecular docking are presented. Therefore, from the bibliographic review, it is concluded that *R. palmarum* larvae are not only a high source of proteins, but also have a potential antiviral activity due to their composition.

For the initiation of the in-silico molecular docking studies, the ACE2 protein was chosen as the study target, because it is one of the enzymes that are

recognized by the protein S of the SARS-CoV-2 virus in the cell membrane. After establishing the target enzyme, we proceeded to reconstruct 3D and optimize the fatty acids found in *R. palmarum* larvae, using the Avogadro program. Meanwhile, the ACE enzyme was obtained from the PDB database. For its selection, as shown in Chapter 5, a validation of each model chosen was carried out, from a total of six models. A total of 15 molecular couplings were performed, where it was found that arachidonic (-6.4), linoleic (-5.8), oleic (-5.6), caprylic (-5.4), alpha-linoleic (-5.4), behenic (-5.4), palmitic (-5.3), tricosanoic (-5.3), myristic (-5.2), margaric (-5.2), palmitoleic (-5.1) and stearic (-5.1) have relevant interactions against the ACE2 enzyme, which is part of the SARS-CoV-2 virus replication cycle, allowing it to enter the cell cytoplasm. In conclusion, chontacuro does have potential antiviral activity.

## Bibliography

- Abram, M., Ferris, A., Shao, W., Alvord, W., & Hughes, S. (2010). Nature, position, and frequency of mutations made in a single cycle of HIV-1 replication. *J. Virol*, *84*(19), 9864-78. <https://doi.org/doi: 10.1128/JVI.00915-10>.
- Agostonia, C., Moreno, L., & Shamir, R. (2016). Palmitic Acid and Health: Introduction. *Critical Reviews in Food Science and Nutrition*, *56*(12), 1941-2. <https://doi.org/doi: 10.1080/10408398.2015.1017435>.
- Ahipo Dué, E., Zabri, H. C., Kouadio, J. P., & Kouamé, L. P. (2009). Fatty acid composition and properties of skin and digestive fat content oils from *Rhynchophorus palmarum* L. larva. *African Journal of Biochemistry Research*, *3*(4), 89-94. <http://internationalscholarsjournals.org/journal/ajmr>
- Aldana de la Torre, R., Aldana de la Torre, J., Moya, O., & Bustillo Pardey, A. (2015). Anillo rojo en palma de aceite. *Boletín Técnico No. 36*.
- Amicone, M., Borges, V., Alves, M. J., Isidro, J., Zé-Zé, L., Duarte, S., . . . Gordo, I. (2022). Mutation rate of SARS-CoV-2 and emergence of mutators during experimental evolution. *Evolution, Medicine, and Public Health*, *10*(1), 142-155. <https://doi.org/https://doi.org/10.1093/emph/eoac010>
- Andersen, J., Westi, E., & Jakobsen, E. (2021). Astrocyte metabolism of the medium-chain fatty acids octanoic acid and decanoic acid promotes GABA synthesis in neurons via elevated glutamine supply. *Mol Brain*, *132*. <https://doi.org/https://doi.org/10.1186/s13041-021-00842-2>
- Antwi-Boasiako, O., & Sander, K. (2020). Mechanisms of Action of trans Fatty Acids. *Advances in Nutrition*, *11*(3), 697-708. <https://doi.org/https://doi.org/10.1093/advances/nmz125>
- AOAC, I. (2007). *Official methods of analysis, 18th edn*. AOAC International, Gaithersburg.
- Araujo, Y., & Beserra, P. (2007). Diversidad de invertebrados consumidos por las etnias Yanomami y Yekuana del alto Orinoco, Venezuela. *INTERCIENCIA*, *32*(5), 318-323.
- Arrese, E., & Soulages, J. (2010). Insect Fat Body: Energy, Metabolism, And Regulation. *Annu Rev Entomol*, *55*, 207-25. <https://doi.org/doi: 10.1146/annurev-ento-112408-085356>
- Aurand, L., Woods, A., & Wells, M. (1987). *Food composition and analysis*. Van Nostrand Reinhold, New York.
- Ávalos, Y., Hernández-Cáceres, M., & Lagos, P. (2022). Palmitic acid control of ciliogenesis modulates insulin signaling in hypothalamic neurons through an autophagy-dependent mechanism. *Cell Death Dis*, *13*(659). <https://doi.org/https://doi.org/10.1038/s41419-022-05109-9>
- Balvers, M., Verhoeckx, K., Plastina, P., Wortelboer, H., & Meijerink, J. (2010). Docosahexaenoic acid and eicosapentaenoic acid are converted by 3T3-L1 adipocytes to N-acyl ethanolamines with anti-inflammatory properties. *Biochim Biophys Acta*, *10*, 1107-1114. <https://doi.org/DOI: 10.1016/j.bbalip.2010.06.006>

- Baral, P., Amin, M., Rashid, M., & Hossain, M. (2022). Assessment of Polyunsaturated Fatty Acids on COVID-19-Associated Risk Reduction. *Rev Bras Farmacogn.*, 32(1), 50-64. <https://doi.org/doi:10.1007/s43450-021-00213-x>.
- Batalha, M. d., Goulart, H. F., Santana, A. E., Barbosa, L. A., Ticiano, G. N., Da Silva, M. K., . . . Grillo, L. A. (2020). Chemical composition and antimicrobial activity of cuticular and internal lipids of the insect *Rhynchophorus palmarum*. *Insect Biochemistry and Physiology*, 105(1), e21723. <https://doi.org/https://doi.org/10.1002/arch.21723>
- Baujard, P. (1989). Remarques sur les genres des sous-familles Bursaphelenchinae Paramonov. *Nematoda: Aphelenchoididae. Revue de Nematologie*, 12, 323-324.
- Belouzard, S., Millet, J. K., Licitra, B. N., & Whittaker, G. R. (2012). Mechanisms of coronavirus cell entry mediated by the viral spike protein. *Viruses*, 4(6), 1011-1033. <https://doi.org/https://doi.org/10.3390/v4061011>
- BeMiller, J. N. (2010). Carbohydrate Analysis. In S. Nielsen, *Food Analysis* (pp. 147-179). Springer.
- Berembaum, M. R. (1995). *Bugs in the System: Insects and Their Impact on Human Affairs*. Addison-Wesley.
- Bergsson, G., Arnfinnsson, J., Steingrímsson, O., & Thormar, H. (2001). In vitro killing of *Candida albicans* by fatty acids and monoglycerides. *Antimicrob Agents Chemother*, 45(11), 3209-12. <https://doi.org/doi:10.1128/AAC.45>.
- Berman, H., Westbrook, J., Feng, Z., Gilliland, G., Bhat, T., Weissig, H., . . . Bourne, P. (2021). RCSB Protein Data Bank: powerful new tools for exploring 3D structures of biological macromolecules for basic and applied research and education in fundamental biology, biomedicine, biotechnology, bioengineering and energy sciences. *Nucleic Acids Research*, 49, D437–D451. <https://doi.org/doi:10.1093/nar/gkaa1038>
- BioRender. (2023). *BioRender*. BioRender: <https://app.biorender.com/illustrations/63bbfe34ffef52dd8d98b75e>
- Blondeau, N., Lipsky, R., Bourourou, M., Duncan, M., Gorelick, P., & Marini, A. (2015). Alpha-linolenic acid: an omega-3 fatty acid with neuroprotective properties-ready for use in the stroke clinic? *Biomed Res, PMC4350958*, 519830. <https://doi.org/doi:10.1155/2015/519830>.
- Bosch, B. J., van der Zee, R., de Haan, C. A., & Rottier, P. J. (2003). The coronavirus spike protein is a class I virus fusion protein: structural and functional characterization of the fusion core complex. *J. Virol.*, 77(16), 8801–8811. <https://doi.org/doi:10.1128/jvi.77.16.8801-8811.2003>.
- Bradley, R. L. (2010). Chapter 6: Moisture and Total Solids. In S. Nielsen, *Food Analysis Fourth Edition* (pp. 85-105 ). Springer .
- Brussel, K. V., & Holmes, E. C. (2022). Zoonotic disease and virome diversity in bats. *Current Opinion in Virology*, 52, 192-202. <https://doi.org/https://doi.org/10.1016/j.coviro.2021.12.008>.

- Caravaca, F., Castel, J., Guzman, J., Delgado, M., Mena, Y., Alcalde, M., & Gonzalez, P. (2003). Composicion analitica de los alimentos. In C. Rodríguez, *Bases de la produccion*. Universidad de Sevilla.
- Carrera, M. (1993). A entomologia na história natural de Plínio. *Revista Brasileira de Entomologia*, 37(2), 387-396.
- Carrillo, M., Cavia, M., & Torre, A. (2012). Role of oleic acid in immune system; mechanism of action; a review. *Nutr Hosp*, 27(4), 978-990. <https://doi.org/DOI:10.3305/nh.2012.27.4.5783>
- Carta, G., Murru, E., Banni, S., & Manca, C. (2017). Palmitic Acid: Physiological Role, Metabolism and Nutritional Implications. *Front. Physiol.*, 8(902). <https://doi.org/doi:10.3389/fphys.2017.00902>
- Cartay, R. (2016). *La mesa amazónica peruana. Ingredientes, corpus, símbolos*. Lima: Universidad San Martín de Porres.
- Cartay, R., Dimitrov, V., & Feldman, M. (2020). An Insect Bad for Agriculture but Good for Human Consumption: The Case of *Rhynchophorus palmarum*: A Social Science Perspective. In H. Mikkola, *Edible Insects*. IntechOpen. <https://doi.org/DOI:10.5772/intechopen.87165>
- Cerda, H., Martinez, R., Briceno, N., Pizzoferrato, L., Manzi, P., Tommaseo Ponzetta, M., . . . Paoletti, M. (2001). Palm worm: (*Rhynchophorus palmarum*) traditional food in Amazonas, Venezuela—nutritional composition, small scale production and tourist palatability. *Ecology of Food and Nutrition*, 40(1), 13-32. <https://doi.org/DOI:10.1080/03670244.2001.9991635>
- Césard, N., Deturche, J., & Erikson, P. (2003). Les insectes dans les pratiques médicinales et rituelles d'Amazonie indigène. In J. M. Thomas, *Insects in oral litterature and traditions* (pp. 395-406). Paris Louvain : Peeters-SELAF (Ethnoscience).
- Chang, S. (2010). Protein Analysis. In S. Nielsen, *Food Analysis* (pp. 133-147). Springer.
- Charles, E. I., Litov, R. E., & Halldor, T. (1995). Antimicrobial activity of lipids added to human milk, infant formula, and bovine milk. *The Journal of Nutritional Biochemistry*, 6(7), 362 - 366. [https://doi.org/https://doi.org/10.1016/0955-2863\(95\)80003-U](https://doi.org/https://doi.org/10.1016/0955-2863(95)80003-U).
- Chaves, J. A., Ortiz, D. P., Bahos, E. M., Ordoñez, G. A., & Villota, D. C. (2020). Análisis del perfil de ácidos grasos y propiedades fisicoquímicas del aceite de palma de mil pesos (*Oenocarpus Bataua*) . *Perspectivas en Nutrición Humana* , 22(2), 175-188. <https://doi.org/DOI:10.17533/udea.penh.v22n2a05>
- Chico-Avelino, M., López-Mejía, A., Ramos-Frías, J., Villafuentes-Téllez, H. A., Menchaca-Armenta, I., Montoya-Ayala, R., . . . Manning-Cela, R. G. (2022). Synanthropic triatomines in Hidalgo state, Mexico: Spatial-temporal distribution, domestic transmission cycle, and natural infection with *Trypanosoma cruzi*. *Acta Tropica*, 234(106618). <https://doi.org/https://doi.org/10.1016/j.actatropica.2022.106618>.
- Chinchilla, C., & Escobar, R. (2007). El anillo rojo y otras enfermedades de la palma aceitera en Centro y Suramérica. *ASD Oil Palm Papers.*, 30, 1-27.

- Choque, B., Catheline, D., Rioux, V., & Legrand, P. (2014). Linoleic acid: Between doubts and certainties. *Biochimie*, *96*, 14-21. <https://doi.org/https://doi.org/10.1016/j.biochi.2013.07.012>
- Choudhary, P., Kumar Sharma, A., Kumar Mishra, Y., & Nayak, S. (2022). Entomotherapy medicinal significance of insects: A review. *The Pharma Innovation Journal*, *11*(4), 25-29. [https://doi.org/ISSN \(E\): 2277- 7695](https://doi.org/ISSN(E):2277-7695)
- Conconi, J., & Pino, J. (1988). The utilization of insects in the empirical medicine of ancient Mexicans. *Journal of Ethnobiology*, *8*, 195-202.
- Costa Neto. (1999). *“Barata é um santo remédio”: introdução à zooterapiapopular no Estado da Bahia*. Universidade Estadual de Feira de Santana. [https://doi.org/857395017X, 9788573950175](https://doi.org/857395017X,9788573950175)
- Costa Neto, E. (2002). The Use of Insects in Folk Medicine in the State of Bahia, Northeastern Brazil, with Notes on Insects Reported Elsewhere in Brazilian Folk Medicine. *Human Ecology*, *30*, 245-263. <https://doi.org/https://doi.org/10.1023/A:1015696830997>
- Costa Neto, E. (2003). *Etnoentomologia no povoado de Pedra Branca, município de Santa Terezinha, Bahia. Um estudo de caso das interações seres humanos/insetos*. São Carlos: Tese (Doutorado em Ciências Biológicas) - Universidade Federal de São Carlo. <https://doi.org/https://repositorio.ufscar.br/handle/ufscar/1651>
- Costa Neto, E., & Melo, M. (1998). Entomotherapy in the country of Matinha dos Pretos. *The Food Insects Newsletter*, *11*(2), 1-3.
- Costa-Neto, E. (2005). Entomotherapy, or the medicinal use of insects. *Journal of Ethnobiology and Ethnomedicine*, *25*, 93-114.
- Dahms, S., Pautsch, A., & Brandstetter, H. (2022). X-ray structure of furin in complex with the dichlorophenylpyridine-based inhibitor 1. [https://doi.org/doi: 10.1021/acscchembio.2c00103](https://doi.org/doi:10.1021/acscchembio.2c00103)
- Dalbon, V., Acevedo, J., Ribeiro Junior, K., Ribeiro, T., da Silva, J., Fonseca, H., . . . Porcelli, F. (2021). Perspectives for Synergic Blends of Attractive Sources in South American Palm Weevil Mass Trapping: Waiting for the Red Palm Weevil Brazil Invasion. *Insects*, *12*(828). <https://doi.org/https://doi.org/10.3390/insects12090828>
- Davies, J. (2008). Arachidonic Acid. *Elsevier Inc.*, 1-4.
- Dayrit, F. (2015). The Properties of Lauric Acid and Their Significance in Coconut Oil. *J Am Oil Chem Soc*, *92*, 1–15. <https://doi.org/https://doi.org/10.1007/s11746-014-2562-7>
- De La Mora Castañeda, J. G., Chan Cupul, W., Durán Puga, N., González Eguiarte, D. R., Ruiz Corral, J. A., & Muñoz Urias, A. (2022). Eficacia de trampeo y fluctuación poblacional de *Rhynchophorus palmarum* en dos plantaciones de coco. *II Simposio Internacional de Parasitología Agrícola*, *26*(2). [https://doi.org/DOI: https://doi.org/10.53897/RevAIA.22.26.12](https://doi.org/DOI:https://doi.org/10.53897/RevAIA.22.26.12)
- De La Mora, J. G., Chan, W., Durán, N., González, D., Ruiz, J., & Muñoz, A. (2022). Eficacia de trampeo y fluctuación poblacional de *Rhynchophorus palmarum* en dos plantaciones de coco. *II Simposio Internacional de Parasitología Agrícola. AIA. 2022. 26*

(Suplemento): 5-6. México: AVANCES EN INVESTIGACIÓN AGROPECUARIA.  
<https://doi.org/http://doi.org/10.53807/revAIA.22.26.12>

- De la Mora-Castañeda, J. G., Chan-Cupul, W., Durán-Puga, N., González-Eguiarte, D. R., Ruíz-Corral, J. A., & Muñoz-Urias, A. (2022). Cost-benefit of trapping and population fluctuation of *Rhynchophorus palmarum* L. in coconut (*Cocos nucifera* L.) genotypes. *Revista Chapingo Serie Ciencias Forestales y del Ambiente*, 28(3), 447-463.  
<https://doi.org/doi:https://doi.org/10.5154/r.rchscfa.2022.02.010>
- Delgado, C., Romero, R., Vásquez Espinoza, R., Trigozo, M., & Correa, R. (2019). *Rhynchophorus palmarum* used in Traditional Medicine in the Peruvian Amazon. *Ethnobiology Letters*, 10(1), 120-128.  
<https://doi.org/https://doi.org/10.14237/ebl.10.1.2019.1271>
- Dennis, E., & Norris, P. (2015). Eicosanoid storm in infection and inflammation. *Nat Rev Immunol.*, 15(8), 511-23. <https://doi.org/doi:10.1038/nri3859>.
- Eberhardt, J., Santos-Martins, D., Tillack, A., & Forli, S. (2021). AutoDock Vina 1.2.0: New Docking Methods, Expanded Force Field, and Python Bindings. *Journal of Chemical Information and Modeling.*, 61(8), 3891–3898.  
<https://doi.org/https://doi.org/10.1021/acs.jcim.1c00203>
- Ellefson, W. (2017). Fat Analysis. In S. Nielsen, *Food Analysis. Food Science Text Series* (pp. 299-314). Springer.
- EPPO. (2020). *Rhynchophorus palmarum*. EPPO datasheets on pests recommended for regulation.: <https://gd.eppo.int>
- Espinosa, A. M., Hidalgo, A. A., & Mayorga, E. L. (2020). THE NUTRITIONAL VALUE AND CHARACTERIZATION OF THE FATTY ACIDS OF CHONTACURO *Rhynchophorus palmarum* L. *InfoANALÍTICA*, 8(1), 127-138. <https://doi.org/DOI:10.26807/ia.v8i1.122>
- Esser, R., & Meredith, J. (1987). Red ring nematode. *Nematology Circular of the Florida Department of Agriculture*, 141.
- Feng, M., Fei, S., Xia, J., Labropoulou, V., Swevers, L., & Sun, J. (2020). Antimicrobial Peptides as Potential Antiviral Factors in Insect Antiviral Immune Response. *Front. Immunol*, 11(2030). <https://doi.org/doi:10.3389/fimmu.2020.02030>
- Flores-Pacheco, J. A., Ruiz Zolano, E. A., & Obregón Hernández, A. J. (2022). Epidemiología del picudo del cocotero como vector de la enfermedad del anillo rojo en plantaciones de palma africana. *Wani*, 38(76), 70-83.  
<https://doi.org/https://doi.org/10.5377/wani.v38i76.13377>
- Florindo, H., Kleiner, R., & Vaskovich-Koubi, D. (2020). Immune-mediated approaches against COVID-19. *Nat. Nanotechnol*, 15, 630–645.  
<https://doi.org/https://doi.org/10.1038/s41565-020-0732-3>
- Food And Agriculture Organization Of The United Nations. (2013). *Edible insects: future prospects for food and feed security*. FAO. <https://doi.org/ISBN978-92-5-107595-1>
- Frémy, E. (1842). *Memoire sur les produits de la saponification de l'huile de palme*. Diario de Pharmacie et de Chimie. XII : 757.



- Frigolet, M. E., & Gutiérrez-Aguilar, R. (2017). The Role of the Novel Lipokine Palmitoleic Acid in Health and Disease. *Advances in Nutrition*, 8(1), 1735-1812. <https://doi.org/https://doi.org/10.3945/an.115.011130>
- Gagnon, L., Leduc, M., Thibodeau, J.-F., & Zhang, M.-Z. (2018). A Newly Discovered Antifibrotic Pathway Regulated by Two Fatty Acid Receptors: GPR40 and GPR84. *The American Journal of Pathology*, 188(5), 1132-1148. <https://doi.org/https://doi.org/10.1016/j.ajpath.2018.01.009>.
- Gebhardt, J. T., Thomson, K. A., Woodworth, J. C., Dritz, S. S., Tokach, M. D., DeRouchey, J. M., . . . Burkey, T. E. (2020). Effect of dietary medium-chain fatty acids on nursery pig growth performance, fecal microbial composition, and mitigation properties against porcine epidemic diarrhea virus following storage. *Journal of Animal Science*, 98(1), skz358. <https://doi.org/https://doi.org/10.1093/jas/skz358>
- Giblin-Davis, R., Faleiro, J., Jacas, J., Peña, J., & Vidyasagar, P. (2013). Biology and management of the red palm weevil, *Rhynchophorus ferrugineus*. In J. E. Peña, *Potential Invasive Pests of Agricultural Crops*, (pp. 1-34). CABI Publishing Oxfordshire, U.K.
- Giblin-Davis, R., Gerber, K., & Griffith, R. (1989). Laboratory rearing of *Rhynchophorus cruentatus* and *R. palmarum* (Coleoptera: Curculionidae). *Florida Entomologist*, 72(3), 480-488. <https://doi.org/https://doi.org/10.2307/3495186>
- Giske, C., Monnet, D., Cars, O., & Carmeli, Y. (2008). Clinical and economic impact of common multidrug-resistant gram-negative bacilli. *Antimicrob Agents Chemother*, 52(3), 813-21. <https://doi.org/doi:10.1128/AAC.01169-07>.
- Goc, A., Niedzwiecki, A., & Rath, M. (2021). Polyunsaturated  $\omega$ -3 fatty acids inhibit ACE2-controlled SARS-CoV-2 binding and cellular entry. *Sci Rep*, 11, 5207. <https://doi.org/https://doi.org/10.1038/s41598-021-84850-1>
- Gogna, S., Kaur, J., Sharma, K., Bhadariya, V., Singh, J., Kumar, V., . . . Vipasha, V. (2022). A systematic review on the role of alpha linolenic acid (ALA) in combating non-communicable diseases (NCDs). *Nutrition & Food Science*. <https://doi.org/https://doi.org/10.1108/NFS-01-2022-0023>
- Gómez-Marco, F., Klompen, H., & Hoddle, M. S. (2021). Phoretic mite infestations associated with *Rhynchophorus palmarum* (Coleoptera: Curculionidae) in southern California. *Systematic and Applied Acarology*, 26(10), 1913-1926. <https://doi.org/https://doi.org/10.11158/saa.26.10.6>
- Gudger, E. (1925). Sticking wounds with the mandibles of ants and beetles. *Journal of the American Medical Association*, 84(24), 1861-1864.
- Gunduz, F., Aboulnasr, F., Chandra, P., Hazari, S., Poat, B., Baker, D., . . . Dash, S. (2012). Free fatty acids induce ER stress and block antiviral activity of interferon alpha against hepatitis C virus in cell culture. *Virology Journal*, 9(143), 1-12. <https://doi.org/DOI:10.1186/1743-422X-9-143>
- Gunstone, F., Harwood, J., & Dijkstra, A. (2007). *The Lipid Handbook with CD-ROM*. Third ed. CRC Press.

- Hagley, E. A. (1965). On the life history and habits of the palm weevil, *Rhynchophorus palmarum*. *Annals of the Entomological Society of America*, 58(1), 22-28. <https://doi.org/https://doi.org/10.1093/aesa/58.1.22>
- Halgren, T. (1996). Merck molecular force field. I. Basis, form, scope, parameterization, and performance of MMFF94. *Journal of Computational Chemistry*, 17(5-6), 490-519. [https://doi.org/https://doi.org/10.1002/\(SICI\)1096-987X\(199604\)17:5/6<490::AID-JCC1>3.0.CO;2-P](https://doi.org/https://doi.org/10.1002/(SICI)1096-987X(199604)17:5/6<490::AID-JCC1>3.0.CO;2-P)
- Hamming, I., Timens, W., Bulthuis, M., Lely, A., Navis, G., & van Goor, H. (2004). Tissue distribution of ACE2 protein, the functional receptor for SARS coronavirus. A first step in understanding SARS pathogenesis. *J Pathol.*, Jun;203(2), 631-7. <https://doi.org/doi:10.1002/path.1570>.
- Hanwell, M. D., Curtis, D. E., Lonie, D. C., Vandermeersch, T., Zurek, E., & Hutchison, G. R. (2012). Avogadro: An advanced semantic chemical editor, visualization, and analysis platform. *Journal of Cheminformatics*, 4(17). <https://doi.org/https://doi.org/10.1186/1758-2946-4-17>
- Hasan, A., Paray, B. A., Hussain, A., Qadir, F. A., Attar, F., Aziz, F. M., . . . Mehrabi, M. (2020). A review on the cleavage priming of the spike protein on coronavirus by angiotensin-converting enzyme-2 and furin. . *Journal of Biomolecular Structure and Dynamics*, 39(8), 3025-3033. <https://doi.org/doi:10.1080/07391102.2020.1754293>.
- Hathaway, D., Pandav, K., Patel, M., Riva-Moscoso, A., Singh, B., Patel, A., . . . Abreu, R. (2020). Omega 3 Fatty Acids and COVID-19: A Comprehensive Review. . *Infect Chemother*, 52(4), 478-495. <https://doi.org/doi:10.3947/ic.2020.52.4.478>.
- Hayata, H., Miyazaki, H., Niisato, N., Yokoyama, N., & Marunaka, Y. (2014). Lowered extracellular pH is involved in the pathogenesis of skeletal muscle insulin resistance. *Biochemical and Biophysical Research Communications*, 445(1), 170-174. <https://doi.org/https://doi.org/10.1016/j.bbrc.2014.01.162>.
- He, M., & Ding, N.-Z. (2020). Plant Unsaturated Fatty Acids: Multiple Roles in Stress Response. *Frontiers in Plant Science*, 11(562785), 1-15. <https://doi.org/https://doi.org/10.3389/fpls.2020.562785>
- He, M., He, C. Q., & Ding, N. Z. (2018). Abiotic stresses: General defenses of land plants and chances for engineering multistress tolerance. *Frontiers in Plant Science*, 9(1771). <https://doi.org/https://doi.org/10.3389/fpls.2018.01771>
- Henry, G. E., Momin, R. A., Nair, M., & Dewitt, D. L. (2002). Antioxidant and cyclooxygenase activities of fatty acids found in food. *J. Agric Food Chem*, 50(8), 2231-2234. <https://doi.org/doi:10.1021/jf0114381>.
- Hermans, W., Senden, J., Churchward-Venne, T., Paulussen, K., Fuchs, C., Smeets, J., . . . Van Loon, L. (2021). Insects are a viable protein source for human consumption: from insect protein digestion to postprandial muscle protein synthesis in vivo in humans: a double-blind randomized trial. *Am J Clin Nutr.*, 114(3), 934-944. <https://doi.org/doi:10.1093/ajcn/nqab115>. PMID: 34020450; PMCID: PMC8408844.

- Hoddle, M. S. (2022). *Rhynchophorus palmarum* egg. *Rhynchophorus palmarum* (RHYCPA). EPPO Global Database.
- Hoddle, M. S., Hoddle, C. D., & Milosavljevi, I. (2021). Quantification of the Life Time Flight Capabilities of the South American Palm Weevil, *Rhynchophorus palmarum* (L.) (Coleoptera: Curculionidae). *Insects*, *12*(126).  
<https://doi.org/https://doi.org/10.3390/insects12020126>
- Hoffmann, M., Kleine-Weber, H., Schroeder, S., Krüger, N., Herrler, T., Erichsen, S., . . . Pöhlmann, S. (2020). SARS-CoV-2 Cell Entry Depends on ACE2 and TMPRSS2 and Is Blocked by a Clinically Proven Protease Inhibitor. *Cell.*, *181*(2), 271-280.e8.  
<https://doi.org/doi:10.1016/j.cell.2020.02.052>.
- Hofmann, H., Pyrc, K., & van der Hoek, L. G. (2005). Human coronavirus NL63 employs the severe acute respiratory syndrome coronavirus receptor for cellular entry. *Proceedings of the National Academy of Sciences*, *102*(22), 7988–7993.  
<https://doi.org/https://doi.org/10.1073/pnas.0409465102>
- Huang, X., Dong, W., Milewska, A., Golda, A., Qi, Y., Zhu, Q. K., . . . Sui, J. (2015). Human Coronavirus HKU1 spike protein uses O-acetylated sialic acid as an attachment receptor determinant and employs hemagglutinin-esterase protein as a receptor-destroying enzyme. *Journal of Virology*, *89*(14), 7202–7213.  
<https://doi.org/https://doi.org/10.1128/JVI.00854-15>
- Huang, Y., Yang, C., & Xu, X. (2020). Structural and functional properties of SARS-CoV-2 spike protein: potential antiviral drug development for COVID-19. *Acta Pharmacol Sin*, *41*, 1141–1149. <https://doi.org/https://doi.org/10.1038/s41401-020-0485-4>
- Hulbert, A. J. (2021). The under-appreciated fats of life: the two types of polyunsaturated fats. *Journal of Experimental Biology*, *224*(8), jeb232538.  
<https://doi.org/https://doi.org/10.1242/jeb.232538>
- Hwabin, J., Lee, Y. J., & Yoon, W. B. (2018). Effect of Moisture Content on the Grinding Process and Powder Properties in Food: A Review. *Processes*, *6*(69).  
<https://doi.org/doi:10.3390/pr6060069>
- Iannacone, J., & Alvareño, L. (2006). Diversity Of Terrestrial Arthropofauna From The Junin Natural Reserve, Peru. *Ecología Aplicada*, *5*(1,2). <https://doi.org/ISSN1726-2216>
- Ibrahim, I. M., Abdelmalek, D. H., Elshahat, M. E., & Elfiky, A. A. (2020). COVID-19 spike-host cell receptor GRP78 binding site prediction. *Journal of Infection*, *80*(5), 554–562.  
<https://doi.org/https://doi.org/10.1016/j.jinf.2020.02.026>
- Iijima, H., Kasai, N., Chiku, H., Murakami, S., Sugawara, F., Sakaguchi, K., . . . Mizushima, Y. (2006). The inhibitory action of long-chain fatty acids on the DNA binding activity of p53. *Lipids*, *41*(6), 521-527. <https://doi.org/doi:10.1007/s11745-006-5000-2>.
- Innes, J., & Calder, P. (2020). Marine Omega-3 (N-3) Fatty Acids for Cardiovascular Health: An Update for 2020. *Int J Mol Sci.*, *21*(4), 1362. <https://doi.org/doi:10.3390/ijms21041362>.
- Jaimes, J., André, N., Chappie, J., Millet, J., & Whittaker, G. (2020). Phylogenetic Analysis and Structural Modeling of SARS-CoV-2 Spike Protein Reveals an Evolutionary Distinct and

- Proteolytically Sensitive Activation Loop. *J Mol Biol.*, 432(10), 3309-3325. <https://doi.org/doi:10.1016/j.jmb.2020.04.009>.
- Jandacek, R. J. (2017). Linoleic Acid: A Nutritional Quandary. *Healthcare*, 5(2), 25. <https://doi.org/https://doi.org/10.3390/healthcare5020025>
- Jensen, R. G., Ferris, A. M., Lammi-Keefe, C. J., & Henderson, R. A. (1990). Lipids of Bovine and Human Milks: A Comparison. *Journal of Dairy Science*, 73(2), 223-240. [https://doi.org/https://doi.org/10.3168/jds.S0022-0302\(90\)78666-3](https://doi.org/https://doi.org/10.3168/jds.S0022-0302(90)78666-3)
- Kalaimathi, R., Krishnaveni, K., Murugan, M., Basha, A., Gilles, A., Kandeepan, C., . . . Dhakar, R. (2022). ADMET informatics of Tetradecanoic acid (Myristic Acid) from ethyl acetate fraction of *Moringa oleifera* leaves. *JDDT*, 12(4-S), 101-111. <http://jddtonline.info/index.php/jddt/article/view/5533>
- Karacor, K., & Cam, M. (2015). Effects of oleic acid. *Medical Science and Discovery*, 2(1), 125-132. <https://doi.org/https://doi.org/10.17546/msd.25609>
- Katdare, A., Thakkar, S., Dhepale, S., Khunt, D., & Misra, M. (2019). Fatty acids as essential adjuvants to treat various ailments and their role in drug delivery: A review. *Nutrition*, 65(ISSN 0899-9007), 138-157. <https://doi.org/https://doi.org/10.1016/j.nut.2019.03.008>.
- Kenar, J. A., Moser, B. R., & List, G. R. (2017). Naturally Occurring Fatty Acids: Source, Chemistry, and Uses. In M. U. Ahmad, *Fatty Acids: Chemistry, Synthesis, and Applications* (p. 39). Elsevier Inc.
- Keweloh, H., & Heipieper, H. J. (1996). Trans unsaturated fatty acids in bacteria. *Lipids*, 31(2), 129-137. <https://doi.org/https://doi.org/10.1007/BF02522611>
- Khan, R. J., Jha, R. K., Amera, G., Jain, M., Singh, E., Pathak, A., . . . Singh, A. K. (2020). Targeting SARS-CoV-2: A systematic drug repurposing approach to identify promising inhibitors against 3C-like proteinase and 2'-O-RiboseMethyltransferase. *Journal of Biomolecular Structure and Dynamics*, 39(8), 2679-2692. <https://doi.org/doi:10.1080/07391102.2020>.
- Kim, S., Chen, J., Cheng, T., Gindulyte, A., He, J., He, S., . . . Bolton, E. E. (2019). PubChem in 2021: new data content and improved web interfaces. *Nucleic Acids Res.*, 49(D1), D1388–D1395. <https://doi.org/https://doi.org/10.1093/nar/gkaa971>
- Kim, Y.-G., Lee, J.-H., Park, S., Kim, S., & Lee, J. (2021). Inhibition of polymicrobial biofilm formation by saw palmetto oil, lauric acid and myristic acid. *Microbial Biotechnology*, 15(2), 590-602. <https://doi.org/https://doi.org/10.1111/1751-7915.13864>
- Kirk, R., Sawyer, R., & Egan, H. (1996). *Composicion y analisis de los alimentos*. Pearson.
- Kleinehr, J., Wilden, J., Boergeling, Y., Ludwig, S., & Hrinčius, E. (2021). Metabolic Modifications by Common Respiratory Viruses and Their Potential as New Antiviral Targets. *Viruses*, Oct 14;13(10), 2068. <https://doi.org/doi:10.3390/v13102068>.
- Kohn, A., Gitelman, J., & Inbar, M. (1980). Unsaturated free fatty acids inactivate animal enveloped viruses. *Arch. Virol.*, 66(4), 301-307. <https://doi.org/DOI:10.1007/BF01320626>

- Kothapalli, K., Park, H., & Brenna, J. (2020). Polyunsaturated fatty acid biosynthesis pathway and genetics. implications for interindividual variability in prothrombotic, inflammatory conditions such as COVID-19☆☆☆,★,★★. *Prostaglandins Leukot Essent Fatty Acids.*, Nov;162:102183. <https://doi.org/doi: 10.1016/j.plefa.2020.102183>.
- Kuklinski, C. (2003). *Nutricion Y Bromatologia*. Omega. <https://doi.org/ISBN: 9788428213301>
- Lake, M. (2020). What we know so far: COVID-19 current clinical knowledge and research. *Clin. Med.*, 20(2), 124-127. <https://doi.org/doi: 10.7861/clinmed.2019-coron>.
- Lan, J., & Jiwan Ge, J. Y. (n.d.).
- Lan, J., Ge, J., Yu, J., Shan, S., Zhou, H., Fan, S., . . . Wang, X. (2020). Structure of the SARS-CoV-2 spike receptor-binding domain bound to the ACE2 receptor. *Nature*, 581, 215-220. <https://doi.org/https://doi.org/10.1038/s41586-020-2180-5>
- Lan, J., Ge, J., Yu, J., Shan, S., Zhou, H., Fan, S., . . . Wang, X. (2020). Structure of the SARS-CoV-2 spike receptor-binding domain bound to the ACE2 receptor. *Nature.*, May;581(7807), 215-220. <https://doi.org/doi: 10.1038/s41586-020-2180-5>.
- Lan, Q., Chan, J., Xu, W., Wang, L., Jiao, F., Zhang, G., . . . Wang, Q. (2022). A Palmitic Acid-Conjugated, Peptide-Based pan-CoV Fusion Inhibitor Potently Inhibits Infection of SARS-CoV-2 Omicron and Other Variants of Concern. *Viruses*, 14(3:549), 1-11. <https://doi.org/doi: 10.3390/v14030549>.
- Lemarié, F., Beauchamp, E., Legrand, P., & Rioux, V. (2016). Revisiting the metabolism and physiological functions of caprylic acid (C8:0) with special focus on ghrelin octanoylation. *Biochimie*, 120(ISSN 0300-9084), 40-48. <https://doi.org/https://doi.org/10.1016/j.biochi.2015.08.002>.
- Li, F. (2016). Structure, Function, and Evolution of Coronavirus Spike Proteins. *Annu Rev Virol.*, 3(1), 237-261. <https://doi.org/doi: 10.1146/annurev-virology-110615-042301>.
- Li, F., Berardi, M., Li, W., Farzan, M., Dormitzer, P., & Harrison, S. (2006). Conformational states of the severe acute respiratory syndrome coronavirus spike protein ectodomain. *J Virol.*, Jul;80(14), 6794-800. <https://doi.org/doi: 10.1128/JVI.02744-05>.
- Liang, X., Huang, Y., Pan, X., Hao, Y., Chen, X., & Jiang, H. (2020). Erucic acid from *Isatis indigotica* Fort. suppresses influenza A virus replication and inflammation in vitro and in vivo through modulation of NF-κB and p38 MAPK pathway. *Journal of Pharmaceutical Analysis*, 10(2), 130-146. <https://doi.org/https://doi.org/10.1016/j.jpha.2019.09.005>.
- Lieberman, S., Enig, M. G., & Preuss, H. G. (2006). A Review of Monolaurin and Lauric Acid: Natural Virucidal and Bactericidal Agents. *Alternative and Complementary Therapies.*, 12(6), 310-314. <https://doi.org/http://doi.org/10.1089/act.2006.12.310>
- Liebert, M. (1987). Final Report on the Safety Assessment of Oleic Acid, Laurie Acid, Palmitic Acid, Myristic Acid, and Stearic Acid. *Journal Of The American College Of Toxicology*, 6(3), 321-401.

- Lindwasser, O., & Resh, M. (2002). Myristoylation as a target for inhibiting HIV assembly: unsaturated fatty acids block viral budding. *Proc Natl Acad Sci U S A*, *99*(20), 13037-42. <https://doi.org/doi:10.1073/pnas.212409999>.
- Linnaeus, C. (1758). *Systema Naturae* (10th Edition ed.). Books, LLC. <https://doi.org/115691034X,9781156910344>
- Lippi, G., Lavie, C., Henry, B., & Sanchis-Gomar, F. (2020). (COVID-19)?, Do genetic polymorphisms in angiotensin converting enzyme 2 (ACE2) gene play a role in coronavirus disease 2019. *Clinical Chemistry and Laboratory Medicine (CCLM)*, *58*(9), 1415-1422. <https://doi.org/https://doi.org/10.1515/cclm-2020-0727>
- List, G. R., Kenar, J. A., & Moser, B. R. (2017). History of Fatty Acids Chemistry. In M. U. Ahmad, *Fatty Acids: Chemistry, Synthesis, and Applications* (pp. 2-18). Elsevier Inc.
- Loften, J., Linn, J., Drackley, J., Jenkins, T., Soderholm, C., & Kertz, A. (2014). Invited review: Palmitic and stearic acid metabolism in lactating dairy cows. *Journal of Dairy Science*, *97*(8), 4661-4674. <https://doi.org/https://doi.org/10.3168/jds.2014-7919>.
- Löhr, B., Vásquez-Ordóñez, A., & Becerra Lopez-Lavalle, L. (2015). *Rhynchophorus palmarum* in disguise: Undescribed polymorphisms in the 'black' palm weevil. . *PLoS One*, *10*(12), e0143210. <https://doi.org/https://do.org/10.1371/journal.pone.0143210>
- López-Luján, L. M., Ramírez-Restrepo, S., Bedoya-Pérez, J. C., Salazar-Yepes, M., Arbeláez-Agudelo, N., & Granada-García, D. (2022). Bioactivity of fungi isolated from coconut growing areas against *Rhynchophorus palmarum*. *Pesquisa Agropecuária Brasileira*, *57*(e02882), 2-8. <https://doi.org/DOI:10.1590/S1678-3921.pab2022.v57.02882>
- Lorgeril, M., & Salen, P. (2004). Alpha-linolenic acid and coronary heart disease. *Cardiovascular Diseases*, *14*(3), 162-169. [https://doi.org/https://doi.org/10.1016/S0939-4753\(04\)80037-1](https://doi.org/https://doi.org/10.1016/S0939-4753(04)80037-1)
- Luo, J., & Hu, H. (2014). Chapter Twelve - Thermally Activated TRPV3 Channels. *Current Topics in Membranes*, *74*, 325-364. <https://doi.org/https://doi.org/10.1016/B978-0-12-800181-3.00012-9>
- Maceda, J., & Chiñi, L. (2021). Larva of *Rhynchophorus palmarum* L. (Coleoptera: Curculionidae): Effect of diet on the synthesis of essential fatty acids. *Revista Verde de Agroecología e Desenvolvimento Sustentável*, *16*(2), 122-130. <https://doi.org/https://doi.org/10.18378/rvads.v16i2.8258>
- Mahmoudi, R., Ghareghani, M., Zibara, K., Tajali, A. M., Jand, Y., Azari, H., . . . Ghanbari, A. (2019). Alyssum homolocarpum seed oil (AHSO), containing natural alpha linolenic acid, stearic acid, myristic acid and  $\beta$ -sitosterol, increases proliferation and differentiation of neural stem cells in vitro. *BMC Complementary and Alternative Medicine.*, *19*(1), 113. <https://doi.org/https://doi.org/10.1186/s12906-019-2518-4>
- Mansky, L., & Temin, H. (1995). Lower in vivo mutation rate of human immunodeficiency virus type 1 than that predicted from the fidelity of purified reverse transcriptase. *J. Virol*, *69*(8), 5087-94. <https://doi.org/doi:10.1128/JVI.69.8.5087-5094.1995>.
- Marshall, M. R. (2010). Ash Analysis. In S. Nielsen, *Food Analysis* (pp. 105 - 117). Springer Science.

- Mazaleuskaya, L., Theken, K., Gong, L., Thorn, C., FitzGerald, G., Altman, R., & Klein, T. (2015). PharmGKB summary: ibuprofen pathways. *Pharmacogenet Genomics.*, 25(2), 96-106. <https://doi.org/doi:10.1097/FPC.0000000000000113>.
- Mexzón, R. G., Chinchilla, C. M., Castrillo, G., & Danny, S. (1994). Biología y hábitos de *Rhynchophorus palmarum* L. asociado a la palma aceitera en Costa Rica. *ASD Oil Palm Papers*, 8(8), 14-21.
- Meyer-Rochow, B. (2017). Therapeutic arthropods and other, largely terrestrial, folk-medicinally important invertebrates: a comparative survey and review. *Journal of Ethnobiology and Ethnomedicine*, 13(9), 1-31. <https://doi.org/DOI10.1186/s13002-017-0136-0>
- Min, D. B., & Ellefson, W. C. (2010). Fat Analysis. In S. Nielsen, *Food Analysis* (pp. 117-133). Springer.
- Mohd, A. S., Giribabu, N., Yelumalai, S., Shahzad, H., Kumar, E., & Salleh, N. (2021). Myristic acid defends against testicular oxidative stress, inflammation, apoptosis: Restoration of spermatogenesis, steroidogenesis in diabetic rats. *Life Sciences*, 278(ISSN 0024-3205), 119605. <https://doi.org/https://doi.org/10.1016/j.lfs.2021.119605>.
- Montgomery, R., Conway, T. W., & Spector, A. A. (1999). *Bioquímica: Casos y Textos*. Harcourt Brace de España, S.A. <https://doi.org/ISBNediciónoriginal:0-8151-6483-1>
- Morge, G. (1973). Entomology in the western world in antiquity and in medieval times. In R. Smith (Ed.), *History of Entomology* (pp. 37-80). Palo Alto : Annual Reviews.
- Mori, N., & Yoshinaga, N. (2011). Function and evolutionary diversity of fatty acid amino acid conjugates in insects. *Journal of Plant Interactions*, 6(2-3). <https://doi.org/https://doi.org/10.1080/17429145.2010.544412>
- Murphy, R. (2015). Chapter 1:Fatty Acids. In R. Murphy, *Tandem Mass Spectrometry of Lipids: Molecular Analysis of Complex Lipids*, (pp. 1-39). DOI: 10.1039/9781782626350-00001.
- Nair, M., Joy, J., Vasudevan, P., Hinckley, L., Hoagland, T., & Venkitanarayanan, K. (2005). Antibacterial Effect of Caprylic Acid and Monocaprylin on Major Bacterial Mastitis Pathogens. *Journal of Dairy Science*, 88(10), 3488-3495. [https://doi.org/https://doi.org/10.3168/jds.S0022-0302\(05\)73033-2](https://doi.org/https://doi.org/10.3168/jds.S0022-0302(05)73033-2).
- Nakajima, Y., Onohara, Y., Ito, K., & Yoshimoto, T. (2006). *Crystal Structure of Aminopeptidase N from Escherichia coli*. RCSB Protein Data Bank: DOI: 10.2210/pdb2DQ6/pdb
- National Center for Biotechnology Information . (2022, November 2). *PubChem Compound Summary for CID 11005, Myristic acid*. PubChem: <https://pubchem.ncbi.nlm.nih.gov/compound/Myristic-acid>.
- National Center for Biotechnology Information . (2022, November 1 ). *PubChem Compound Summary for CID 16898, Heneicosanoic acid*. PubChem: <https://pubchem.ncbi.nlm.nih.gov/compound/Heneicosanoic-acid>.
- National Center for Biotechnology Information . (2022, November 1). *PubChem Compound Summary for CID 444899, Arachidonic acid*. PubChem: <https://pubchem.ncbi.nlm.nih.gov/compound/Arachidonic-acid>.

National Center for Biotechnology Information . (2022, November 1). *PubChem Compound Summary for CID 445638, Palmitoleic acid*. PubChem: <https://pubchem.ncbi.nlm.nih.gov/compound/Palmitoleic-acid>.

National Center for Biotechnology Information . (2022, November 1). *PubChem Compound Summary for CID 445639, Oleic acid*. PubChem: <https://pubchem.ncbi.nlm.nih.gov/compound/Oleic-acid>.

National Center for Biotechnology Information. (2022, November 1). *PubChem Compound Summary for CID 10465, Heptadecanoic acid*. PubChem: <https://pubchem.ncbi.nlm.nih.gov/compound/Heptadecanoic-acid>.

National Center for Biotechnology Information. (2022, November 1). *PubChem Compound Summary for CID 17085, Tricosanoic acid*. PubChem: <https://pubchem.ncbi.nlm.nih.gov/compound/Tricosanoic-acid>.

National Center for Biotechnology Information. (2022, November 2). *PubChem Compound Summary for CID 2969, Decanoic acid*. . PubChem: <https://pubchem.ncbi.nlm.nih.gov/compound/Decanoic-acid>.

National Center for Biotechnology Information. (2022, November 1). *PubChem Compound Summary for CID 379, Octanoic acid*. PubChem: <https://pubchem.ncbi.nlm.nih.gov/compound/Octanoic-acid>

National Center for Biotechnology Information. (2022, November 2). *PubChem Compound Summary for CID 3893, Lauric acid*. PubChem: <https://pubchem.ncbi.nlm.nih.gov/compound/Lauric-acid>.

National Center for Biotechnology Information. (2022, November 1). *PubChem Compound Summary for CID 5280450, Linoleic acid*. PubChem: <https://pubchem.ncbi.nlm.nih.gov/compound/Linoleic-acid>.

National Center for Biotechnology Information. (2022, November 1). *PubChem Compound Summary for CID 5281, Stearic Acid*. PubChem: <https://pubchem.ncbi.nlm.nih.gov/compound/Stearic-Acid>.

National Center for Biotechnology Information. (2022, November 1). *PubChem Compound Summary for CID 8215, Docosanoic acid*. PubChem: <https://pubchem.ncbi.nlm.nih.gov/compound/Docosanoic-acid>

National Center for Biotechnology Information. (2022, November 2). *PubChem Compound Summary for CID 985, Palmitic Acid*. PubChem: <https://pubchem.ncbi.nlm.nih.gov/compound/Palmitic-Acid>.

National Center for Biotechnology Information. (2022, November 1). *PubChem Compound Summary for SID 16898, Heneicosanoic acid*. Guri Giaever, Pharmaceutical Sciences, University of British Columbia: <https://pubchem.ncbi.nlm.nih.gov/compound/Heneicosanoic-acid>

National Center for Biotechnology Information. (2023, 01 03). *Compound Summary Sialic Acid For Cid 906*. PubChem : <https://pubchem.ncbi.nlm.nih.gov/compound/Sialic-acid>



- Natto, Z., Yaghmoor, W., Alshaeri, H., & Van, D. T. (2019). Omega-3 Fatty Acids Effects on Inflammatory Biomarkers and Lipid Profiles among Diabetic and Cardiovascular Disease Patients: A Systematic Review and Meta-Analysis. . *Sci Rep.*, *9*(1), 18867. <https://doi.org/doi: 10.1038/s41598-019-54535-x>.
- Nematologists, S. o. (2020). Symptoms. *Rhadinaphelenchus cocophilus (red ring nematode)*. The Invasive Species Compendium (ISC), Wallingford.
- Neto, E., & Ramos-Elorduy, J. (2006). Los insectos comestibles de Brasil: etnicidad, diversidad e importancia en la alimentación. *Boletín Sociedad Entomológica Aragonesa.*, *38*, 423-442.
- Ngamnikom, P., & Songsermpong, S. (2011). The effects of freeze, dry, and wet grinding processes on rice flour properties and their energy consumption. *Journal of Food Engineering*, *104*(4), 632-638. <https://doi.org/https://doi.org/10.1016/j.jfoodeng.2011.02.001>
- Nie, W., Xu, F., Zhou, K., Yang, X., Zhou, H., & Xu, B. (2022). Stearic acid prevent alcohol-induced liver damage by regulating the gut microbiota. *Food Research International*, *155*, 111095. <https://doi.org/https://doi.org/10.1016/j.foodres.2022.111095>
- Nitbani, F. O., Pama, P. J., Nitti, F., Jumina, J., & Rohi, A. I. (2022). Antimicrobial Properties of Lauric Acid and Monolaurin in Virgin Coconut Oil: A Review. *ChemBioEng Reviews*, *9*(5), 442-461. <https://doi.org/https://doi.org/10.1002/cben.202100050>
- Njoroge, G., Kaibui, I., Njenga, P., & Odhiambo, P. (2010). Utilisation of priority traditional medicinal plants and local people's knowledge on their conservation status in arid lands of Kenya (Mwingi District). *J Ethnobiology Ethnomedicine*, *6*(22), 1-8. <https://doi.org/https://doi.org/10.1186/1746-4269-6-22>
- Ortega, E. (2022). *Origenes EC*. CHONTACURO, el mejor alimento de la Amazonía: <https://origenesec.com/amazonia/chontacuro/>
- O'Shea, M., Bassaganya-Riera, J., & Mohede, I. C. (2004). Immunomodulatory properties of conjugated linoleic acid. *The American Journal of Clinical Nutrition*, *79*(6), 1199S–1206S. <https://doi.org/https://doi.org/10.1093/ajcn/79.6.1199S>
- Ou, X., Liu, Y., & Lei, X. (2020). Characterization of spike glycoprotein of SARS-CoV-2 on virus entry and its immune cross-reactivity with SARS-CoV. . *Nat Commun*, *1620*. <https://doi.org/https://doi.org/10.1038/s41467-020-15562-9>
- Paladino, J. A., Sunderlin, J. L., Price, C. S., & Schentag, J. J. (2002). Economic Consequences of Antimicrobial Resistance. *Surgical Infections.*, *3*(3), 259-267. <https://doi.org/http://doi.org/10.1089/109629602761624225>
- Palomer, X., Pizarro-Delgado, J., Barroso, E., & Vázquez-Carrera, M. (2018). Palmitic and Oleic Acid: The Yin and Yang of Fatty Acids in Type 2 Diabetes Mellitus. *Trends Endocrinol Metab.*, *29*(3), 178-190. <https://doi.org/doi: 10.1016/j.tem.2017.11.009>.
- Park, J.-Y., Choi, H.-W., Park, K.-M., & Chang, P.-S. (2023). An improved method for rapid evaluation of enzymatic cis/trans isomerization of C18:1 monounsaturated fatty acids. *Food Chemistry*, *404*(A), 134618. <https://doi.org/https://doi.org/10.1016/j.foodchem.2022.134618>

- Pászti-Gere, E., Czimmermann, E., Ujhelyi, G., Balla, P., Maiwald, A., & Steinmetzer, T. (2016). In vitro characterization of TMPRSS2 inhibition in IPEC-J2 cells. *J Enzyme Inhib Med Chem.*, 31((sup2)), 123-129. <https://doi.org/doi: 10.1080/14756366.2016.1193732>.
- Paucar-Cabrera, A. (2005). A catalog and distributional analysis of the Rutelinae (Coleoptera: Scarabaeidae) of Ecuador. *Zootaxa*, 948(1), 20. <https://doi.org/DOI: https://doi.org/10.11646/zootaxa.948.1.1>
- Pelley, J. W. (2012). *ELSEVIER'S INTEGRATED REVIEW BIOCHEMISTRY SECOND EDITION*. Elsevier Inc. <https://doi.org/ ISBN: 978-0-323-07446-9>
- Pettersen, E., Goddard, T., Huang, C., Couch, G., Greenblatt, D., Meng, E., & Ferrin, T. (2004). UCSF Chimera--a visualization system for exploratory research and analysis. *J Comput Chem.*, 13, 1605-12. <https://doi.org/DOI: 10.1002/jcc.20084>
- Pfeuffer, M., & Jaudszus, A. (2016). entadecanoic and Heptadecanoic Acids: Multifaceted Odd-Chain Fatty Acids. *Advances in Nutrition*, 7(4), 730-734. <https://doi.org/https://doi.org/10.3945/an.115.011387>
- Pomeranz, Y. (2013). *Food Analysis: Theory and Practice*. Springer Science & Business Media. <https://doi.org/ISBN-1461569982>
- Ponce-Méndez, M., García-Martínez, M., Serna-Lagunes, R., Lasa-Covarrubias, R., Presa-Parra, E., Murguía-González, J., & Larena-Hernández, C. (2022). ocal Agricultural Management Filters Morphological Traits of the South American Palm Weevil (*Rhynchophorus palmarum* L.; Coleoptera: Curculionidae) in Ornamental Palm Plantations. *Agronomy*, 12(10), 2371. <https://doi.org/https://doi.org/10.3390/agronomy12102371>
- Quast, K. (2016). The use of zeta potential to investigate the pKa of saturated fatty acids. *Advanced Powder Technology*, 27(1), 207-214. <https://doi.org/https://doi.org/10.1016/j.apr.2015.12.003>.
- Quinteros, M., Martínez, J., Barrionuevo, A., Rojas, M., & Carrillo, W. (2022). Functional, Antioxidant, and Anti-Inflammatory Properties of Cricket Protein Concentrate (*Gryllus assimilis*). *Biology (Basel)*. *Biology (Basel)*, 11(5), 776. <https://doi.org/doi: 10.3390/biology11050776>.
- Ramos Elorduy, J., Motteflorac, E., & Pino, J. (2001). Chinchas medicinales de México (Insecta: Hemiptera). *In Memorias del 15 congreso internacional de medicina tradicional y alternativas terapéuticas*. Ciudad de México: Academia Mexicana de Medicina Tradicional.
- Rawling, T., MacDermott-Opeskin, H., Roseblade, A., Pazderka, C., Clarke, C., Bourget, K., . . . Murray, M. (2020). Aryl urea substituted fatty acids: a new class of protonophoric mitochondrial uncoupler that utilises a synthetic anion transporter. *The Royal Society of Chemistry*, 11, 12677-12685. <https://doi.org/DOI: 10.1039/D0SC02777D>
- Restrepo, G. L., Rivera, A. F., & Raigosa, B. J. (1982). Ciclo de vida, hábitos y morfometría de *Metamasius hemipterus* Olivier y *Rhynchophorus palmarum* L. (Coleoptera: Curculionidae) en caña de azúcar (*Saccharum officinarum* L.). *Acta Agronómica*, 32, 33-44. <https://doi.org/DOI: 10.15446/acag>

- Rioux, V. (2016). Fatty acid acylation of proteins: specific roles for palmitic, myristic and caprylic acids. *OCL*, 3(D304), 23. <https://doi.org/DOI: 10.1051/ocl/2015070>
- Robinson, D. F., Abdel-Latif, A., & Roffe, P. (2017). *Protecting Traditional Knowledge: The WIPO Intergovernmental Committee on Intellectual Property and Genetic Resources, Traditional Knowledge and Folklore*. Routledge. <https://doi.org/1317354850, 9781317354857>
- Rogero, M., Leão, M., Santana, T., Pimentel, M., Carlini, G., da Silveira, T., . . . Castro, I. (2020). Potential benefits and risks of omega-3 fatty acids supplementation to patients with COVID-19. *Free Radic Biol Med.*, Aug 20;156:190-199. <https://doi.org/doi: 10.1016/j.freeradbiomed.2020.07.005>.
- Sales-Campos, H., Reis de Souza, P., Crema Peghini, B., Santana da Silva, J., & Ribeiro Cardoso, C. (2013). An Overview of the Modulatory Effects of Oleic Acid in Health and Disease. *Bentham Science Publishers*, 13(2), 201-210. <https://doi.org/DOI: https://doi.org/10.2174/138955713804805193>
- Sam, Q., Ling, H., Yew, W., Tan, Z., Ravikumar, S., Chang, M., & Chai, L. (2021). The Divergent Immunomodulatory Effects of Short Chain Fatty Acids and Medium Chain Fatty Acids. *Int. J. Mol.*, 22(11), 6453. <https://doi.org/https://doi.org/10.3390/ijms22126453>
- Sánchez, P., & Cerda, H. (1993). The complex *Rhynchophorus palmarum* / *Bursaphelenchus cocophilus* in palms. *Boletín de Entomología Venezolana*, 8, 1-18.
- Sancho, D., Landivar Valverde, D., Sarabia, D., & Alvarez Gil, M. d. (2015). Caracterización del extracto graso de larvas de *Rhynchophorus palmarum* L. *Ciencia y Tecnología de Alimentos*, 25(2), 39-44. <https://doi.org/ISSN 0864-4497>
- Santana, C., Nascimento, J., de M. Costa, M., da Silva, A., Dornelas, C., & Grillo, L. (2014). Avaliação do desenvolvimento e reservas energéticas de larvas de *Rhynchophorus palmarum* (Coleoptera: Curculionidae) em diferentes dietas. *Agrária - Revista Brasileira de Ciências Agrárias*, 9(2), 205-209. <https://doi.org/https://doi.org/10.5039/agraria.v9i2a3885>
- Santivañez, J. C., & Paucar, L. O. (2021). Larva de *Rhynchophorus palmarum* L. (Coleoptera: Curculionidae): Efecto de la dieta en la síntesis de ácidos grasos esenciales. *Revista Verde de Agroecología e Desenvolvimento Sustentável*, 16(2). <https://doi.org/http://dx.doi.org/10.18378/rvads.v16i2.8258>
- Sarria, G., Riascos-Ortiz, D., Medina, H., Mestizo, Y., Lizarazo, G., & De Agudelo, F. (2020). Molecular identification of *Bursaphelenchus cocophilus* associated to oil palm (*Elaeis guineensis*) crops in Tibu (North Santander, Colombia). *The Journal of Nematology*, 30(52), e2020-117. <https://doi.org/doi: 10.2130/jofnem-2020-117>
- Schlickmann-Tank, J. A., Enciso-Maldonado, G. A., Haupenthal, D. I., Luna-Alejandro, G., & Badillo-López, S. E. (2020). Detección y variación temporal de *Rhynchophorus palmarum* (Linnaeus) (Coleoptera: Dryophthoridae) en cultivos de *Acrocomia aculeata* (Jacq.) Lodd. ex Mart. en Itapúa, Paraguay. *Revista Chilena de Entomología*, 46(2), 163-169. <https://doi.org/https://doi.org/10.35249/rche.46.2.20.04>

- Segré, D., Ben-Eli, D., & Deamer, D. (2001). The Lipid World. *Orig Life Evol Biosph*, 31, 119-145. <https://doi.org/https://doi.org/10.1023/A:1006746807104>
- Senesi, N., & Loffredo, E. (1998). The Chemistry of Soil Organic Matter. In N. S. Donald L. Sparks, *Soil Physical Chemistry* (p. 132). CRC Press. <https://doi.org/https://doi.org/10.1201/9780203739280>
- Serrano-González, R., Guerrero-Martínez, F., Pichardo-Barreiro, Y., & Serrano-Velázquez, R. (2013). Los artrópodos medicinales en tres fuentes novohispanas del siglo XVI. *Etnobiología*, 11(2), 23-24. <https://doi.org/ISSN 1665 - 2703>
- Smith, N. (1996). *The Enchanted Amazon Rain Forest: Stories from Vanishing World*. Gainesville: The University Press of Florida;
- Solines Reyes, P. J. (2022). *Eficiencia del uso de feromona sintética y cebos vegetales en la captura del picudo negro (Rhynchophorus palmarum) en el cultivo de palma africana (Elaeis guineensis Jacq.)*. Universidad Católica de Santiago de Guayaquil. <http://repositorio.ucsg.edu.ec/handle/3317/19191>
- Srivastava, S., Babu, N., & Pandey, H. (2009). Traditional insect bioprospecting – As human food and medicine. *CSIR*, 8(4), 485-494. <https://doi.org/http://nopr.niscpr.res.in/handle/123456789/6263>
- Stark, A. H., Crawford, M. A., & Reifen, R. (2008). Update on alpha-linolenic acid. *Nutrition Reviews*, 66(6), 326-332. <https://doi.org/https://doi.org/10.1111/j.1753-4887.2008.00040.x>
- Stephenson, C., Coker, E., Wisely, S., Liang, S., Dinglasan, R., & Lednicky, J. (2022). Imported Dengue Case Numbers and Local Climatic Patterns Are Associated with Dengue Virus Transmission in Florida, USA . *Insects*, 13(2). <https://doi.org/https://doi.org/10.3390/insects13020163>
- Takato, T., Iwata, K., Murakami, C., Wada, Y., & Sakane, F. (2017). Chronic administration of myristic acid improves hyperglycaemia in the Nagoya–Shibata–Yasuda mouse model of congenital type 2 diabetes. *Diabetologia*, 60, 2076-2083. <https://doi.org/doi:10.1007/s00125-017-4366-4>.
- Tallima, H., & Ridi, E. R. (2017). Arachidonic acid: Physiological roles and potential health benefits - A review. *J Adv Res.*, 11, 33-41. <https://doi.org/doi:10.1016/j.jare.2017.11.004>.
- Tay, M., Poh, C., Rénia, L., MacAry, P., & Ng, L. (2020). *Nat. Rev Immunol.*, 20, 363-374. <https://doi.org/https://doi.org/10.1038/s41577-020-0311-8>.
- Tormar, H., Isaacs, C. E., Brown, H. R., Barshatzky, M. R., & Pessolano, T. (1987). Inactivation of enveloped viruses and killing of cells by fatty acids and monoglycerides. *Antimicrob Agents Chemother.*, 31(1), 27-31. <https://doi.org/doi:10.1128/AAC.31.1.27>.
- Torres, I. D. (2021). *Manejo integrado de bursaphelenchus cocophilus causante del anillo rojo en las palmas aceiteras*. Universidad Técnica de Babahoyo. <http://dspace.utb.edu.ec/handle/49000/9353>

- Towler, P., Staker, B., & Prasad, S. (2004). *Native Human Angiotensin Converting Enzyme-Related Carboxypeptidase (ACE2)*. Protein Data Base: DOI: 10.2210/pdb1R42/pdb
- Trott, O., & Olson, A. J. (2010). AutoDock Vina: improving the speed and accuracy of docking with a new scoring function, efficient optimization, and multithreading. *Journal of computational chemistry*, 31(2), 455-461. <https://doi.org/doi:10.1002/jcc.21334>
- Trujillo-Gonzalez, J., Santan-Castaña, E., & Torres Mora, M. (2011). La palma de Moriche (*Mauritia Flexuosa* L.f.) un ecosistema estratégico. *Revista ORINOQUIA*, 8(4), 62-70. <https://doi.org/ISSN:0121-3709>
- Universal Biologicals. (2022, November 1). *HENEICOSANOIC ACID*. Universal Biologicals Life Science Research Products: <https://www.universalbiologicals.com/heneicosanoic-acid-1241>
- Vargas, G. E., Espinoza, G., Ruiz, C., & Rojas, R. (2013). Valor nutricional de la larva de *Rhynchophorus palmarum* L.: comida tradicional en la amazonía peruana. *Rev. Soc. Quím. Perú*, 79(1), 64-70. <https://doi.org/ISSN1810-634X>
- Venugopal, E., Ramadoss, G., Krishnan, K., Subash, S. E., & Rajendran, S. (2017). Stimulation of human osteoblast cells (MG63) proliferation using decanoic acid and isopropyl amine fractions of *Wattakaka volubilis* leaves. *Journal of Pharmacy and Pharmacology*, 69(11), 1578-1591. <https://doi.org/https://doi.org/10.1111/jphp.12801>
- Vera, C., & Brand, A. (2014). Aramanday guasu (*Rhynchophorus palmarum*) como alimento tradicional entre os Guarani Ñandéva na aldeia Pirajuí. *Tellus*, 23, 97-126. <https://doi.org/DOI:10.20435/tellus.v0i23.258>
- Vetter, W., Darwisch, V., & Lehnert, K. (2020). Erucic acid in Brassicaceae and salmon – An evaluation of the new proposed limits of erucic acid in food. *NFS Journal*, 19(ISSN 2352-3646), 9-15. <https://doi.org/https://doi.org/10.1016/j.nfs.2020.03.002>
- Viesca, F., & Romero, A. (2009). La Entomofagia en México. Algunos aspectos culturales. *Revista El Periplo Sustentable*, 16, 57-83. <https://doi.org/ISSN:1870-9036>
- Vilharva, K., Leite, D., & Dos Santos, H. (2021). *Rhynchophorus palmarum* (Linnaeus, 1758) (Coleoptera: Curculionidae): Guarani-Kaiowa indigenous knowledge and pharmacological activities. *PLoS ONE*, 4(16), 1-17. <https://doi.org/https://doi.org/10.1371/journal.pone.0249919>
- Volkamer, A., Griewel, A., Grombacher, T., & Rarey, M. (2010). Analyzing the topology of active sites: on the prediction of pockets and subpockets. *J Chem Inf Model*, 50(11), 2041-52. <https://doi.org/DOI:https://doi.org/10.1021/ci100241y>
- Volkamer, A., Kuhn, D., Grombacher, T., Rippmann, F., & Rarey, M. (2012). Combining global and local measures for structure-based druggability predictions. *J Chem Inf Model*, 52(2), 360-72. <https://doi.org/DOI:https://doi.org/10.1021/ci200454v>
- Wang, B., Wu, L., & Chen, J. (2021). Metabolism pathways of arachidonic acids: mechanisms and potential therapeutic targets. *Sig Transduct Target Ther*, 6(94). <https://doi.org/https://doi.org/10.1038/s41392-020-00443-w>

- Wattanapongsiri, A. (1966). *A Revision of the Genera Rhynchophorus and Dynamis*. Oregon State University.  
[https://ir.library.oregonstate.edu/concern/graduate\\_thesis\\_or\\_dissertations/6d570047d?locale=en](https://ir.library.oregonstate.edu/concern/graduate_thesis_or_dissertations/6d570047d?locale=en)
- Weiss, H. B. (1946). An Old Use for Cockroaches. *Journal of the New York Entomological Society*, 54(2), 166–166. <https://doi.org/http://www.jstor.org/stable/25005159>
- Whelan, J., & Fritsche, K. (2013). Linoleic Acid. *Advances in Nutrition*, 4(3), 311-312. <https://doi.org/https://doi.org/10.3945/an.113.003772>
- Wijaya, C. H., Wijaya, W., & Mehtac, B. M. (2015). General Properties of Major Food Components. *Handbook of Food Chemistry*, 1-32. [https://doi.org/DOI 10.1007/978-3-642-41609-5\\_35-1](https://doi.org/DOI 10.1007/978-3-642-41609-5_35-1)
- Wille, J., & Kydonieus, A. (2003). Palmitoleic Acid Isomer (C16:1Δ6) in Human Skin Sebum Is Effective against Gram-Positive Bacteria. *Skin Pharmacol Appl Skin Physiol*, 16, 176-187. <https://doi.org/https://doi.org/10.1159/000069757>
- Williams, C., Headd, J., Moriarty, N., Prisant, M., Videau, L., Deis, L., . . . Richardson, D. (2018). MolProbity: More and better reference data for improved all-atom structure validation. *Protein Sci*, 27(1), 293-315. <https://doi.org/doi: 10.1002/pro.3330>
- Wisniewska, M., Karlberg, T., & Arrowsmith, C. (2009). *Crystal structure of the human 70kDa heat shock protein 5 (BIP/GRP78) ATPase domain in complex with ADP*. Protein Data Bank: DOI: 10.2210/pdb3IUC/pdb
- World Health Organization. (2022). *Coronavirus disease (COVID-19) pandemic*. World Health Organization. <https://www.who.int/europe/emergencies/situations/covid-19#:~:text=This%20led%20WHO%20to%20declare,have%20died%20from%20the%20disease.>
- World Health Organization. (2022). *Zoonosis*. WHO. <https://www.who.int/es/news-room/fact-sheets/detail/zoonoses>
- Wu, Q., Liu, T., Liu, H., & Zheng, G. (2009). Unsaturated fatty acid: Metabolism, synthesis and gene regulation. *African Journal of Biotechnology*, 8(9), 1782-1785. <https://doi.org/ISSN 1684-5315>
- Xu, C., Wu, P., Gao, J., Zhang, L., Ma, T., Ma, B., . . . Zhang, B. (2019). Heptadecanoic acid inhibits cell proliferation in PC-9 non-small-cell lung cancer cells with acquired gefitinib resistance. *Oncology Reports*, 41(6), 3499-3507. <https://doi.org/https://doi.org/10.3892/or.2019.7130>
- Xu, X., Chen, P., Wang, J., Feng, J., Zhou, H., Li, X., . . . Hao, P. (2020). Evolution of the novel coronavirus from the ongoing Wuhan outbreak and modeling of its spike protein for risk of human transmission. *Sci China Life Sci.*, 63(3), 457-460. [https://doi.org/doi: 10.1007/s11427-020-1637-5.](https://doi.org/doi: 10.1007/s11427-020-1637-5)
- Yaqoob. (2002). Monounsaturated fatty acids and immune function. *Eur J Clin Nutr.*, Aug;56, Suppl 3:S9-S13. <https://doi.org/doi: 10.1038/sj.ejcn.1601477>. PMID: 12142954.

- Yaqoob, R. (2022). *iBiologia*. Fatty Acid Structure | Examples | Types | Physical & Chemical Properties: <https://ibiologia.com/fatty-acid-structure/>
- Yen, A. (2009). Entomophagy and insect conservation: some thoughts for digestion. *Journal Insect Conserv*, *13*, 667-670. <https://doi.org/https://doi.org/10.1007/s10841-008-9208-8>
- Yu, C., Griffiths, L., & Haupt, L. (2017). Exploiting Heparan Sulfate Proteoglycans in Human Neurogenesis—Controlling Lineage Specification and Fate. *Front. Integr. Neurosci.*, *11*(28). <https://doi.org/https://doi.org/10.3389/fnint.2017.00028>
- Yuan, Q., Xie, F., Huang, W., Hu, M., Yan, Q., Chen, Z., . . . Liu, L. (2021). The review of alpha-linolenic acid: Sources, metabolism, and pharmacology. *Phytotherapy Research*, *36*(1), 164-188. <https://doi.org/https://doi.org/10.1002/ptr.7295>
- Zhan, W., Tian, W., Zhang, W., Tian, H., & Sun, T. (2022). ANGPTL4 attenuates palmitic acid-induced endothelial cell injury by increasing autophagy. *Cellular Signalling*, *98*, 110410. <https://doi.org/https://doi.org/10.1016/j.cellsig.2022.110410>.
- Zhou, T., Tsybovsky, Y., Olin, A., & Kwong, P. (2020). *Structure of SARS-CoV-2 spike at pH 4.0*. Protein Data Bank: DOI: 10.2210/pdb6XLU/pdb
- Zimian, D., Yonghua, Z., & Xiwu, G. (1997). Medicinal insects in China. *Ecology of Food and Nutrition*, *36*(2-4), 209-220. <https://doi.org/https://doi.org/10.1080/03670244.1997.9991516>